Final Design Report

Pseudo Satellite for Military Purpose

July 4, 2017

DSE group 22

Final Design Report

Pseudo Satellite for Military Purpose

July 4, 2017

Team members		Course staff	
Büller, M.B.	4166566	Dr. Ir. Vos, R.	Tutor
Claes, A.P.K.	4276450	Ir. Jongbloed, B.C.P.	Coach
Drenth, M.J.	4296850	Ir. Baptista, C.P.	Coach
Griffioen, M.A.	4377745	L.T. Willems, J.	External expert
Groot, D.J.	4354583		
Janowski, J.T.	4347900		
Marchena Esteban, C.	4308891		
Post, P.J.A	4351037		
Wedemeijer, R.	4289404		
Willemsen, J.D.	4354028		

TU Delft

Preface

This report is written as part of the Design Synthesis Exercise at the TU Delft University of Technology by 10 students in 10 weeks. The team had to design a high altitude, long endurance aircraft for military purpose. Throughout the report the entire conceptual design process is explained and all design decisions are elaborated on. Furthermore, it contains analysis about the expected market, possible missions, the design cost and the way in which the design is sustainable. Readers that are especially interested in the final design are referred to chapter 9.

Acknowledgments

We would like to thank all parties involved in helping us reach our goal. Without these parties this project would not have been possible. Special thanks has to be given to Dr.ir. R. Vos, for his support and knowledge. We are grateful for the support of Lt. J. Willems, Ir. B. Jongbloed and Ir. C.F. Baptista on who we could count when having questions concerning their specialty. We would like to thank Dr. M. Voskuijl and Y. Teeuwen for their help in developing the power and propulsion algorithms. We would like to acknowledge the "Aviation Department of the VSV Leonardo da Vinci" and Steve Whitby of Airbus Defence & Space for organizing the Zephyr lunch-lecture, which allowed us to get insight in the Airbus Defence & Space design methods of a similar design. We would also like to show gratitude to Delft University of Technology for allowing us to use their facilities on a daily basis. Lastly, some companies deserve extra acknowledgment for giving information, directly leading to a better design: Alta Devices[1], NovoPolymers[2], Fokker [3] and Dunmore[4].

DSE Group 22

[1]https://www.altadevices.com/
[2]http://www.novopolymers.com/
[3]http://www.fokker.com
[4]http://www.dunmore.com/

Nomenclature

α	Angle of attack	[°]
β	Sideslip angle	[°]
η_p	Propeller efficiency	$[-]$
$\eta_{Batteries}$	Battery efficiency including battery management system	$[-]$
$\eta_{Propeller_{climb}}$	Efficiency of propellers during climb	$[-]$
$\eta_{Propeller_{cruise}}$	Efficiency of propellers during cruise	$[-]$
$\eta_{Propulsiontrain}$	Efficiency of propellers, motors and ESC	$[-]$
$\eta_{Solarpanels}$	Solar foil efficiency	$[-]$
Λ_{LE}	Leading edge sweep angle	[°]
ρ_{people}	Population density	$[people/km^2]$
ζ	Damping ratio	$[-]$
A	Availability	[%]
A_{exp}	Expected area	$[km^2]$
AR	Aspect ratio	$[-]$
b	Span	$[m]$
c	Chord	$[-]$
C_D	Aircraft drag coefficient	$[-]$
C_L	Aircraft lift coefficient	$[-]$
C_{L_α}	Lift coefficient with respect to angle of attack	$[-]$
C_{l_β}	Derivative of the roll moment with respect to sideslip	$[-]$
C_{l_β}	Rolling coefficient with respect to sideslip	$[-]$
$C_{L_{max}}$	Maximum wing lift coefficient	$[-]$
C_{l_p}	Rolling coefficient with respect to roll rate	$[-]$
C_{L_q}	Lift coefficient with respect to q	$[-]$
C_{l_r}	Rolling coefficient with respect to yaw rate	$[-]$
$C_L^{\frac{3}{2}}/C_D$	Endurance parameter	$[-]$
C_{m_α}	Moment coefficient with respect to angle of attack	$[-]$
C_{m_q}	Moment coefficient with respect to q	$[-]$
C_{m_u}	Moment coefficient with respect to airspeed	$[-]$
C_{n_β}	Static directional stability derivative	$[-]$
C_{n_β}	Yawing moment coefficient with respect to sideslip	$[-]$
C_{n_p}	Yawing moment coefficient with respect to roll rate	$[-]$

C_{n_r}	Yawing moment coefficient with respect to yaw rate	$[-]$
C_{X_α}	X-force coefficient with respect to angle of attack	$[-]$
C_{X_u}	X-force coefficient with respect to airspeed	$[-]$
C_{Y_β}	Y-force coefficient with respect to sideslip	$[-]$
C_{Y_p}	Y-force coefficient with respect to roll rate	$[-]$
C_{Y_r}	Y-force coefficient with respect to yaw rate	$[-]$
C_{Z_u}	Z-force coefficient with respect to airspeed	$[-]$
D	Diameter of the propeller	$[m]$
$D_{propeller}$	Diameter of the propeller	$[m]$
E	Young's Modulus	$[MPa]$
J	Advance ratio	$[-]$
L	Rolling moment	$[Nm]$
$M_{landinggear}$	Total mass of landing gears	$[kg]$
M_{oew}	Operative empty mass	$[kg]$
M_{other}	Mass of payload and other equipment	$[kg]$
$M_{payload}$	Payload mass	$[kg]$
$M_{Powerstorage}$	Total mass of batteries and battery management system	$[kg]$
$M_{powertrain}$	Mass of the complete powertrain	$[kg]$
$m_{propeller}$	Mass of the propeller	$[kg]$
$M_{Propulsion}$	Total mass of ESCs, motors and propellers	$[kg]$
M_{Ribs}	Total mass of wing ribs	$[kg]$
M_{Rod}	Total mass of wing rods	$[kg]$
M_{Skin}	Total mass of skin foil	$[kg]$
M_{solar}	Total mass solar foil and maximum power point trackers	$[kg]$
$M_{structure}$	Structural mass	$[kg]$
M_{TO}	Take-off mass	$[kg]$
MAC	Mean aerodynamic chord	$[m]$
MDT	Mean Down Time	$[hours]$
$MTBF$	Mean Time Between Failure	$[-]$
$MTBF$	Mean Time Between Failure	$[hours]$
n_p	Propeller's rotational speed	$[rotations/s]$
N_{rudder}	Moment caused by rudders	$[Nm]$
P	Eigenmotion period	$[s]$
$P_{climb_{shaft}}$	Required shaft power during climb	$[W]$
$P_{cruise_{shaft}}$	Required shaft power during cruise	$[W]$
P_{fatal}	The chance of a fatal injury	$[-]$
S	Wing surface area	$[m^2]$
t/c	Airfoil thickness to chord ratio	$[-]$
T_2	Time to double amplitude	$[-]$

$T_{1/2}$	Time to half amplitude	$[-]$
T_{min}	Minimum operation temperature	$[C°]$
UTS	Ultime Tensile Strength	$[MPa]$
V	Free stream fluid velocity	$[m/s]$
V_{cruise}	Cruise Velocity	$[m/s]$
W/P	Power loading	$[N/W]$
W/S	Wing loading	$[N/m^2]$
x_{cg}	Center of gravity	$[m]$

Summary

Currently surveillance and reconnaissance missions by the Royal Netherlands Air Force are being performed with aircraft or helicopters which have limited endurance due to their fuel dependence. This limits the gathering of intelligence. Hence, the need for a new platform to provide continuous flow of information arises. The military applications of this platform are measurement and signature intelligence (MASINT) gathering including infrared, laser, spectroscopic data and synthetic aperture radar (SAR). Also signal en electronic intelligence can be gathered. This platform could also possibly be used for civil application such as communication, monitoring of weather and/or climate and remote sensing.

The need for a continuous information flow can be solved by designing a high altitude, long endurance aircraft which can carry a interchangeable, 25 kg payload. This should be done by 2023. More specifically, the mission duration is 30 days flying above 15 km. This is elevated to 18 km to avoid the jet stream. This goal can be fulfilled by a lightweight design with an efficient power train.

During the concept selection phase a trade off was made between a flying wing and a conventional wing tail for the configuration. The power train trade off included electric, hybrid and fuel power. The flying wing with electric power generation and propulsion was chosen due to its lower weight, smaller size and ease of operation while still maintaining the highest possible aerodynamic efficiency.

The final design was optimized to be lightweight and dimensionally small. The take off mass budget is set to 405 kg and the maximum allowable span was set to 50 m. An isometric representation of the aircraft is shown in figure 1 and the important parameters can be found in table 1. To achieve this optimized design three design groups were created: a structural, power & propulsion and wing (aerodynamics, stability & control) group. The design parameters that affect multiple design groups such as aspect ratio, sweep angle and thickness over chord ratio are determined and can also be found in table 1. It is chosen to not use dihedral as this decreases directional stability and increases the structural weight. To achieve maximum aerodynamic efficiency the wing has a taper ratio, a root to tip twist angle of 1.8° leading edge down and two different airfoils at the root and tip. The wing is segmented in 3 spanwise sections, the outer 25% is the MH81 airfoil, the other 75% of the wing is a gradual transition to the SM701 airfoil.

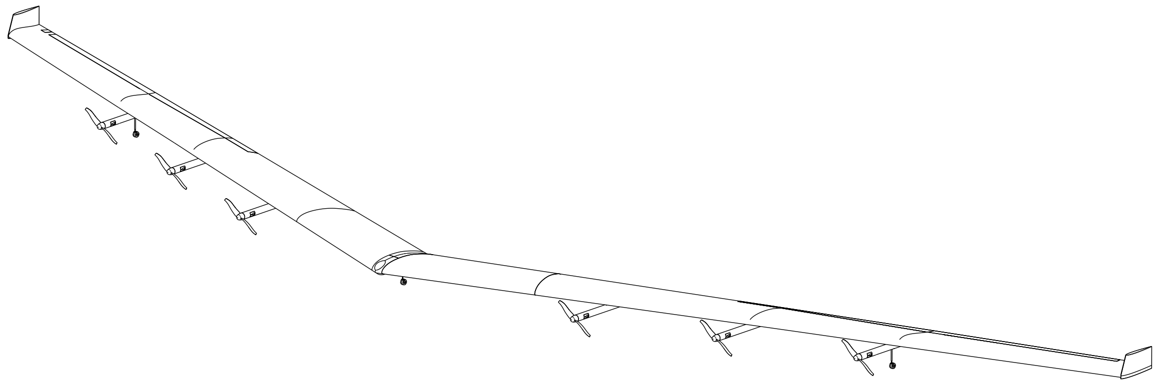

Figure 1: Isometric view of the aircraft.

Stability wise all eigenmotions are stable except for the spiral. Due to its time to double amplitude of 30 seconds the aircraft still categorized to have level 1 flying qualities. The Dutch Roll performs the worst and is categorized as level 3. This is not due to the damping ratio, which almost categorizes as level 1. But due to the low frequency of the Dutch roll Although stable, in the future design, attention should be given to designing a PID controller and yaw damping system. To control the aircraft longitudinally and laterally elevons are used which run along 50% of the entire span and cover $0.2c$. Split drag rudders are used for directional control. To increase the yaw stability by a factor of 2.5 wingtips of 0.7 m high are added to the aircraft.

To comply with the 30 day flight requirement the aircraft surface area is driven by the solar panel area. Gallium arsenide solar panels with an efficiency of 31.6% are used. This does not comply with the requirement stating no toxic materials may be used during production. However, if Silicon type solar panels would be used the size and mass of the aircraft would be driven to unacceptable numbers. This solar array powers 6 electrical engines and charges the batteries during the day. At the end of each day the aircraft ascends to 23 km to store potential energy to glide down with engines off during the night. Once 18 km is reached again the engines run on battery power until first sunlight, where the cycle begins again.

The structure is lightweight by using a carbon fibre composite rod to cope with all loads. Plastic ribs hold the Mylar polyester skin. The aircraft can be disassembled into the following sections: a mid section, two wing halves and six engine pods. This is done to fulfill the transportation requirement which states that three aircraft including support equipment should be able to be transported using a C-17 transport aircraft.

The aircraft is equipped with 6 engine pods. These pods contain the engines, batteries, battery management systems and the two outer pods also contain a landing gear system. By using these pods (dis)assembly is easy, maintenance can be easily performed and during designing the aircraft these can easily be moved to affect the stability characteristics. A representation of one of these pods including landing gear can be found in figure 2.

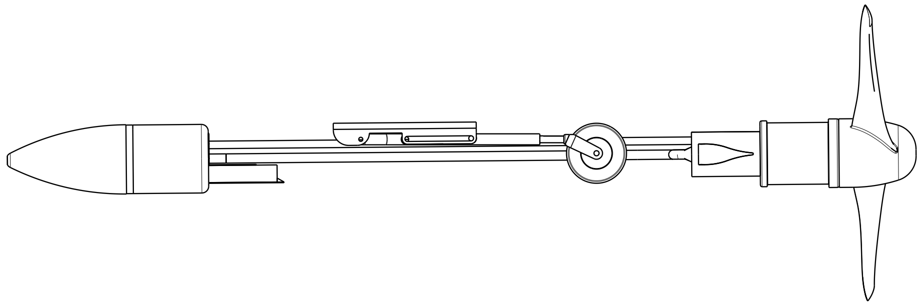

Figure 2: Pod layout including landing gear

Once arrived at the destination take-off can be done within approximately one or two days. Next to the unloading and assembling time this is also dependent on the weather conditions. The aircraft operates between ±40° latitude year-round and can reach higher latitudes seasonally. For take-off the aircraft will be towed on a trailer to obtain enough velocity. It is equipped with a landing gear system to perform the landing.

Table 1: Important aircraft parameters

Parameter	**Value**	**Parameter**	**Value**	**Parameter**	**Value**
S $[m^2]$	83	M_{to} $[kg]$	307	$P_{cruise_{shaft}}$ (18 km) $[kW]$	2.1
AR [-]	25	M_{oew} $[kg]$	283	$P_{cruise_{shaft}}$ (23 km) $[kW]$	3.2
b $[m]$	45.6	$M_{\text{structure}}$ $[kg]$	139	$P_{climb_{shaft}}$ $[kW]$	4.5
Taper ratio [-]	0.6	-M_{Rod} $[kg]$	58	$\eta_{Solarpanels}$ [%]	31.6
Tip chord $[m]$	1.3	-M_{Ribs} $[kg]$	20	$\eta_{Batteries}$ [%]	98
Root chord $[m]$	2.2	-M_{Skin} $[kg]$	23	$\eta_{Propulsiontrain}$ [%]	78
Sweep_{LE} $[deg]$	20	-$M_{\text{landinggear}}$ $[kg]$	13	$\eta_{Propeller_{cruise}}$ [%]	85
t/c [%]	18	$M_{\text{Powertrain}}$ $[kg]$	131	$\eta_{Propeller_{climb}}$ [%]	75
W/S $[N/m^2]$	35.8	-M_{Solar} $[kg]$	19	η_{Engine} [%]	93
W/P $[N/W]$	0.89	-$M_{\text{Power storage}}$ $[kg]$	92	Number of engines [-]	6
L/D [-]	52	-$M_{\text{Propulsion}}$ $[kg]$	14	Propeller diameter $[m]$	1.5
$C_L^{\frac{3}{2}}/C_D$ [-]	45	M_{other} $[kg]$	12		
V_{cruise} (18 km) $[m/s]$	26	M_{payload} $[kg]$	25		

The aircraft can be controlled from the ground station based in The Netherlands via satellite communication using the Iridium network. For local checks and maintenance, line of sight control can be performed from a small suitcase containing the necessary equipment. Due to the Veronte autopilot system by Embention 10 aircraft can be controlled by 2 operators. As stated before, the payload is interchangeable by means of a simple to use rail system. The payload establishes it's own communication link to send data.

Regarding reliability all critical systems are at least one time redundant. It is decided that the aircraft returns to base in case of critical system failure. The mean time between component failure is estimated to be approximately 5200 hours. This is due to the relatively high failure rate of the line-of-sight antennas and servos (numbers?). The lifetime os the aircraft is expected to easily(numbers?) surpass the 20,000 flight hour requirement. The batteries will be replaced once per year, or every 300 cycles. In case of no failures maintenance will take 24 hours. The mean down time is two days, accounting for possibles failures fixable at the deployment site and the periodical battery replacement. This leads to an availability of 99% The aircraft safety is assessed by chance of causing fatal injury. This can be caused by catastrophic failure, loss of structural parts and complete loss of control. To comply with the fatal injury requirement the maximum failure rate for the first two failure types was set at 10^{-8} and complete loss of control only occurs with a rate of $4.8 \cdot 10^{-7}$.

A sensitivity analysis was performed to determine the effects of certain design choices. The design parameters with the largest influence on the design is the battery energy density. It is assumed that by 2023 an energy density of 450 Wh/kg can be used. If this would be e.g. 300 Wh/kg, the surface area would increase from 83 m^2 to 133 m^2.

The total cost of a single aircraft is €5.5M including maintenance throughout its operational lifetime. The cost per flight hour is €260. Comparing this to a flight hour of an AH-64 Apache, the Apache is 2000% more expensive.

The manufacturing and assembly of the aircraft will be performed in The Netherlands. The landing gear and pods are produced by KVE Composites Group. The propeller and rod are made by the NLR. The ribs are 3D printed at the RNLAF and assembly will be performed at a factory to be built.

The sustainable development mainly focuses on the production and end-of-life. Due to the high required performances the choice in different technologies is limited. For production the main focus is minimizing transport and material usage. The end-of-life solution is to be decided by the customer but most of the subsystems can be re-used.

Furthermore, the CO2 emissions during production and transport have been calculated at 450 tonnes of CO2. This will be mitigated by promoting the usage of green energy to all manufacturers. All remaining unmitigated CO2 will be covered by buying emission credits.

Recommendations for further design are to put more emphasis on the stability, especially the Dutch roll. Also propeller design at high altitude is a relatively large uncertainty factor, more research is recommended. The skin material and its replaceability and repairability should also be further investigated.

Contents

ATA 100

In table 2 the Air Transport Association (ATA) numbering system can be found. This is a numbering system that applies to common aircraft documentation. Not all chapters of the numbering system are implemented, as not all chapters apply to the aircraft, or some chapters are for detailed design.

Table 2: ATA 100 [5]

ATA number	Title	Section
05-00	MAINTENANCE CHECKS	9.4.3
06-00	DIMENSIONS AND AREAS	9
08-00	LEVELING AND WEIGHING	5.2.1
09-00	TOWING AND TAXIING	8.2
20-00	STANDARD PRACTICES - AIRFRAME	7
21-00	AIR CONDITIONING	6.4
22-00	AUTO FLIGHT	8.4
23-00	COMMUNICATIONS	8.4
24-00	ELECTRICAL POWER	6.1
27-00	FLIGHT CONTROLS	5.2.3
32-00	LANDING GEAR	7.8
34-00	NAVIGATION	8.4
36-00	PNEUMATIC	7.7
39-00	ELECTRICAL	6.1
45-00	CENTRAL MAINTENANCE SYSTEM	8.4
49-00	AIRBORNE AUXILIARY POWER	6.2
51-00	STANDARD PRACTICES AND STRUCTURES	7
54-00	NACELLES / PYLONS	7.7
55-00	STABILIZERS	5.2.3
57-00	WINGS	5.1
60-00	PROPELLERS / PROPULSORS	6.3
70-00	STANDARD PRACTICES - ENGINE	6.2
75-00	BLEED AIR	6.2
76-00	ENGINE CONTROLS	8.4
77-00	ENGINE INDICATION	8.4

[5] URL: http://www.s-techent.com/ATA100.htm [Retrieved on: 27-06-2017]

1. Introduction

The Royal Netherlands Air Force (RNLAF) performs missions in which surveillance, reconnaissance and communication are a key factor. An example of such a mission is MINUSMA in the northern and central parts of Mali[1], a peacekeeping mission which comprises of protecting civilians and other security-related stabilization tasks. Part of this contains the gathering of intelligence with respect to possible terrorist attacks. Currently, this task is performed by a group of special forces using Apache helicopters and other platforms of which the range and endurance are limited and operational costs are very high. Hence data gathering with these platforms is very inefficient in terms of cost efficiency and time. As such, there is a need from the Royal Netherlands Air Force (RNLAF) to increase its reconnaissance and surveillance capabilities in order to increase the effectiveness of its operations. One system that can satisfy this need effectively is an unmanned, long-endurance aircraft that can operate autonomously. A fleet of up to 10 such aircraft can be controlled from a single ground unit with only two operators while performing tasks such as in-theatre relay of communications, missile detection, navigation and continuous imagery. The mission profile for such an aircraft is shown in figure 1.1. A more detailed mission profile is shown in chapter 8.

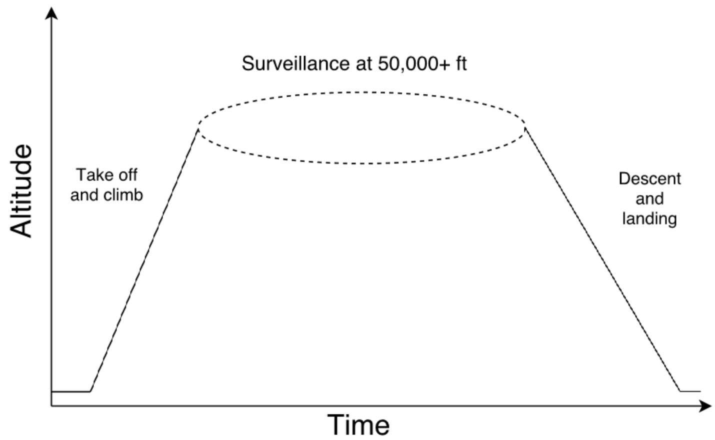

Figure 1.1: Probable mission profile for long endurance aircraft

While the autonomous flight and long mission radius are key requirements for the RNLAF, these are not the main drivers for the design of the aircraft. The challenge in the design lies in the endurance and high altitude required for completing the mission successfully. With energy densities of batteries

[1]URL: http://www.un.org/en/peacekeeping/missions/minusma/background.shtml [Retrieved on 26-6-2017]

increasing every year [2], companies and civilian service are beginning to show interest in very long endurance platforms. An example of this are Airbus and Facebook with their Zephyr and Aquila platforms respectively.

The goal of this project is to make a class II conceptual design of the complete system including the operational strategy, manufacturing process and the ground station. Since the RNLAF is the primary customer, the system should be manufactured using mostly technology that is currently present in Dutch companies. This is the final report of a series of four design reports. In the previous report, three concepts have been evaluated and constraints with the resulting design space has been set up. To set up this design space a wing and power loading diagram has been used. For a conventional aircraft, this would contain constraints due to CS-23 and CS-25 requirements combined with other specific requirements for the design. For the current aircraft however, there are only some specific requirements present. Therefore the only constraints for the design space are the cruise condition (MPS-FLT-1) and the climb requirement (MPS-FLT-5). This climb requirements states that the aircraft should be able to climb to its ceiling altitude within 9 hours and 20 minutes, which is the shortest daylight duration it will encounter in the required latitude range. The take-off field length has no influence because take-off is done from a trailer, as evaluated in chapter 8. The wing-loading and power loading diagram is shown in figure 1.2. Note that since the climb requirement is always more limiting than the cruise requirement, this is the only constraint shown in the diagram.

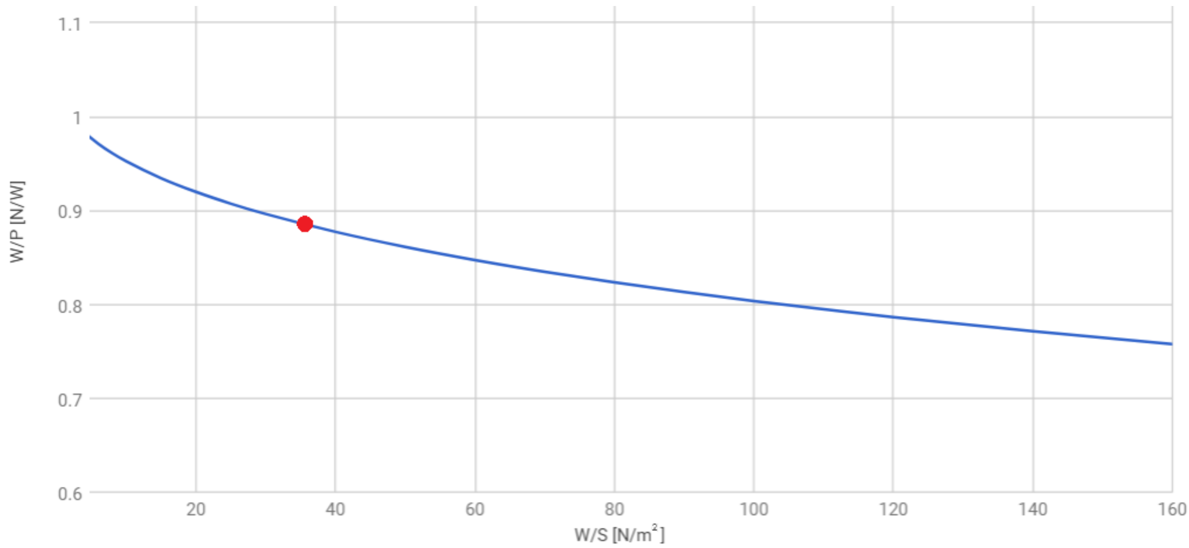

Figure 1.2: Wing- & Power loading diagram including the final design point ($AR = 25$, $C_L^{3/2}/C_D = 45$, $\rho = 0.186$)

This report will present final class II conceptual design for this project, which includes final design drawings, subsystem design, operational analysis, cost analysis, resource allocation and a sustainable

[2] URL: https://www.enterpriseirregulars.com/103492/future-electric-utilities-change-disruption-ahead/ [Retrieved on 27-6-2017]

development approach.

The report starts with an overview of the current market and other opportunities in the market analysis in chapter 2. After that, the steps made before the actual design phase, such as identifying all requirements, are explained in chapter 3. Then a description of the design approach is given in chapter 4, after which the wing geometry & aircraft stability, power & propulsion system and aircraft structure are elaborated on in chapters 5 to 7, respectively. The operational strategy, which includes deployment, take-off and landing, the ground station amongst other topics is described in chapter 8. Chapter 9 subsequently includes an overview of the final design, as well as an evaluation of requirement compliance, the RAMS analysis and a sensitivity analysis. The development and production of the aircraft are discussed in chapter 10. Finally, the sustainable development approach is given in chapter 11 and the conclusion and recommendations are given in chapter 12.

2. Market analysis

The pseudo-satellite will be designed keeping the RNLAF in mind as primary customer. In this chapter, other potential customers who can benefit from this design also are investigated. Key strengths and differences between this project and similar projects will be discussed.

2.1. Military applications

The main stakeholder of this design project is the Royal Netherlands Air Force which require an increase in their capabilities in communication, surveillance and reconnaissance. The main intelligence gathering missions performed by airborne/spaceborne vehicles are:

- Measurement and signature intelligence (**MASINT**)
  - Infrared
  - Laser
  - Spectroscopic
  - Multispectral Imagery
- Radar **MASINT**
  - Line-of-Sight radar
  - Synthetic aperture radar (SAR)
- Signals intelligence—gathered from interception of signals **SIGINT**
  - Communications Intelligence **COMINT**
  - Electronic Intelligence: gathered from electronic signals that do not contain speech or text **ELINT**

Aside from data gathering applications airborne vehicles can perform as Battlefield Airborne Communications Nodes[1]. These nodes serve as communication relays between dissimilar data links but also aid in communication over greater distances and around obstructions which does allow, for example, to use a short range VHF radio to communicate over distances which usually would not be possible.

[1]URL: https://web.archive.org/web/20120422094233/http://www.afc2ic.af.mil/news/story.asp?id=123160766 [Retrieved on 27-7-2017]

2.2. Civilian applications

A High Altitude Pseudo Satellite (HAPS), as requested by the RNLAF, is a platform that can be utilizable in more sectors than only military. Civilian UAVs can for example can be used in [2]:

- Communication (e.g. Global 3G)
- Monitoring Weather and Climate
  - Weather Forecasting
  - Global Change Research
  - Long-Term Monitoring of Climate and Other Earth Systems
- Land Remote Sensing
  - Mapping and Planning
  - Terrestrial Monitoring and Natural Resource Management
    - ◇ Crop monitoring
    - ◇ Managing national lands
    - ◇ Environmental regulation
    - ◇ Geology and Mining
- Ocean Remote Sensing
- Public safety (e.g. Analyzing drug trafficking routes)

Currently Facebook [3] and Airbus Defence & Space [4] are attempting to enter the civilian market with HAPS platforms.

[2] URL: https://www.princeton.edu/~ota/disk1/1994/9403/940305.PDF [Retrieved on 2-5-2017]
[3] URL: https://www.facebook.com/notes/mark-zuckerberg/the-technology-behind-aquila/10153916136506634/ [Retrieved on 27-6-2017]
[4] URL: http://www.airbus.com/newsroom/news/en/2016/04/zephyr-the-high-altitude-pseudo-satellite-is-taking-off-2.html [Retrieved on 27-6-2017]

2.3. Market Sizing

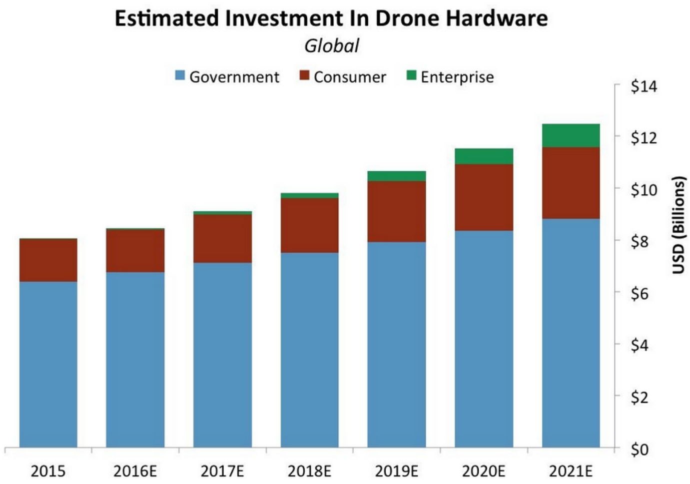

Figure 2.1: Growth of Global UAV Market 2015-2021.[5]

In the next years the militarized UAV market is expected to grow from $4 billion now, to $11.5 billion by 2023. [1] This market is segmented with large, small, armed and unarmed UAVs. In figure 2.1 the global market size of UAVs is shown to increase [5]. It is important to note that government branch does not only consist of military but also civilian sections, such as Forest Service, police and others. A large number of competition comes along with the possibilities of this new market. Currently there are a number of projects being developed which have a large number of similarities with the aircraft requested by RNLAF. Most notable is the Airbus Zephyr which is strikingly similar. The Airbus Zephyr has flown for 14 days continuously at an altitude of 65,000 ft. Currently a version is being developed which will be able to carry a 20 kg payload, called the Zephyr T [6]. This project could prove to be a major competitor for potential customers outside the RNLAF due to the large number of similarities as well as the maturity of the project. Another similar project is Facebook's Aquila which targets the communication market by creating a drone network which will be used to provide internet access to regions where there is no cabled infrastructure yet. The first test flight was done in June 2016 [7], however it ended in a crash [8]. In the field of Earth Observation, UAV's are not the only competitors. Space satellites have been used for earth observation for a long time already and may prove to become more efficient with the rise of cheaper launch vehicles. Satellites provide the advantage of a large payload at the cost of high costs and limited temporal resolution [9].

[5]URL:http://www.businessinsider.com/european-first-responders-are-learning-to-pilot-drones-2016-4?international=true&r=US&IR=T [Retrieved on 2-5-2017]
[6]URL:https://airbusdefenceandspace.com/our-portfolio/military-aircraft/uav/zephyr/ [Retrieved on 2-5-2017]
[7]URL:https://www.facebook.com/notes/mark-zuckerberg/the-technology-behind-aquila/10153916136506634/ [Retrieved on 2-5-2017]
[8]URL:https://www.ntsb.gov/_layouts/ntsb.aviation/brief.aspx?ev_id=20160701X62525&key=1 [Retrieved on 27-6-2017]
[9]URL: http://www.satimagingcorp.com/satellite-sensors/terrasar-x-radar-satellite/ [Retrieved on 27-6-2017]

3. Functional discovery

This chapter includes the functional discovery that is done at the start of every design process. First, the list of requirements is set up in section 3.1. Then the functional analysis, which shows all the functions that the system needs to fulfill, is given in section 3.2. Finally, a technical risk assessment is done in section 3.3.

3.1. Requirements

In order to make sure that the designed system is able to fulfill the mission successfully, a list of requirements is set up. Even though some of the top level requirements were already given by the customer, more requirements were discovered in the design process. Most of the new system requirements were set to include new boundaries on the design, which were not present in the initial requirement list. Examples of such requirements are the zone in which the aircraft should be operable year-round (MPS-FLT-4), the operational temperature (MPS-PLAT-6) and the payload dimension (MPS-PLD-6). Other requirements were adapted due to new insights. For example, it was concluded that the initial 300 watts that were budgeted for the payload were very limiting, and as such the power required to be delivered to the payload was increased to 400 watts (MPS-PLD-1). The complete set of top-level requirements is given in table 3.1. The abbreviation work as follows: **FLT** are flight requirements, **PLAT** are platform requirements, **PLD** are payload requirements, **COST** are cost requirements, **PRD** are production requirements and **MISC** are miscellaneous requirements.

Table 3.1: Requirements

Number	Requirement
MPS-FLT-1	The station keeping altitude shall be more than 50,000 ft.
MPS-FLT-2	The loiter time of the aircraft shall be more than one month, unrefuelled.
MPS-FLT-3	The mission radius shall be more than 800 km.
MPS-FLT-4	The aircraft should be operable year-round between $\pm$ 40° latitude.
MPS-FLT-5	The aircraft shall be able to climb to its ceiling in 9 hours, 20 minutes
MPS-PLAT-1	The aircraft shall be able to fly autonomously.
MPS-PLAT-2.1	The take-off and landing field length shall be less than 2300 m.
MPS-PLAT-2.2	The aircraft shall be able to take-off from a gravel surface.
MPS-PLAT-3	The operational lifetime shall be more than 20,000 flight hours.
MPS-PLAT-4.1	Three aircraft with support material shall fit in the cargo hold of one C-17.
MPS-PLAT-4.2	The weight budget of the total system to be transported with the C-17 shall be less than 77,000 kg.
MPS-PLAT-5	The preliminary design shall be a fixed-wing aircraft.

MPS-PLAT-6	The platform shall be operational in a temperature range of $\pm 70°$ Celsius.
MPS-PLAT-7	The clearance angle during take-off and landing shall be more than 3°.
MPS-PLD-1	The aircraft shall be able to continuously provide 400 W of power to the payload.
MPS-PLD-2	The aircraft shall be able to support a payload of 25 kg.
MPS-PLD-3	The on-board computer shall be able to store up 500 GB worth of data.
MPS-PLD-4	The payload shall include its own telecommunication system for receiving and sending data.
MPS-PLD-5	The aircraft shall be able to carry a payload which is no larger than 0.4 m in diameter and 0.5 m in length.
MPS-PLD-6	The payload shall be positioned to obtain a clear view towards the ground.
MPS-COST-1	The fly-away cost per aircraft shall be less than €10 million.
MPS-COST-2	The ground station cost shall be less than €30 million.
MPS-COST-3	The maintenance and take-off material cost shall be less than 10% of the aircraft cost.
MPS-COST-4	The annual maintenance cost shall be less than 5% of the aircraft cost.
MPS-PRD-1	75% of the total design & production cost shall be contracted to Dutch parties.
MPS-PRD-2	The system shall enter service in 2023.
MPS-PRD-3.1	The production of the complete system shall be carried out with zero effective CO_2 emissions.
MPS-PRD-3.2	No production processes shall be employed where toxins or other environmentally harmful by-products are being produced.
MPS-MISC-1	A fleet of 10 aircraft shall be able to be controlled by 2 operators.
MPS-MISC-2	The third-party probability of fatal injury shall be lower than 10^{-9} per hour.

3.2. Functional analysis

Functional flow block diagram

The functional flow block diagram in section 3.2 divides the systems functions into three levels of increasing details. A clear distinction is made in the "Perform mission objective" (4.3) function between the payload and aircraft task. The payload shall receive its own commands, perform the mission and process and send data via its own, separate communication link.

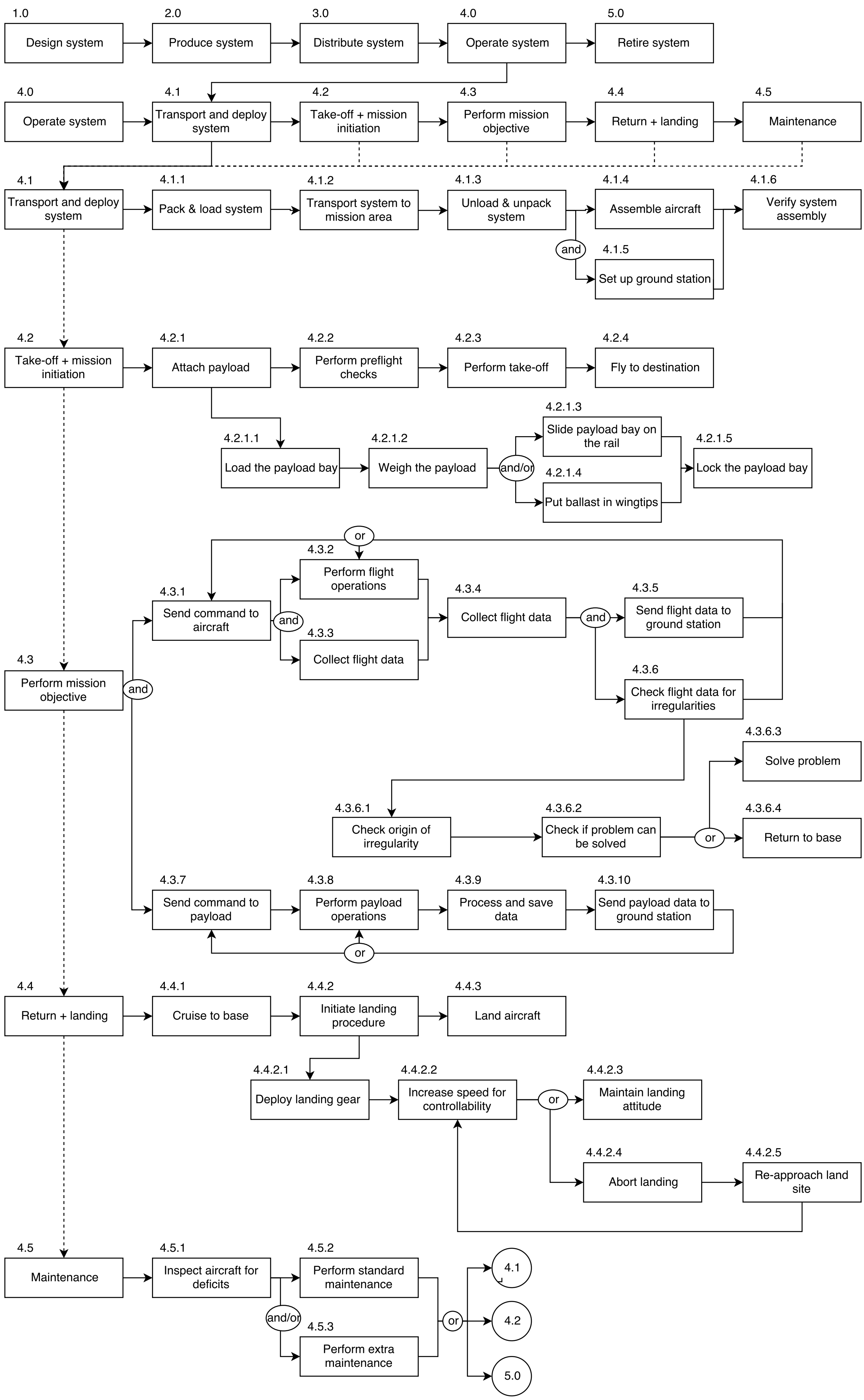

Figure 3.1: The functional flow block diagram of the HAPS system

Functional breakdown structure

The functional breakdown structure in figure 3.2 breaks the system down into different groups with the critical functions to be performed.

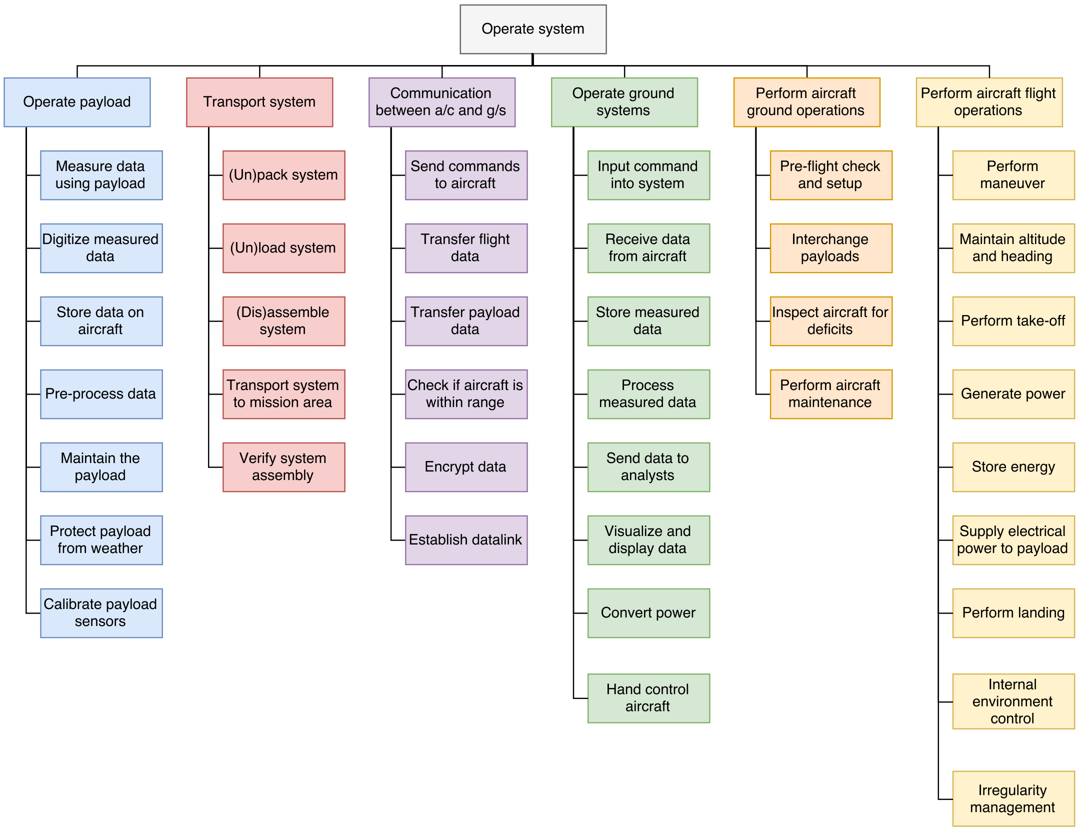

Figure 3.2: The functional breakdown structure of the HAPS system

3.3. Technical risk assessment

In order to assist the design trade-off a risk analysis is used to determine problems which could be encountered whilst designing the system. A risk map is used to identify possible problems with the designs as early as possible. The identified risks can be found below and the complete risk map can be found in table 3.2

1 Aircraft cannot fly in all defined mission areas at all times.
2 Endurance is less than 30 days.
3 The aircraft does not fit inside a C-17.
4 Communication link can not be sustained at all times.
5 The up- and down-link data rate is not sufficient.
6 The altitude requirement cannot be met.
7 Aircraft cannot be manufactured by 75% Dutch contractors.

8 The manufacturing of the design turns out to be highly impractical.

9 The total costs of the aircraft are higher by a small amount than the requirements stipulate.

10 The total costs of the aircraft are higher by a large amount than the requirements stipulate.

11 The design tools turn out to differ significantly from reality.

12 Subsystem integration deems impossible.

Table 3.2: Risk map before implementation of contingency plans.

Very Likely		1		
Likely		7,9		
Not Likely		4	2, 3, 5, 10	8, 11, 12
Almost Impossible			6	
	Negligible	Marginal	Critical	Catastrophic

Contingency plans

Contingency plans for the most important risks are formulated below.

1 Aircraft can not fly in all defined mission areas at all times: If the aircraft needs to be deployed in areas which are not within ±40° latitude, a solar powered design will likely not be able to fly for more than 30 days. The solutions are to design the aircraft for the most critical day (which is the day during which the amount of solar energy is at a minimum) and to fly missions for a shorter period of time might the mission be extended beyond ±40° latitude.

2 Endurance is less than 30 days: Margins need to be implemented in the energy storage so during nominal operation, unexpected shortages due to slight inefficient flight can be compensated.

3 The aircraft does not fit inside a C-17: Throughout the design phase the transportability and folding or disassembly mechanisms should be monitored and/or implemented. Another alternative would be to choose another means of transportation. This is, however, not favourable due to the availability of the C-17 transportation aircraft to the RNLAF.

5 The up- and down-link data rate is not sufficient. Might the up- or down-link data rate be temporarily insufficient, the data can be stored on memory and be retrieved later.

7 Aircraft design and manufacturing cost can not be contracted to 75% Dutch parties: This would not have a very big impact on the design, although in some cases going for a Dutch company may be preferable even though this has a slightly negative effect on the performance. One thing that can be done is to see if the manufacturing can be contracted through Dutch parties in case it is done in a foreign country.

8 The manufacturing of the design turns out to be highly impractical: Do thorough research on manufacturing beforehand, or postpone production for redesign.

9 The total costs of the aircraft are higher by a small amount than the requirements stipulate: Margins in the budget will prevent small changes to result in going over the budget.

10 The total costs of the aircraft are higher by a large amount than the requirements stipulate: Might this be the case, other design options have to be reconsidered to significantly lower the costs.

11 The design tools turn out to differ significantly from reality: Validate the tool immediately once it is finished. The impact of a tool not working is less severe if the flaw is found before the actual aircraft design, in comparison to after this phase.

12 Subsystem integration deems impossible: During the design, the configurator should stay updated on every subsystem. The configurator should be double checked by the other systems engineer.

The risk map is redone after implementation of these contingency plans and is found in table 3.3

Table 3.3: Risk map after implementation of contingency plans. The values that changed with respect to the original risk map are underlined.

Very Likely				
Likely	1, 7			
Not Likely	4	5, 9, 11, 12		
Almost Impossible			2, 3, 6, 10, 8	
	Negligible	Marginal	Critical	Catastrophic

4. General Design Approach

In this chapter, a general outline of the design approach will be given in section 4.1. After this, the reasoning behind some large design decisions which have been made will be explained in section 4.2. Finally, the baseline mass and power budgets which are used for the initial iterations are given in section 4.3

4.1. Design approach

Throughout the project the design was optimized to be as small (span) and as light (take-off mass) as possible. This was done since in general, smaller and lighter aircraft are more easily operated and less costly to build and maintain.

In order to create an optimal design, the project was split up into 4 phases as seen in figure 4.1. At the end of the first three phases (until "Creating class I conceptual designs") one concept was selected to be further developed into a class II design. The process until and including this selection is summarized in section 4.1.1. The approach for the class II conceptual design is described in section 4.1.2.

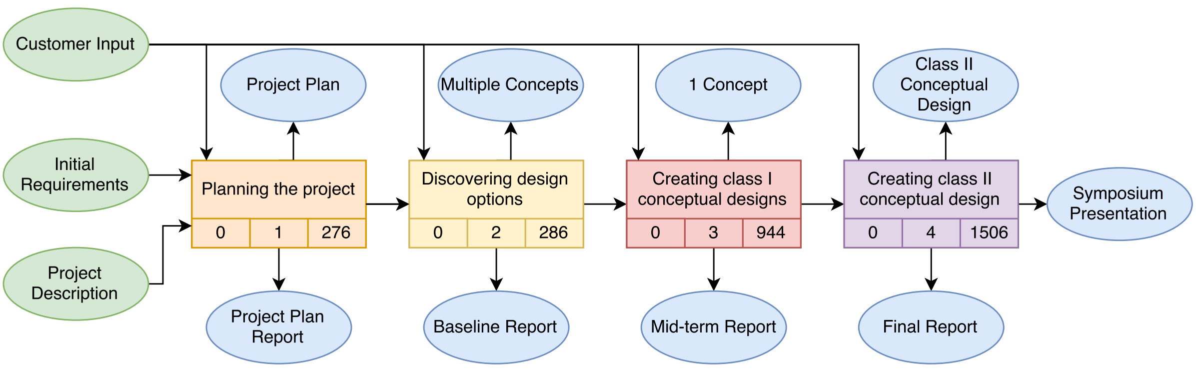

Figure 4.1: The method used to evaluate the designs

4.1.1. Concept selection

First the project planning was made. This included a schedule until the final report as well as task distributions, both technical and organizational. [2] The second phase consisted of discovering design options. After making an extensive list of concepts a trade-off was performed based on the following criteria: aerodynamic efficiency, weight of the design, development risk, propulsion efficiency, cost and sustainability. During the trade-off a separation was made between planform and the power system.

The planform concepts that were further analyzed were flying wing and conventional planform. The flying wing was chosen because of high theoretical aerodynamic efficiency, the conventional planform was chosen because of good stability and controllability. For the propulsive system three concepts were chosen: Fully fuel, hybrid and fully electric. Electric has a theoretical infinite mission duration, but is limited in the locations where it could be used. Fuel has the exact opposite, as it has limited mission duration but can fly anywhere as it is not dependent on the sun. A hybrid concept was the third to be analyzed. This would give the most flexibility, as it is able to fly its mission successfully while also being able to fly multiple days above 40° latitude. For the trade-off, the optimal fuel-to-solar energy ratio was found using weight as the deciding parameter, and this was then taken into the trade-off. [3]

The previous named concepts were further developed into class I conceptual designs. These designs were then evaluated in a trade-off. For the planform trade-off the following criteria were used: mass performance, size performance, aerodynamic performance (endurance parameter), design risk, total cost and ease of operation. For the power system trade-off the following criteria were used: mass performance, size performance, readiness of technology, performance risk, total cost, ease of operation and sustainability. During the trade-offs the mass, size and aerodynamic performance were considered most important. This was to ensure the aircraft would be effective and easy to operate. The trade-off table for the planform can be found in table 4.1, the table for the power system can be found in table 4.2. The fully electric flying wing was chosen as the final design as it was deemed to be the easiest in operations while remaining aerodynamically most efficient. Fully electric also allowed it to have the longest mission duration.

Table 4.1: Planform trade-off

	Mass Performance 15%	**Size Performance 18%**	**Aerodynamic Performance 28%**	**Total Costs 15%**	**Ease of Operation 13%**	**Design risk 11%**
Flying Wing	482 kg +	46 m +	40 +	2.75 M ++	Good +	Poor -
Wing + Tail	679 kg ±	64 m ±	42 +	3.08 M +	Poor -	Moderate ±

Table 4.2: Power system trade-off

	Mass Performance 21%	**Size Performance 16%**	**Readiness of Technology 15%**	**Performance Risk 15 %**	**Total Costs 13%**	**Ease of Operation 11%**	**Sustainability 9%**
Electric	482 kg ±	46 m ±	Moderate ±	Moderate ±	2.75 M ±	Good +	Good +
Hybrid	488 kg ±	42 m +	Poor -	Moderate ±	2.43 M +	Moderate ±	Moderate ±
Fuel	1805 kg −	51 m -	Very good ++	Moderate ±	2.25 M ++	Poor -	Very Poor −

4.1.2. Concept detailing

After selecting one concept, the electric flying-wing concept, the more detailed conceptual design was started. For this concept detailing, three main sub system design groups were identified:

- Structural design group (4 people)
- Power and propulsion design group (3 people)
- Wing design, including aerodynamics, stability & control (3 people)

Then, the design decisions for the final design were identified. Based on that the concept detailing was split up into 3 phases:

1. Identify and estimate group-specific design parameters. These parameters could be decided on design group level. Some examples of these are, the materials, sensor package, airfoil or propeller design.

2. Decide on the design parameters which affect more than one design group in a significant manner. This was done by creating a baseline design, changing different design parameters and evaluating the change in mass and size performance in an iterative process. During this process the designs were optimized such that requirements MPS-FLT-1, MPS-FLT-2 and MPS-FLT-4 were just met. The variables which were evaluated in this manner were:

    - Aspect ratio (section 4.2.1)
    - Sweep angle (section 4.2.2)
    - Thickness over chord ratio (section 4.2.3)

    The method used to evaluate the designs can be seen in figure 4.2.

3. Further evaluation, design and component selection of design group specific systems and parameters that require the overall layout and weight of the aircraft to be known.

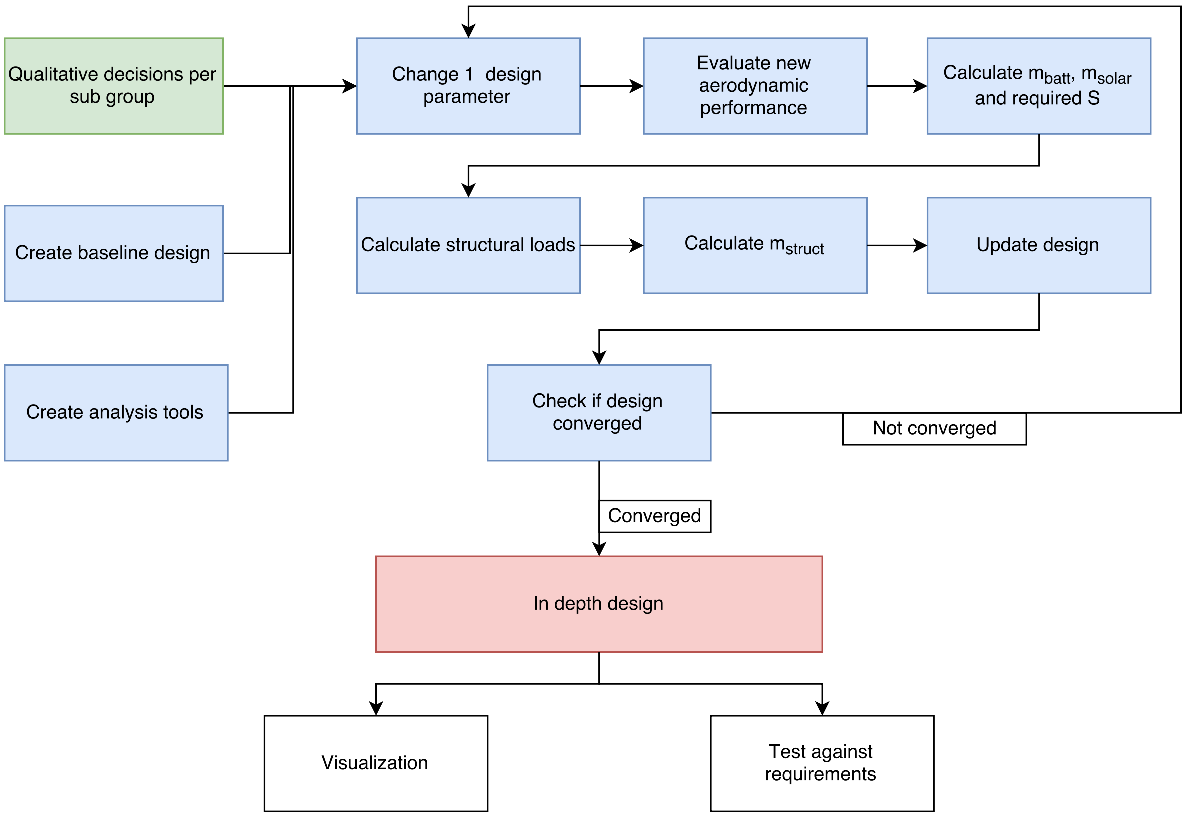

Figure 4.2: The method used to evaluate the designs

4.2. General results

As stated in section 4.1.2, three main design parameters were evaluated by creating a single parameter from a baseline design. The baseline design can be seen in table 4.3. $M_{o}ther$ contains smaller systems such as avionics and thermal protection. Some of these are related to the take-off weight, so this mass changes for different design. In section 4.2.1, section 4.2.2 and section 4.2.3, the effects of aspect ratio, sweep angle and thickness to chord ratio can be seen respectively.

Table 4.3: Summarized baseline design

Parameter	**Value**	**Parameter**	**Value**
S $[m^2]$	100	M_{to} $[kg]$	405
AR [-]	25	$M_{payload}$ $[kg]$	25
b $[m]$	50	M_{oew} $[kg]$	380
Λ_{LE} [°]	15	$M_{structure}$ $[kg]$	128
t/c [%]	18	$M_{powertrain}$ $[kg]$	225
Taper ratio [-]	0.6	M_{other} $[kg]$	27
Root chord $[m]$	2.5	$C_L^{\frac{3}{2}}/C_D$ [-]	43
W/S $[N/m^2]$	40		

4.2.1. The effect of aspect ratio

Generally, a bigger aspect ratio results in a heavier structure but better aerodynamic efficiency. Analysis was done to find the optimum aspect ratio. The results of this analysis can be found in section 4.2.1 and table 4.4. It was found that the baseline aspect ratio of 25 was the most optimal choice.

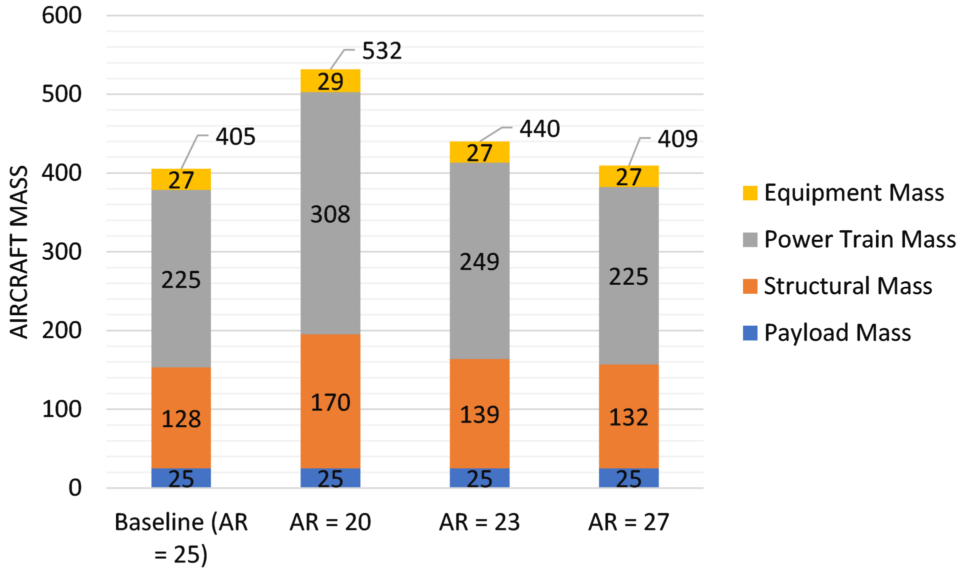

Figure 4.3: Weight comparison of designs with different aspect ratio's. Baseline at an Aspect Ratio of 25.

Table 4.4: Results from the analysis done on the aspect ratio. Baseline at an Aspect Ratio of 25.

	AR = 25	AR = 20	AR = 23	AR = 27
$C_L^{\frac{3}{2}}/C_D$ [-]	43	34	38	43
Take-off Mass [kg]	405	532	440	409
Span [m]	50	54	51	52
% Mass increase	0%	31%	9%	1%
% Span increase	0%	8%	2%	4%

4.2.2. The effect of sweep

Increasing the sweep of a flying wing can increase it's aerodynamic efficiency due to the fact that it is easier to make a swept wing stable. This results in a decrease in power train mass. However; from a structures perspective, sweep has a negative influence. Analysis was done to find an optimum which would results in the smallest and lightest design. The results of this analysis can be found in figure 4.4 and table 4.5. As can be seen, the baseline design here has a different weight and span. This is due to the fact that some efficiency estimations had changed. The concepts with the different sweep angles were all evaluated using the same efficiencies as this baseline to make for a fair comparison. It was found that a sweep angle of 20 degrees was the optimum due to it having the shortest leading edge length, making it the best for transportation.

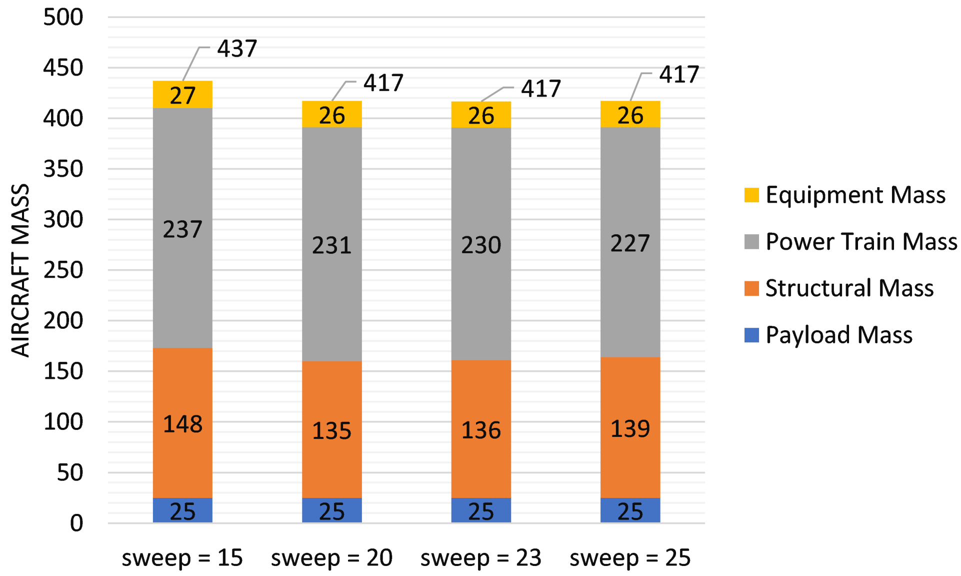

Figure 4.4: Weight comparison of designs with different sweep angles. Baseline at 15° sweep.

Table 4.5: Results from the analysis done on sweep angles. Baseline at 15° sweep.

	$\Lambda_{LE} = 15°$	$\Lambda_{LE} = 20°$	$\Lambda_{LE} = 23°$	$\Lambda_{LE} = 25°$
$C_L^{\frac{3}{2}}/C_D$ [-]	39.3	42.1	42.7	42.9
Take-off Mass [kg]	437	417	417	417
Span [m]	53.6	50.7	50.2	50.0
Length Leading edge [m]	55.	54.0	54.6	55.2
% Mass increase	0%	-5%	-5%	-5%
% Leading edge increase	0%	-3%	-2%	-1%

4.2.3. The effect of thickness to chord ratio

The results from the analysis on the thickness to chord ratio are stated in section 4.2.3 and table 4.6. It was found that a thickness of 18% was the most optimal. Due to the low flight velocity, thicker airfoils not only increased the structural efficiency but also the aerodynamic efficiency.

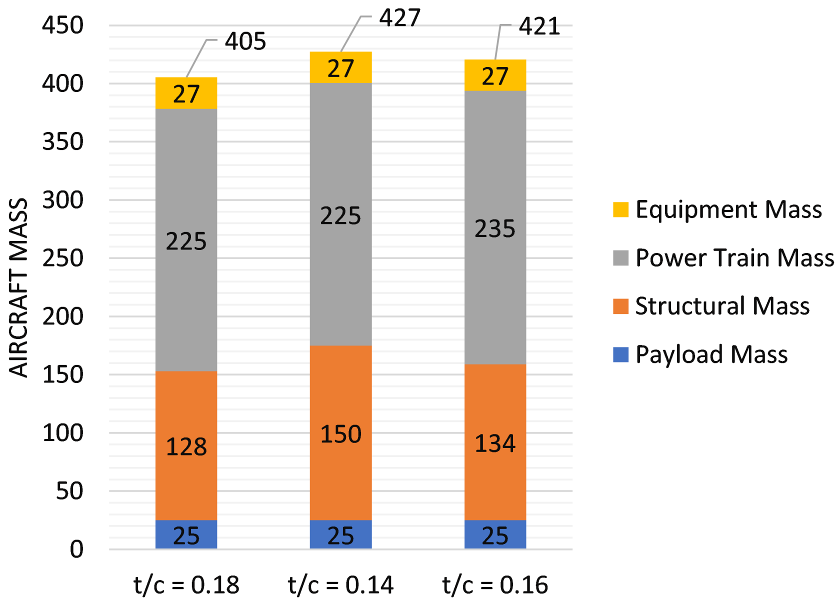

Figure 4.5: Weight comparison of designs with different thickness to chord. Baseline at thickness/chord of 18%.

Table 4.6: Comparison of designs with different thickness/chord ratios. Baseline at thickness/chord of 18%.

	t/c = 0.18	t/c = 0.14	t/c = 0.16
$C_L^{\frac{3}{2}}/C_D$ [-]	43	42	41.7
Take-off Mass [kg]	405.4	424	421
Span [m]	50	50.5	50.5
Mass increase [%]	0%	5%	4%
Span increase [%]	0%	1%	1%

4.3. Mass & Power budgets

To get a good starting point for the design iterations a mass and power budget is made for four different systems, where 'other' includes avionics, landing gear, servos etc. These budgets are estimated from the baseline design and serve as a starting point for the design. They are shown in table 4.7.

Table 4.7: Initial mass and power budgets

Subsystem	**Mass budget** [kg]	**Power budget** [W]
Power & Propulsion	225	4150
Structure	128	0
Payload	25	400
Other	27	300
Total	405	4850

5. Wing geometry, stability & control

This chapter concerns the design of the outer mold line and control systems of the aircraft. In section 5.1, a closer look will be taken at the decisions made with respect to the wing geometry and the airfoil. Even though the aircraft has been continually designed keeping longitudinal stability in mind, a closer look at stability and control is taken in section 5.2. Here, the design will be evaluated not only for static longitudinal stability but also for dynamic, lateral and directional stability and control. The necessary adjustments are made to make sure the aircraft has sufficiently good handling qualities. In section 5.3, the used methods and software will be verified and validated.

5.1. Wing geometry

In this subsection, the geometry of the wing will be presented. The goal of the wing geometry is to maximize the aircraft endurance, while keeping weight as low as possible. The most influential value is the endurance parameter $C_L^{\frac{3}{2}}/C_D$, which should be as high as possible. Therefore, almost all the geometrical decisions made in the wing design are made with a high $C_L^{\frac{3}{2}}/C_D$ in mind.

Wing area and span After an iterative process also involving the structural and power & propulsion group a final planform was found. This planform has a surface of 83 m^2 and a span of 43.6 m. The aspect ratio is 25, which is very high but not unusually for long-endurance aircraft. All of this resulted in a $C_L^{\frac{3}{2}}/C_D$ of 45.

Sweep Usually, sweep can be found on aircraft that fly close to the critical Mach number of the airfoil that is used. The reason for using sweep in this aircraft is irrelevant of velocity, but contributes towards longitudinal stability. A sweep angle of 20° has been chosen. Higher values resulted in a slightly heavier structure, whereas lower values resulted in a decrease in $C_L^{\frac{3}{2}}/C_D$.

Taper ratio By tapering the wing, one can obtain a lift distribution which is closer to an elliptical lift distribution. This decreases the lift induced drag. Yet taper has disadvantages as well. It affects the strength needed for the structure to cope with the loads, and it can result in a large loss off lift in case of tip stall, when the maximum spanwise C_L is near the tip. A taper ratio of 0.6 has been chosen. [4].

Dihedral It is chosen not to use dihedral. It does increase roll stability, but also decreases directional stability. Also, the effective lift will be lower and structurally the aircraft would become heavier if dihedral is introduced. More about the roll dynamics can found in section 5.2.2.

Twist Wing twist can be combined with sweep to stabilize the aircraft. The value for the twist is usually between $0°$ and $-5°$. [5] After analysis, the twist angle needed was determined to be $-1.8°$.

Wing tips The wingtips on the aircraft increase the yaw stability. Adding wingtips of 0.7 m high increases the stabilizing yaw moment by factor 2.5. Besides increasing the stability, these wingtips also will reduce the induced drag slightly due to the reduction of wing tip vertices.

Airfoil Airfoils should generate enough lift, but for a flying wing the airfoil should also have stabilizing effects. This is where reflex airfoils come into play. After performing thorough analysis, two airfoils have been chosen. At the root, the $SM701$ (figure 5.1a) airfoil is used. The $MH81$ (figure 5.1b) airfoil is used at the tip. The first one is a cambered airfoil generating a fair amount of lift and the latter one has a reflex shape which provides stability. The wing is segmented in 3 spanwise sections, the outer 25% of one winghalf is $MH81$, the other 75% of the wing is a gradual transition from $SM701$ to $MH81$. For structural reasons, both airfoils will have a $\frac{t}{c}$ of 18%.

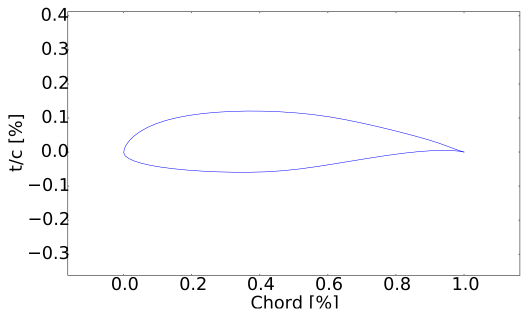

(a) SM701 (root airfoil)

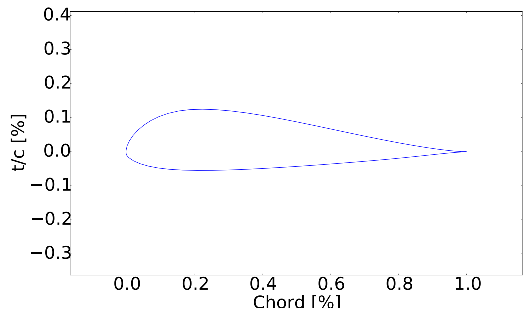

(b) MH81 (tip airfoil)

Figure 5.1: Airfoils

5.1.1. Aerodynamic characteristics

In order to design for long endurance, one wants to design for a high $C_L^{\frac{3}{2}}/C_D$. After analyzing several different planforms, a final design was chosen. figure 5.2 shows the aerodynamic performance of the aircraft, the design point can be seen as well.

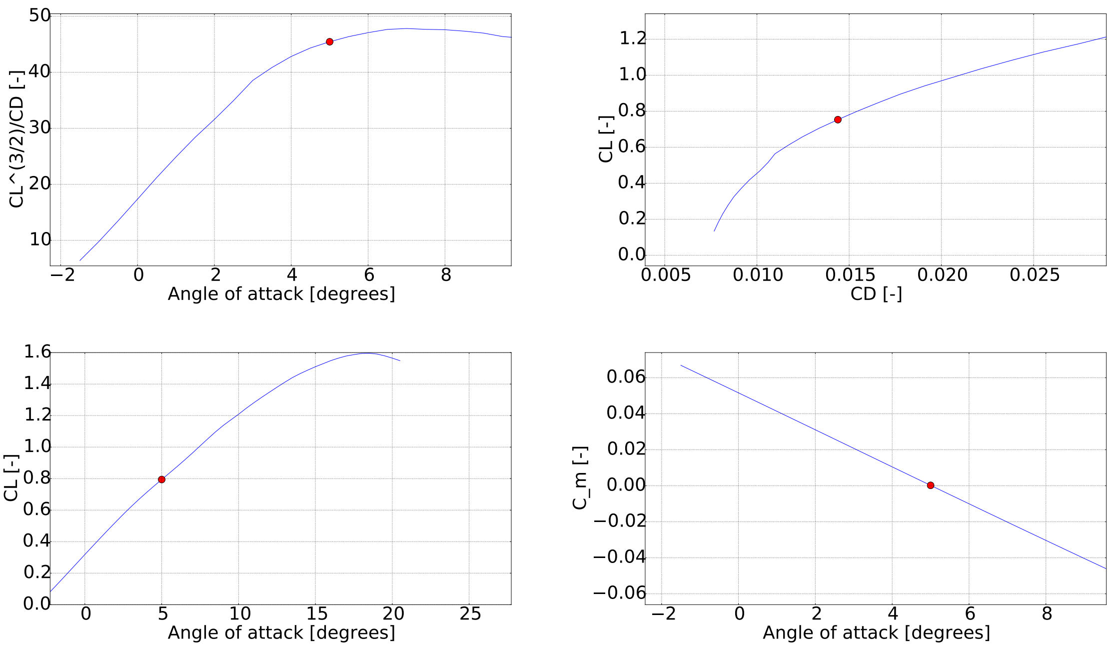

Figure 5.2: Aerodynamic characteristics of the aircraft. The red dots indicate the design cruise condition.

5.1.2. Stall characteristics

A flying wing usually has poor stall characteristics because of the sweep (which decreases the airspeed over the airfoil), taper (decreasing the Reynolds number over the outer wing section) and high aspect ratio. These last two factors lead to the tendency for the wing tips to stall first, leading to dangerous conditions such as pitch-up which causes the aircraft to slow down even more. Also, the thick airfoil (t/c = 18%) that is chosen in the wing design has a tendency to stall from the back to the front. Combined with the tip stalling first, this leads to a stall of the control surfaces which makes the aircraft uncontrollable. To counteract these bad characteristics, two measures are taken. First of all, the wing is twisted downwards by 1.8°. This counteracts the tendency to stall from the trailing edge, instead stalling the wing from the leading edge which is much more controllable. Also, this decreases the local angle of attack at the wing tips, causing the root of the wing to stall first. Secondly during normal operations there is always a margin on the angle of attack of 5°. This is done to ensure that even in case of gusts or other environmental conditions the aircraft will not come close to stall conditions. These conditions are given for different altitudes in table 5.1.

Table 5.1: Stall characteristics

Altitude $[m]$	**Stall** α [°]	$\mathbf{C_{L_{max}}}$ [-]	**Stall velocity** $[m/s]$
0.0 (Sea level)	12.5	1.4	6
10,000	12.5	1.4	8
18,000 (Low cruise)	12.5	1.4	13
23,000 (Ceiling)	12.5	1.4	19

5.2. Stability & control

In this section, the characteristics for the longitudinal, lateral and dynamic stability are presented, together with the way the aircraft is controlled.

5.2.1. Static stability

To determine the center of gravity location of the entire aircraft the subsystem weight and location is used which are found in table 5.2. The aircraft x_{cg} is consequently found using $x_{cg} = \frac{\sum x_{cg_i} \cdot W_i}{\sum W_i}$.

Table 5.2: Weight budget and their center of gravity location

Component	Weight $[kg]$	% of M_{TO}	as % of MAC
Payload	25	8.1	-174
Voltage converter*	1	0.41	-150
Avionics	2	0.61	-150
Thermal system*	4	1.4	16
FCS	2	0.62	284
Wing tips	3	0.91	280
Aircraft structure	**139**	**45**	**15**
Rod	58	19	-2
Ribs	21	6.5	42
Skin	23	7.5	42
Nose landing gear	4	1.3	-123
Aft landing gear	8	2.7	100
Mounts	15	4.8	54
Joints	10	3.3	-75
Power train	**131**	**43**	**40**
Solar cells	13	4.4	42
MPPT's	6	2.0	42
Batteries 1&2	30	9.8	-27
Batteries 3&4	30	9.8	55
Batteries 5&6	30	9.8	138
Battery manager	2	0.49	32
6 Propellers	11	3.7	-49
Engines 1&2	0.68	0.22	-119
Engines 3&4	0.68	0.22	-34
Engines 5&6	0.68	0.22	36
Wiring	7	2.3	11
Total mass / x_{cg}	$\approx$ 307	100	12.9

Static longitudinal stability

In order to ensure longitudinal stability, one has to make sure the centre of gravity of the aircraft is positioned in front of the neutral point of the aircraft, which is the same point as the aerodynamic centre for a flying wing. This can be tweaked using the wing sweep and the wing twist, but also by moving certain masses more aft or forward. For this the center engine pod is used as this pod imposes small contributions to the center of gravity For this aircraft, a minimum stability margin of 5% has been used. The centre of gravity is positioned at 12.9%MAC and the neutral point at 26.4 %MAC This means the aircraft is statically longitudinally stable.

Static lateral and directional stability

The aircraft should be laterally stable as well. To ensure this, one has to investigate the values for C_{n_β} and C_{l_β}. They should be larger and smaller than 0, respectively. These two values are mainly affected by sweep, dihedral and wingtips. The values, as found by XFLR5, are: C_{n_β} = 0.00621 and C_{l_β} = -0.0705. This means that the aircraft has lateral and directional static stability. Section 5.2.2 shows how these values result in the corresponding eigenmotion, the Dutch Roll.

Six engine pods under the wing and the payload stick out of the front of the aircraft, will have an effect on C_{n_β}. This effect is found by calculating the yawing moments caused by the drag due to the sideways velocity component. The drag coefficients are estimated using the length over diameter ratio [1]. At $\beta = 10°$ the pods cause a stabilizing moment of about $N_{pods} = 1.63$ Nm during landing, resulting in $C_{n_{\beta_{pods}}} = 4.10 \cdot 10^{-5}$. Assuming the payload pod to be completely out of the wing, which is a more extreme case than in the design, a destabilizing moment of $N_{payload} = -1.0$ Nm is induced at landing conditions, resulting in $C_{n_{\beta_{payload}}} = 2.53 \cdot 10^{-5}$. In total, these effects will have a slightly stabilizing effect. Due to its small magnitude it will be neglected in further analysis.

5.2.2. Dynamic stability

A dynamic stability analysis is performed using XFLR-5. Several stability derivatives can be found in table 5.3.

Table 5.3: Stability derivatives

Longitudinal derivatives	**Value**	**Lateral derivatives**	**Value**
C_{X_u}	-0.0275	C_{Y_b}	-0.0190
C_{X_α}	0.637	C_{Y_p}	0.138
C_{Z_u}	-0.00156	C_{Y_r}	-0.00775
C_{L_α}	5.42	C_{l_b}	-0.0705
C_{L_q}	5.25	C_{l_p}	-0.714
C_{m_u}	0.000315	C_{l_r}	0.169
C_{m_α}	-0.592	C_{n_b}	0.00621
C_{m_q}	-14.5	C_{n_p}	-0.0938
		C_{n_p}	-0.0938
		C_{n_r}	0.00160

Table 5.4: Estimation of the moments of inertia of the aircraft.

Inertia	**Value** $[kg/m^2]$
I_{xx}	3,500
I_{yy}	1,100
I_{zz}	3,600
I_{xz}	-4.8

[1] URL:https://www.slideshare.net/garapatiavinash/9-drag-and-lift, [Retrieved on 19-06-2017]

The period P, damping ratio ζ, and time to half or double amplitude as well as the stability can be found in table table 5.5 for five eigenmotions: Short period, phugoid. aperiodic roll, Dutch roll and spiral.

Table 5.5: Characteristic values of the different eigenmotions

Eigenmotion	**P** $[s]$	ζ [-]	$T_{1/2}$ $[s]$	T_2 $[s]$	**Stablility**
Short period	3.4	0.84	0.24	-	Stable
Phugoid	22	0.052	46	-	Stable
Aperiodic roll	-	-	0.24	-	Stable
Dutch roll	18	0.13	15	-	Stable
Spiral	-	-	-	30	Unstable

These values have been checked using the military specification MIL-F-8785C.[6] Aircraft can be categorized into 3 levels using these values, 1 being the best. Categorizing the aircraft results in the following levels for different eigenmotions shown in table 5.6.

Table 5.6: Level classification of eigenmotions

Eigenmotion	**Level**
Short period	1
Phugoid	1
Dutch roll	3
Spiral	1

Only the Dutch roll scores a level 3. As the definition of a level 3 aircraft sounds: "Flying qualities such that the airplane can be controlled safely, but pilot workload is excessive or mission effectiveness is inadequate, or both.", it is deemed sufficient as an autopilot is used, relieving a pilot of excessive workload. The Dutch roll is stable and can be controlled by the autopilot, in the detailed design a PID and yaw damping system should be integrated. Besides, the damping ratio of the Dutch roll is good enough to be level 1, however, due to the low frequency of the motion it ends up being level 3.

Categorizing the dynamic stability in an integrated Birhle-Weissman chart found in figure 5.3, the aircraft scores a category A.[7] An explanation is also given in the figure.

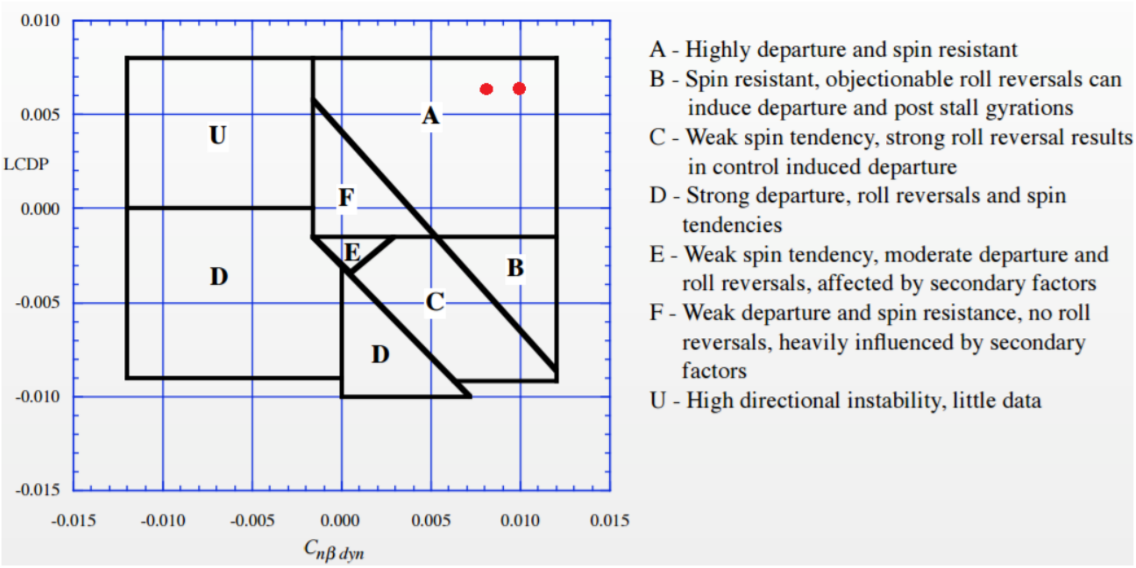

Figure 5.3: The left red dot represents the aircraft during landing and the right dot represents cruise (this is α dependent) in the Birhle-Weissman chart.[7]

Departure resistance is the aircraft ability to resist entering potentially dangerous, uncontrollable or less-controlled maneuvers.

5.2.3. Controllability

This section includes the selection of the control types supported by calculations regarding forces and moment to determine the needed size of the chosen control surfaces.

Control type selection

One of the problems in the design of a flying wing is providing adequate longitudinal control due to the smaller moment arms compared to conventional aircraft. When control surfaces are place towards the wing tips, for high aspect ratio swept back wings, the elevator and ailerons can be combined into a single surface, an "elevon". It is chosen to use elevons for longitudinal and lateral control to reduce complexity. The elevons are a proven concept also used in several Northrop Grumman flying wings, the XB-35, YB-49[2] and B2 spirit bomber.[8]

For directional control it is chosen to use split drag rudders. Also a proven design in the flying wings stated above they prove to be a better option than differential thrust as this induces several unwanted moments. In addition to this, the Facebook Aquila crashed during landing due to structural failure. The maximum loads were exceeded by a combination of a gust and a too high velocity[3]. The current braking capabilities of the aircraft deemed to be insufficient to successfully land, which could probably be prevented by the use of split drag rudders.

[2]URL: http://www.century-of-flight.net/Aviation%20history/flying%20wings/Northrop%20bombers.htm[Retrieved on 06-06-2017]
[3]URL: https://www.ntsb.gov/_layouts/ntsb.aviation/brief.aspx?ev_id=20160701X62525&key=1 [Retrieved on 06-06-2017

Control surface sizing

All of the control surfaces are designed for the landing conditions, as this is the flight phase where most control is required. For each control direction the control parameters are shown in table 5.7 Firstly, the drag rudders are sized by finding the drag of a thin plate in the airfoil. The width of this thin plate is equal to the width of the drag rudder while the height is taken to be the maximum distance to the upper and lower surface, deployed at 25°. The depth of the drag rudder is 0.2c and the width is 0.45 m, equal to the distance between two ribs. The drag rudder is assumed to be placed at the very tip of the wing in order to increase the induced moment while reducing extra drag. This results in a drag rudder capable of producing a moment of 226 Nm, allowing the aircraft to fly at a sideslip angle of 15°. The drag rudder was sized such that, when deployed, the aircraft will sideslip at this angle and will not yaw out of control, which would be the case if the drag rudders are too large. The yaw acceleration induced by the drag rudders at $\beta = 0°$ is 0.4 $°/s^2$. The elevons are sized for roll by finding the rolling moment on the aircraft due to the difference on lift on the wings. A difference in lift coefficient of $dC_l = 2.0$ was found between the downward and upward deployed airfoil at 25° with a hinge at $0.2c$. By dividing the wing into sections the total moment is found. When placing the elevators between the drag rudder and the outermost engine a rolling moment $L = 42$ kNm is found with a elevon width of 52% of each wing half, resulting in a roll acceleration of 69 $°/s^2$. As rolling motion is greatly resisted by the large wing, the maximum rolling speed due to the ailerons is at 6.0°/s. This allows the aircraft to make a roll of 30° in less than 6s, which is a guideline set by regulations for large transport aircraft during landing and thus will be sufficient for the current design. [6]

These elevons are used for pitch control as well. Pitch control is mainly used during landing when the angle of attack is reduced to $\alpha = 2°$ in order to increase landing velocity. This will allow the aircraft to land with stronger winds and makes the aircraft more controllable during landing. When evaluating the elevons, a pitch rate of 6.5°/s is found.

Both the elevon and the drag rudder will have a rather simple actuation mechanism. The elevon will be actuated using one servo with a maximum torque of at least 8.1 Nm at the leading edge of the control surface. The drag rudder will make use of two smaller servos (at least 0.03 Nm) at the leading edge, one for the upper surface and one for the lower surface. This mechanism was chosen because of its low number of moving parts, reducing aircraft complexity and increasing reliability.

The control surfaces can be seen in figure 5.4 in the neutral position. Figure 5.5 shows the deployed drag rudder and the elevon in downward position.

Table 5.7: Parameters for the control of the aircraft. The values are for landing conditions. It should be noted that these roll and pitch parameters cannot be obtained at the same time.

	Moment [kNm]	**Acceleration** [$°/s^2$]	**Maximum rate** [$°/s$]	**Deflection** [°]
Pitch	3.0	275	6.5	25
Roll	42	69	6.0	25
Yaw	0.23	0.4	14.4	25

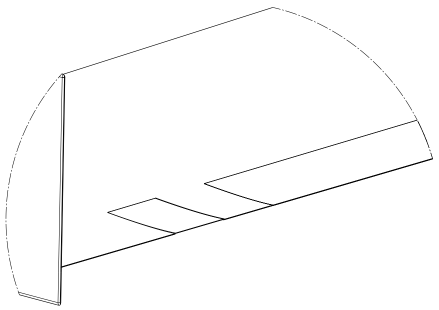

Figure 5.4: Control surfaces in the neutral position.

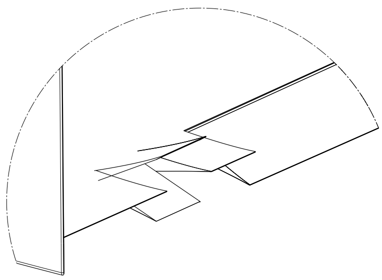

Figure 5.5: Control surfaces in the maximum deployed position. In this figure the elevon is deployed downwards.

5.3. Verification and Validation

First, verification of the 2D analysis have been performed. The verification has been performed by analyzing a thin plate in XFLR5 and by analyzing a symmetric airfoil. At 0 degrees angle of attack, the flat plate should not generate lift, which it does not. Furthermore, the C_p distribution (chordwise) should be nearly constant, which it is. Also, the lift curve for the symmetric airfoil should be approximately 2π, which is true for lower angles of attack.

For the validation of the 2D part, the $NACA63-018$ has been analyzed and compared to experimental data. This comparison can be seen in figure 5.6.

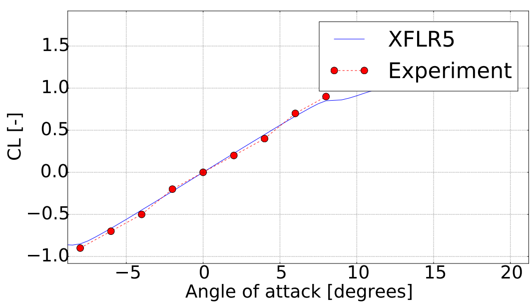

Figure 5.6: Comparison between 2D analysis in XFLR5 and experimental data

The initial wing design has been verified by looking at the values which are calculated by AVL[4] for C_L and C_D. As the C_L is somewhat higher in AVL than in XFLR5, the C_D is also somewhat higher due to lift induced drag. Therefore, the values for C_L/C_D and for $C_L^{\frac{3}{2}}/C_D$ have been compared. This can be seen in figures 5.7 and 5.8.

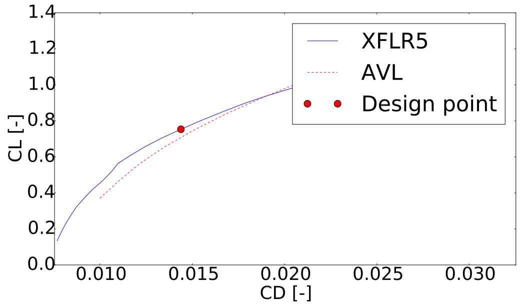

Figure 5.7

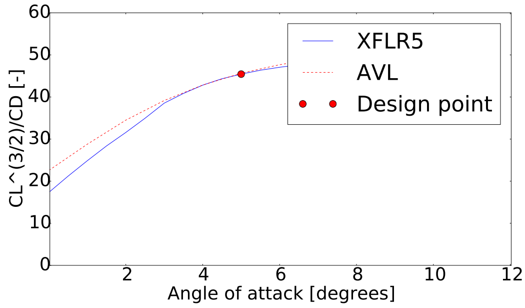

Figure 5.8

As for the validation of this part. For now, the tool has been analyzed by comparing experimental results for a flat plate to the results for a flat plate in XFLR5.[9] The results can be seen in figure 5.9 and figure 5.10. From this validation, it can be concluded that the C_D is underestimated by a average value of 0.004 in XFLR5 compared to reality (see table 5.8). For slightly higher values for C_L, this error decreases and as such the tool is more accurate.

Now this experiment has been performed with a flat plate with an aspect ratio of 3, so it is hard to say how the results for the flying wing with aspect ratio 25 would compare to reality, as there is no experimental data on this type of aircraft. It is known that XFLR5 is usually more accurate with higher aspect ratio wings, but a more accurate evaluation of the aircraft aerodynamics in further design steps is recommended.

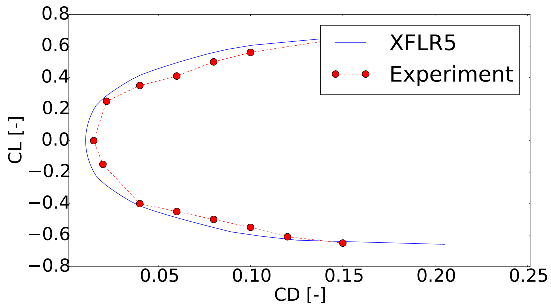

Figure 5.9: AR=3, taper=0

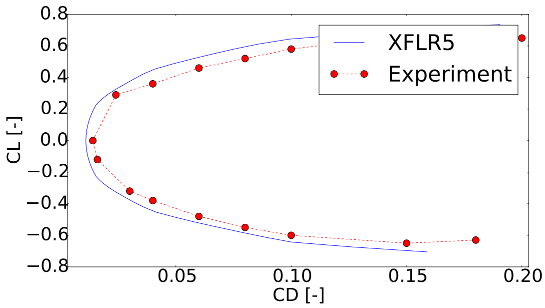

Figure 5.10: AR=4, taper=0.75

[4]URL: http://web.mit.edu/drela/Public/web/avl/

Table 5.8: Comparison between experimental data and XFLR5

		Experiment		**XFLR5**	
		C_L	C_D	C_L	C_D
AR = 3, taper = 0	α = 0	0	0.015	0	0.011
	α = 4	0.25	0.022	0.23	0.017
	α = -2	-0.12	0.016	-0.11	0.012
AR = 4, taper = 0.75	α = 0	0	0.014	0	0.011
	α = 4	0.29	0.024	0.26	0.017
	α = -2	-0.12	0.016	-0.13	0.012

6. Power & propulsion system

This section discusses the design process and decisions for the power and propulsion systems. First the power system design is elaborated on in section 6.1. Then the propulsion system is designed in two parts: Engine design (section 6.2) and Propeller design (section 6.3). The final design step of this chapter is the design of the thermal protection system, which is done in section 6.4. Finally, the tools used in the design process are verified and validated in section 6.5.

6.1. Power system design

Big choices had to be made to define the power system which consists out of energy generation and energy storage. Two system types were considered: A purely solar powered system and a hybrid system, which would fly on solar energy during daytime and on fuel during nighttime. This would also allow the aircraft to fly at even higher latitudes than required, although the mission duration would be limited. However, the hybrid system has some disadvantages:

- Need for refuelling after each flight cycle
- Fuel system is very heavy w.r.t. solar-powered system
- Increased cooling of engines
- Hybrid system needs a fuel-based and electrical system and will therefore become very complex and less reliable
- Heat signature of fossil fuels would disturb the infra-red camera
- High carbon-footprint for combustion engines
- Fuel cells are too big for long endurance missions

After careful consideration, a purely solar energy driven platform was decided on. This was mainly due to excessive weight and size penalties when choosing a hybrid design. Big superchargers, fuel tanks and heating systems had to be designed. The mid-term report of this project is good reference point to find more information on this trade-off.[10] The main downside of the solar-powered system is that the wing is sized by the required solar panel area. This is because in the worst case scenario, which is during winter at 40° latitude, the aircraft will see only 9 hours and 20 minutes of sunlight. To keep the required area as small as possible, different types of solar panel materials were considered. The advantages and disadvantages of these panels are found in table 6.1.

Table 6.1: Advantages and disadvantages of different solar panel types [11] [12]

Type of solar panel	Pro	Con
a-Si	-Cheap	-Not designed for high altitude -Inefficient -Heavy -Lead (Pb)
x-Si	-Good efficiency	-Not designed for high altitude -SiH4: pyrophoric -Bad end-of-life solution -Heavy -Toxic doping gas: POCl3, B2H3
GaAs	-Tertiary-butylgas (makes handling safer) -Very efficient -Lightweight -Foil material	-Toxic hybrid gas: Arsine and Phosphine -Expensive

Since both silicon-type solar panels are not designed for aerospace applications and are heavy, the Gallium-Arsenide panels were chosen, as these would also drastically decrease the area required due to their higher efficiency. This material is a foil, which is lightweight and can easily be morphed to fit on the wing surface. Even though this material is the least environmentally friendly, the high efficiency helps to keep the wing area as small as possible. As every solar panel uses at least one kind of toxic material, so requirement MPS-PRD-3.2 can not be met and is identified as a killer-requirement. The properties of the solar foil can be found in table 6.2.

The next design step is designing the energy storage system. Energy will be stored in two ways: By storing electrical energy in batteries and by storing potential energy. This means that during daytime, the aircraft will use excess power to charge the batteries and after that the excess power is used to climb to an altitude of 23 km. During nighttime the aircraft will gradually glide to its mission altitude, thus not using any power to propel itself. When it reaches its desired altitude, the engines will be started again using energy from the batteries. This is further elaborated in section 6.1.1. Sion power Licerion batteries are chosen based on their recharging capabilities and high efficiency.[13] To prolong the lifetime of the batteries, they will only be discharged to 90% in normal operations. Still, they have to be replaced 3 times during the design lifetime of the aircraft to maintain a sufficient efficiency level. The properties of the Sion power batteries can be found in table 6.3.

Table 6.2: Alta solar film parameters [11]

Parameter	Value
Cell voltage $[V]$	1.1
Area density $[kg/m^2]$	0.17
Theoretical efficiency (2023) [%]	34.0
Design efficiency (2017) [%]	31.6

Table 6.3: Sion Power Licerion© Batteries. [13]

Parameter	Value
Design specific Energy $[MJ/kg]$	1.17
Density $[kg/m^3]$	2000
Pack Efficiency [%]	97.5
Maximum D.O.D [%]	100

6.1.1. P&P system sizing

To size the power and propulsion system, two flight phases are considered: Initial climb and cruise flight. During the initial climb, the aircraft will take-off and climb to its ceiling of 23 km in at most 9 hours and 20 minutes. It will only use power from the solar panels, but it will not have to store any power in this phase as it will take-off with fully charged batteries. The amount of power that needs to be available from the propellers is calculated using the simulation shown in figure 6.1.

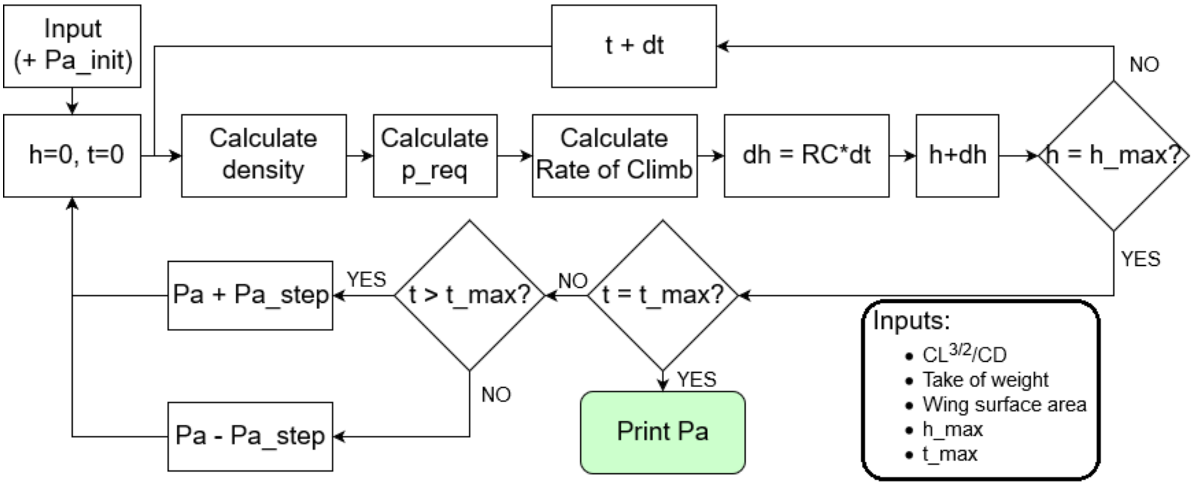

Figure 6.1: Flowchart of power and propulsion sizing program

Since the initial climb is the most demanding flight phase for the propulsion system, the propellers and engines are designed accordingly. The amount of power from the solar film, however, is usually not determined by this phase. This is because although the climb phase required the most power, the batteries are recharged during the cruise phase. The amount of solar area and batteries needed for the cruise phase is evaluated using the simulation shown in figure 6.2. The resulting battery mass is $90kg$ and the resulting area needed for the solar panels is $78m^2$. From this sizing, it is ensured that the aircraft can be powered year-round for at least 30 days on latitudes between plus and minus 40°. It can fly at even higher latitudes, but not year round, as is elaborated on in section 8.2.

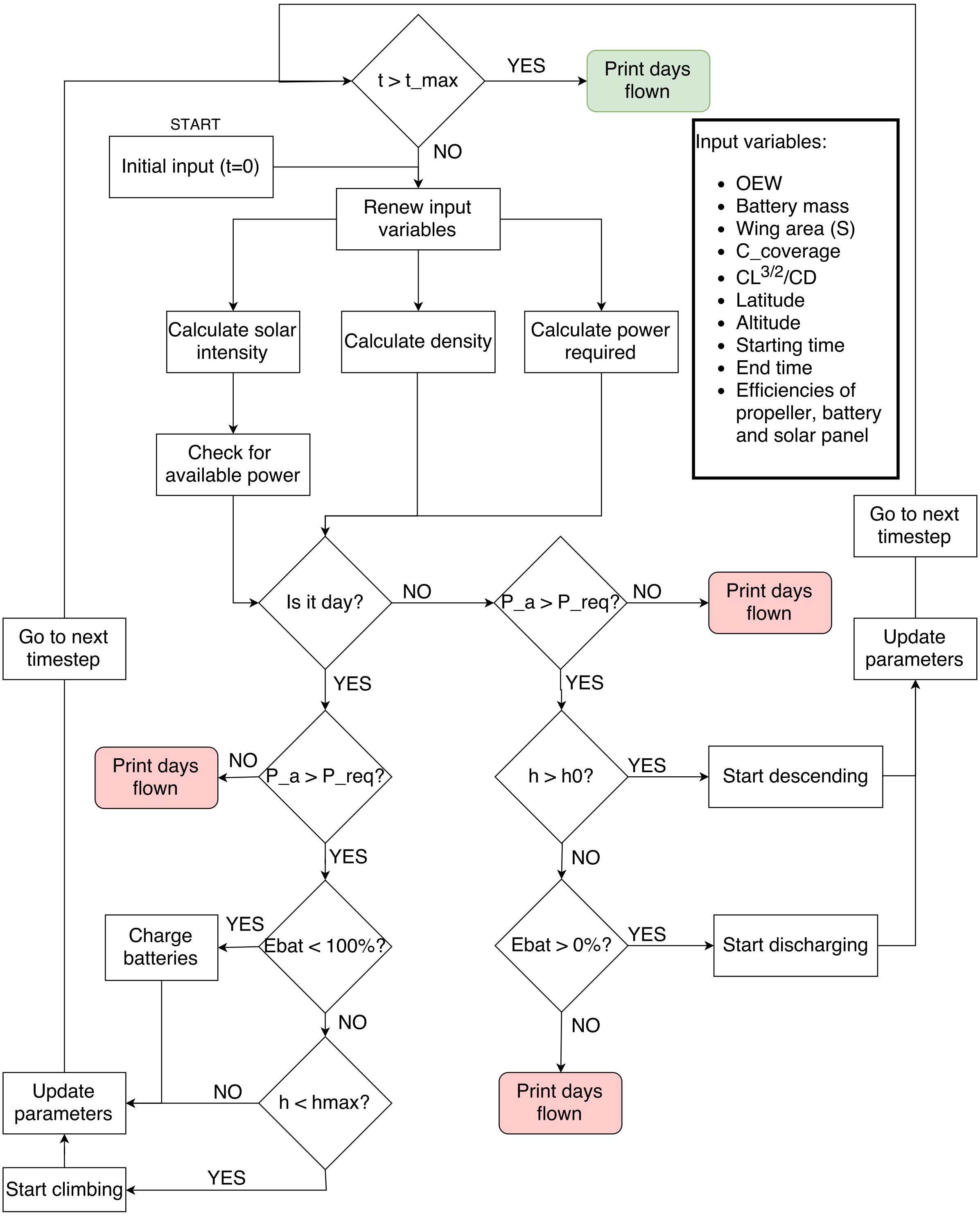

Figure 6.2: Flowchart of power and propulsion sizing program

6.1.2. Electrical system layout

To limit the amount and size of the necessary wiring, it has been decided to split up the power system into six separate sections, one for each engine. Each section will consist of a complete power-train, including solar film area, batteries, a battery manager, etc. All six systems will be connected with each other via the central power system, which regulates power to the payload and flight controls while also being able to 'redirect' some power in case of a failure in one of the pods. This can be both an electric failure, which means that more power is needed for a certain pod, or a propulsive system failure, in which case the power from one pod can be redirected to other pods or the central system. The complete schematic can be seen in section 6.1.2

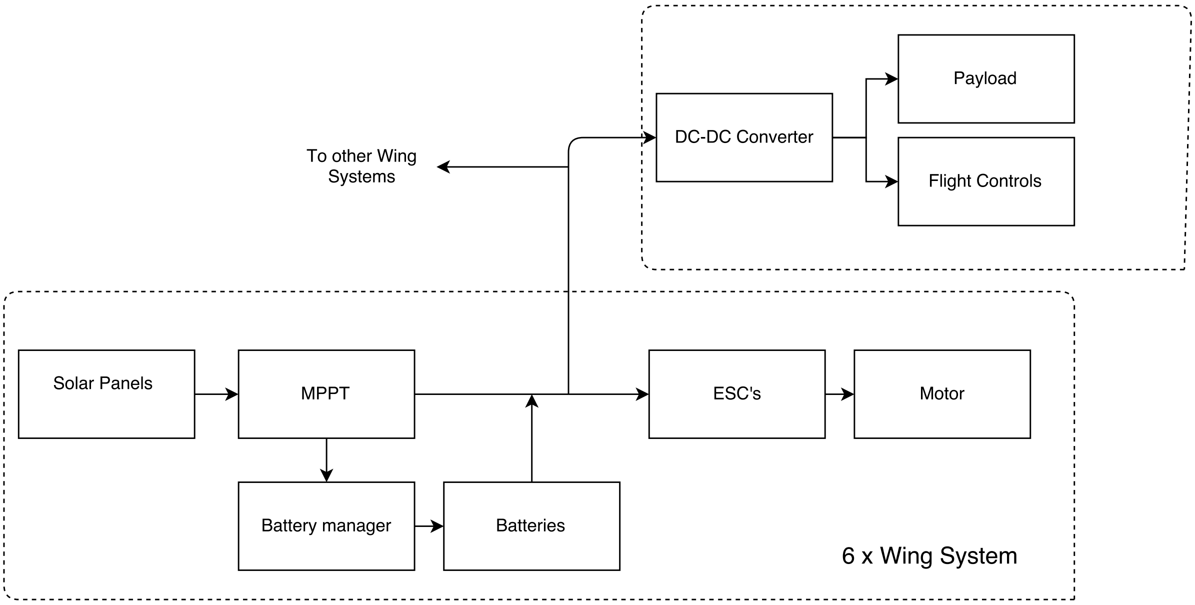

Figure 6.3: Layout of the primary power system

6.2. Engine Design

In this section a conceptual engine design will be made, specifying the most important parameters and specifications. These need to be taken into a further stage of development, since engine selection/design is outside the scope of the conceptual design. The electrical engineering lab of Delft University of Technology is very experienced in electrical engines and therefore is a perfect candidate to lead the development and design. As explanation of some important terms figure 6.4 has been introduced.

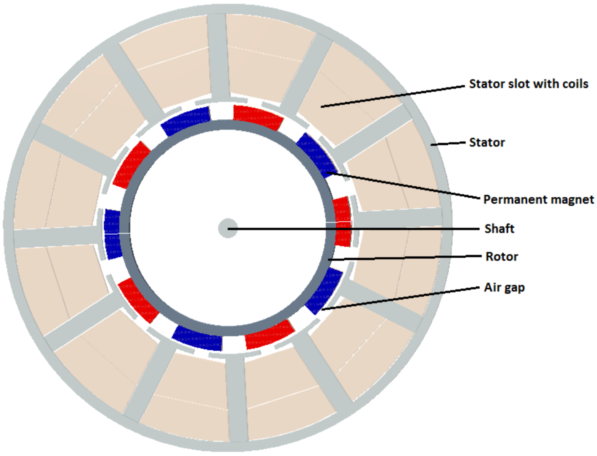

Figure 6.4: Explanation of the basic terminology of a DC engine.

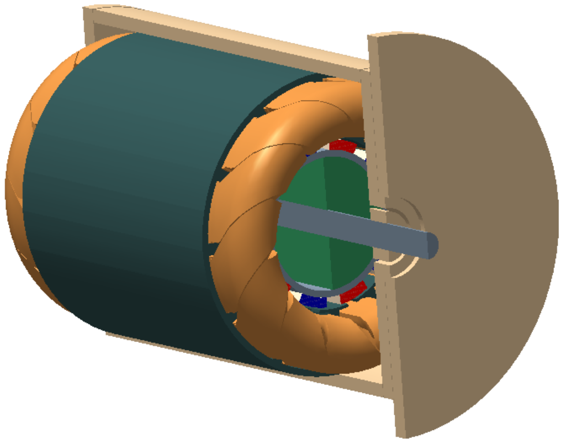

Figure 6.5: Orthographic view of the proposed engine.

Figure 6.6: Engine design.[14]

Amount of engines

The first big decision that was made is the amount of engines to operate the aircraft. Since a flying wing is being designed, no vertical control surface is used. Therefore it is cardinal to design a power distribution that allows for one engine to fail, without jeopardizing the entire aircraft. To increase reliability and keep with a simple design one engine per propeller was decided on, with a total amount of 6 propellers distributed over the wingspan. This design choice will be further explained in section 6.3.

Gearbox

A mechanical gearbox can be used to decrease the RPM of an engine to fit the RPM needed by the propeller. In an electric design however; this need could be eliminated by designing an electric engine which runs at a sufficiently low RPM[1], thus removing the need for a gearbox. In addition, an older design of the Zephyr used a gearbox system, but this proved to be unreliable.[15] A new design without gearbox increased both the efficiency as well as the reliability of the propulsion system. Therefore; it has been decided that in this aircraft design, no gearbox will be used.

Selection of engine type

In figure 6.8 a design option tree of the most important electric motor concepts is depicted. An AC engine is chosen because they are more powerful than DC engines. A synchronous motor is chosen since these are more efficient and they should operate on direct current (DC). Synchronous engines are most often built for outputs larger than 150kW. Only the brushless DC (BLDC) engines are available with a reliable, proven history for smaller sizes. Because the rotor is filled with permanent magnets, instead of coils/slots, this system does not need an extensive amount of cooling, is capable of long running times and has a higher reliability because the copper coils are not moving. This gives BLDC

[1]URL: http://gemsmotor.com/12v-24v-48v-brushless-bldc-motor [Retrieved on 27-06-2017]

motors a clear advantage, in our mission profile, over brushed motors.[16]

After the type of engine was chosen, some design decisions were made to increase reliability and tailor the engine to the needs of the aircraft. The most important decision that was made is the amount of slots, poles and phases of the aircraft engines (and the slots/poles/phases ratio). When the ratio is an integer, the engine is an integral-slot (IS) motor, otherwise it is a fractional-slot (FS) motor. The voltage required for a certain rpm is lower for FS than for IS engines.[17] The peak torque cogging and torque ripple [2] are also positively affected when using FS, compared to IS. The losses are higher in FS machines due to sub-harmonic-induced losses. When adding up the advantages and disadvantages of the FS motors, they are more suiting than the IS motors.

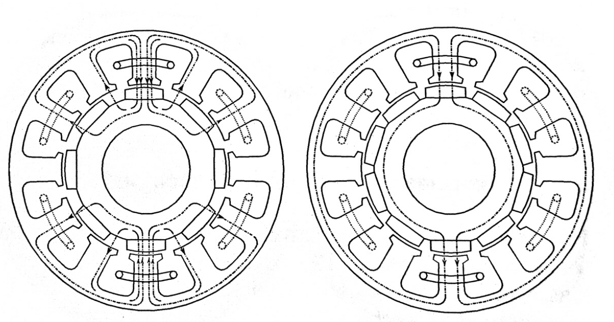

Figure 6.7: Flux pattern for 12/8 (left) and 12/10 (right) engines.[18]

The amount of phases used by the engines is 3. Less phases would be inefficient engine design, because too many coils stay unused. More phases would increase the complexity of the engines drastically, and thereby decrease their reliability.[16]

A 12/10 (slots/poles) engine was decided on. The reduction of the inter-phase coupling from 12/8 to 12/10 makes a 12/10 engine more fault tolerant (see figure 6.7), which means that when/if one of the phases would fail, the overall system performance would not drastically decrease. The only major decrease in performance would be the increase in torque, and DC current ripple.[18] Configurations with smaller numbers of poles or slots would be ineffective use of space while larger numbers would be too complex.

[2]URL: https://www.motioncontrolonline.org/content-detail.cfm/Motion-Control-Tech-Papers/Understanding-the-Distinctions-Among-Torque-Ripple-Cogging-Torque-and-Detent/content_id/675 [Retrieved on 9-6-2017]

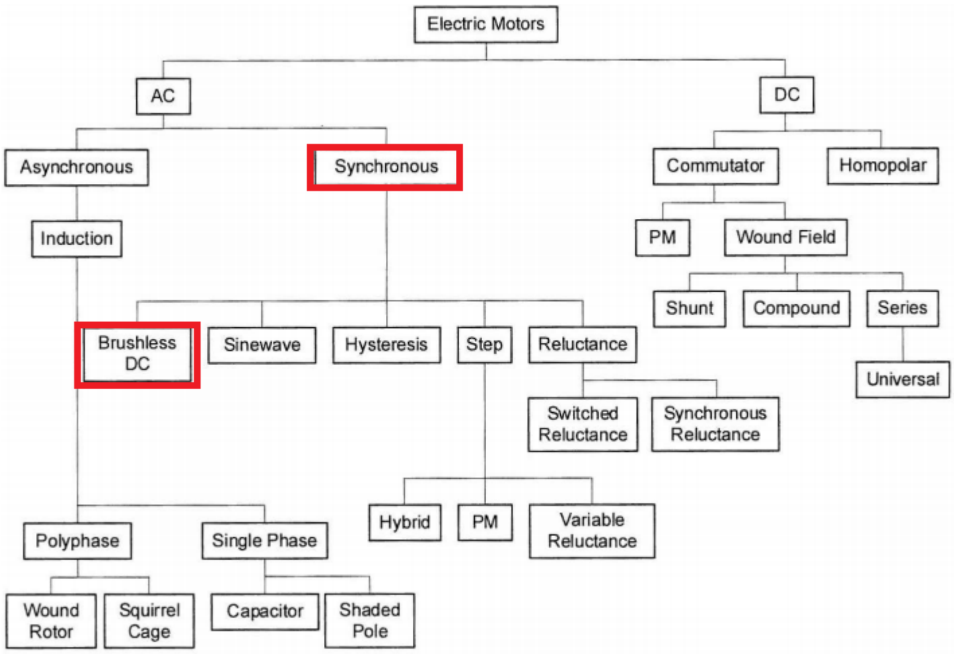

Figure 6.8: Design option tree for electric motor concepts.[16].

To control the phase switches of the motor speed and position, Hall-sensors are often used. These sensors are not desirable because of their cost, maintenance, size and reliability. To eliminate this problem sensorless control could be done, as explained in.[19] As stated, the starting procedure is still a problem and should be looked into in further design steps.In table 6.4 the most important parameters and design goals of the engine are given.

Table 6.4: Engine Parameters

Parameter	**Value**
Torque $[Nm]$	5
Output power $[W]$	750
Angular speed $[rad/s]$	150
Minimum Temperature $[°C]$	-50
Maximum Temperature $[°C]$	100
Slots	12
Poles	10
Phases	3
Control of phase switches	Sensorless
Efficiency $[\%]$	93

Engine Cooling

Cooling the engine is important since the reliability of the propulsion subsection and therefore the reliability of the mission depends on it. An engine that overheats will lose efficiency[3]. The slow turn ratio and high altitude make it so an air-cooled system is enough to manage the heat produced by the

[3]URL: http://www.motioncontroltips.com/understanding-dc-motor-curves-temperature-part-2 [Retrieved on 26-06-2017]

rotations. A valve system has to be designed to prevent overheating and freezing. The NACA intakes, see figure 6.9, will be placed on the side of the pod. In case of stand-still engine tests, the engine will still be cooled through the airflow produced by the propeller wake. This cooling system will be explained later on in the report in section 6.4. The temperature range, as given in table 6.4, is a range that needs to be designed for to reduce the decrease in efficiency. The detailed design of this thermal control system is outside the scope of this report. The critical case is the testing of the engines before take-off in a hot environment. To increase the Dutch portion of production, the valve system will be outsourced to Aeronamic[4].

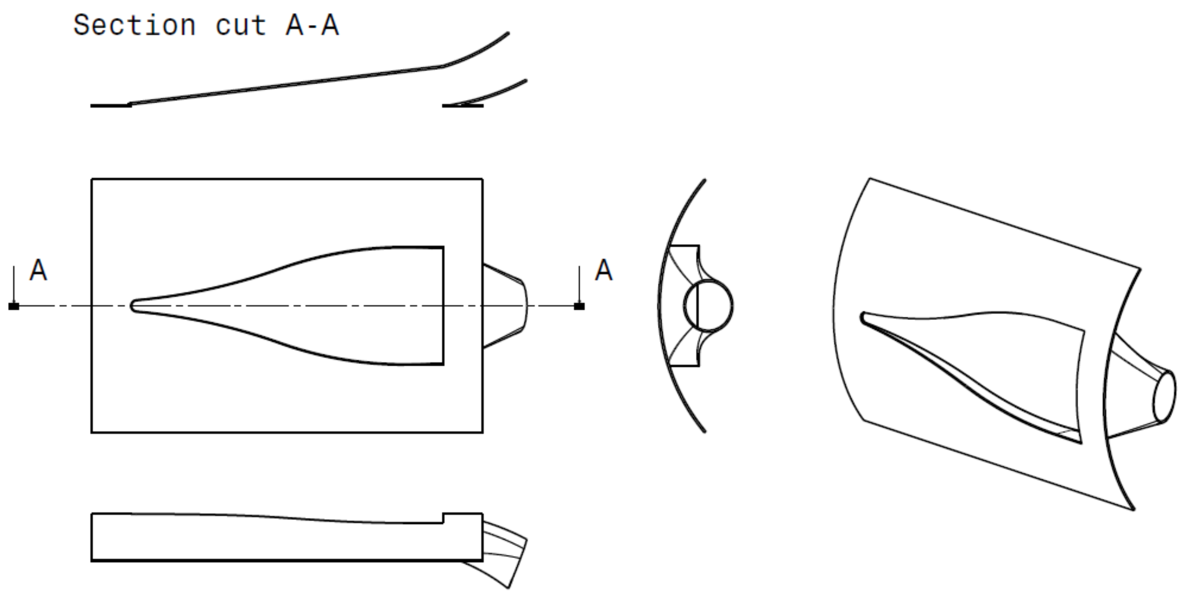

Figure 6.9: NACA intake

6.3. Propeller Design

This section features the design of the outer part of the propulsion system: The propeller. A propeller system is chosen because other aircraft propulsion types like turbojets and turbofans are not efficient at slow speeds. The first choice in the propeller design is the amount of propellers that will deliver the thrust. In theory, this thrust can be delivered by as few as 1 propeller or as many small propellers as can fit on the aircraft. This distributed propulsion concept is currently investigated by many companies as it has a few distinct advantages:

- Increased dynamic pressure over the entire wing, increasing the amount of generated lift. By making good use of this effect the wing size can be optimized.
- Smaller propellers, causing less constraints in operational procedures.

[4]URL: http://www.aeronamic.com/product-range/ [Retrieved on 14-6-2017]

- Capability to precisely steer the aircraft using differential thrust
- Increased redundancy & Increased capability to fly in One-engine-inoperative condition.
- Lighter system. [20]

There are some downsides as well. The complexity increases with each added propeller, as each needs an engine, gearbox, separate wiring etc. Also, propellers generally get less efficient as they get smaller, which is a constraint in the design since the required thrust level is very low. This would make the propellers and engines too small to be efficient. Lastly, the effect of the increased dynamic pressure over the wing would be minimal since the wing span is very large. Taking these advantages and disadvantages into account, it became clear that distributed propulsion is not suited for this aircraft design. So, the amount of propellers would be six or less. An uneven amount of propellers is not preferable, since there would be a resultant torque acting on the aircraft structure. Having just two propellers is a bad option as well, because in case one engine fails the other engine would have to be shut down as well as the control surfaces are not large enough to cope with the resulting yaw moment. To come to a final decision, a trade off was made between four or six engines using relative mass measurements. An estimation was made on the weight of all the components. Since this weight is not accurate, a percentage was used to express the relationship between 6 and 4 pods. "Total Pods Combined" takes the absolute weights of the pod structure, engines and propellers and expresses the relationship again in percentages. This trade-off can be seen in table 6.5.

Table 6.5: Amount of engine pods

Mass	**6 Engine pods**	**4 Engine pods**
Pod structure	100%	92%
Engines	100%	100%
Propeller	100%	88%
Total Pods Combined	100%	91%
Efficiency		
Engine	Due to higher RPM the 4-pod lay-out is approx. 1.7% more efficient.	
Landing gear	The landing gear of 4 engines has to be 60% larger, due to MPS-PLAT-7.	

Because the lower complexity and mass of the landing gear and the better life-time performance due to lower stresses, a 6-propeller pod configuration was chosen. The slightly higher pod mass is offset by the larger landing gear that is necessary due to the fact that the back engines of the six-pod configuration are placed more closely to the wing tips than those of the four-pod configuration. At this point in the design, the pods combined weigh 10 kg, while the landing gears combined weigh 12.3 kg. Therefore; 60% of 12.3 kg heavily outweighs 9% of 10 kg.

A fixed pitch propeller can be efficient, but its efficiency varies with the given advance ratio which is defined by equation (6.1).

$$J = \frac{V}{n_p \cdot D} \tag{6.1}$$

The aircraft will climb during the day to be able to glide during the night. Therefore the flight velocity will vary during the flight. As the engines need to always run at a high RPM to provide enough power during the climbing flight, efficiency will vary. However; if the climb will be done gradually, the efficiency loss can be reduced. A variable pitch propeller is capable of reaching near optimal efficiency's at different advance ratio's. This effect can be seen in Ruijgrok figure 7.4-2.[21] The disadvantages of a variable pitch propeller is the complexity and the associated cost, weight and reliability issues.The decision is made to use a fixed pitch propeller since efficiency loss can be minimized by always operating close to the optimum advance ratio by climbing gradually.

Another influential factor on the efficiency are the number of propeller blades. In general, using less propeller blades increases the propeller efficiency. The benefit of using more than two blades is being able to reduce the propeller blade diameter, mainly for ground clearance reasons. In this design however; propellers will be set horizontally during landing, maximizing ground clearance. Using two propeller blades is therefore the optimal design for both ground clearance as well as efficiency, therefore; two blades will be used. The downside to this is that a propeller brake needs to be developed which is able to stop the propeller accurately in the horizontal position.

The use of contra-rotating propellers can increase the efficiency by reducing the vortices created by the propellers. In piston setups, they require complicated mechanical gearboxes, which increases weight and reduces reliability. In an electric setup however, these problems can be negated by using a "shaft within a shaft" drive arrangement, by using two separate electric motors[5]. The efficiency increase for large-scale transport applications was found to be between 6% and 16%.[22] However; at applications more similar to a HAPS, high altitude airships, the efficiency increase was found to be only between 3% and 8% when performing at near optimal advance ratios.[23] Taking this into consideration, it is decided that the increased efficiency does not outweigh the increased complexity and associated maintenance and therefore, no contra-rotating propellers will be used.

Momentum theory [6] was used to estimate an ideal propeller efficiency. This was then compensated with an assumed nonideal efficiency to get a complete propeller efficiency, which is done by multiplying the ideal and non-ideal efficiency. Based on Gundlach [24], this non-ideal efficiency is assumed to be 0.9.

[5]URL: https://www.electro-flight.com/contra-rotating [Retrieved on 8-6-2017]
[6]URL: http://web.mit.edu/16.unified/www/FALL/thermodynamics/notes/node86.html [Retrieved on 8-6-2017]

From this theory, it is known that increasing disk loading (T/A) of a propeller reduces the efficiency of the propeller. However; at some point the weight increase due to the larger diameter will outweigh the efficiency increase. Due to the difficulty of accurately estimating high-altitude propeller performance, a disk loading similar to the NASA Pathfinder of 7.25 N/m^2 [25] was used. This resulted in a propeller diameter of 1.5 m and an estimated propeller efficiency of 85% as can be seen in figure 6.10. This efficiency is similar to typical values given by the solar impulse team [7].

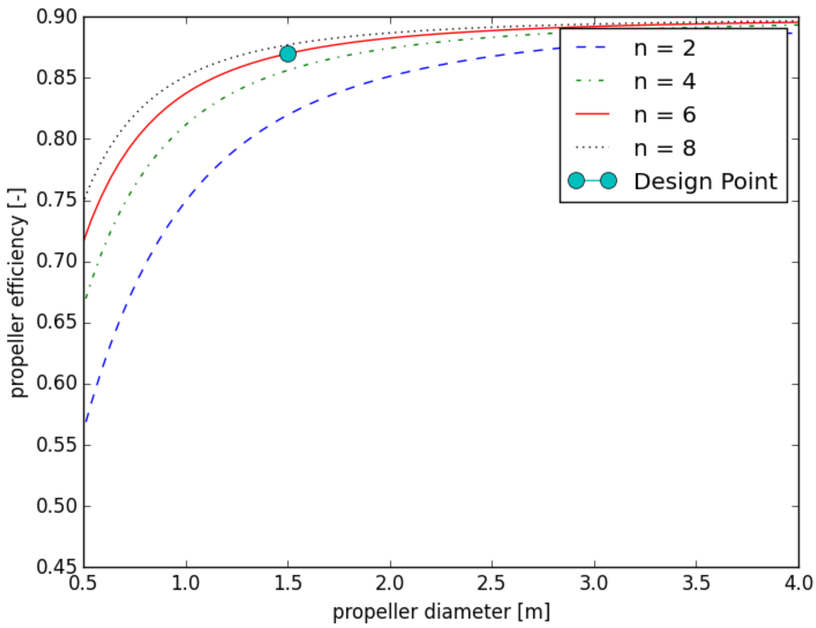

Figure 6.10: Propeller efficiency for different propeller configurations. $V = 26.9m/s$, $h = 18000m$, $P_{req} = 1800W$.

The propeller RPM is an important parameter which determines the possible need for a gearbox. In order to find the RPM for a propeller, in-depth propeller design methods (such as blade element theory) need to be used, which were considered too in-depth for this stage of the design. Therefore the propeller RPM of reference aircraft which use similar propellers was used. The closest reference aircraft which was found is the NASA Pathfinder, which flies at a RPM of 1450 [8]. The motors have a maximum power of 1.5 kW per motor, therefore it seems that the design is very similar. Thus; at this stage of the design, a RPM of 1450 is considered. Due to the propeller Reynolds number and Mach number conditions associated with high-altitude flight, a propeller will need to be designed in the further stages of the design since most likely, no off-the-shelf propellers exist which are optimized for these conditions. The specifications of the propeller as it has been selected so far are summarized in the table 6.6.

[7]URL: http://aviation.aiaa.org/SolarImpulse2 [Retrieved on 12-6-2017]
[8]URL: https://web.archive.org/web/20060911120327/http://www.ecsel.psu.edu/ dbieryla/pathfinder/pathpropellers.html [Retrieved on 13-6-2017]

Table 6.6: Summarized chosen and estimated parameters of the propeller

Parameter	Value
Amount of propellers [-]	6
Amount of blades [-]	2
Pitch [-]	Fixed
Propeller diameter [m]	1.5
Propeller cruise speed [RPM]	1450
Cruise thrust [N]	80.3
Cruise efficiency [-]	0.85
Average climb efficiency [-]	0.75

Propeller weight can be estimated using a modified version of Roskam's weight propeller estimation as described by Gundlach.[24] This resulted in a propeller mass of 0.13 kg per propeller. To validate this method, the solar impulse propellers (5 kg [9] [Retrieved on 15-6-2017]) were compared with their weight estimation from Gundlach (4.0 kg). Thus it seems that Gundlach underestimates the weight of these propellers. In addition, due to the fact that this design will be flying at higher altitudes, a wider chord is needed for the propellers [10], which might result in an increase in weight. To be conservative, the propeller weight was simply estimated using equation (6.2), resulting in a total propeller mass of 11.3 kg.

$$m_{propeller} = \frac{m_{propeller,solarimpulse}}{D_{propeller,solarimpulse}} D_{propeller} \tag{6.2}$$

What has to be taken into account is the fact that the propeller will disturb the incoming flow over the wing. Dependant on the propeller, it can have different effects on the wing. The wake of the propeller will cause a local increase of C_L where the wake moves over the wing, as the flow is accelerated or locally the angle of attack could have been increased. Yet due to this, the Oswald factor will somewhat decrease. The values for the Oswald factor and the lift coefficients are hard to find, thus this needs to be investigated in a later stage of the design. In figure 6.11 and figure 6.12 the interaction between propeller and wing can be seen.

[9] URL: https://www.youtube.com/watch?v=w6dLqkYU7vs

[10] URL: https://web.archive.org/web/20060911120327/http://www.ecsel.psu.edu/ dbieryla/pathfinder/pathpropellers.html [Retrieved on 15-6-2017]

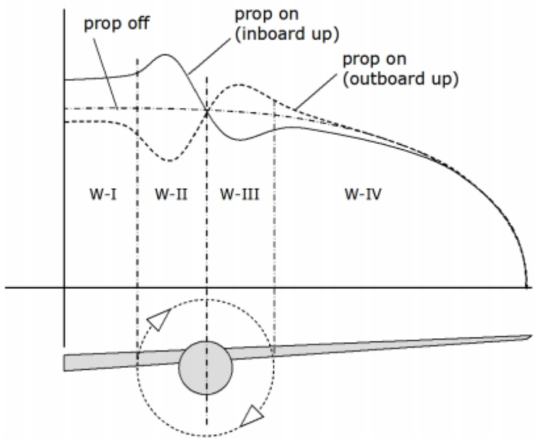

Figure 6.11

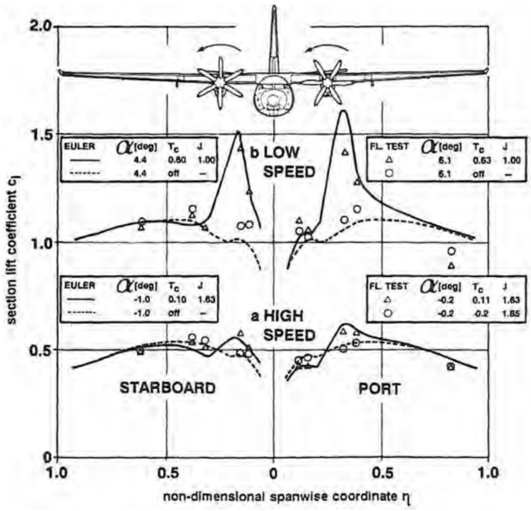

Figure 6.12

Figure 6.13: Propeller wing interaction [26]

6.4. Thermal design

To protect the systems from harsh conditions (temperature and radiation) a thermal system has to be designed. The engine has to be cooled to prevent overheating, as discussed in section 6.2. Other systems that need to be protected are batteries, actuators and avionics. A distinction has to be made between subsystems and components that are constantly used or those that are only used in a infrequent manner. Constantly used components will draw a continuous current and will therefore not require active heating, in some cases (e.g. the batteries) they might even need cooling. Subsystems and parts that are not used regularly (e.g. actuators) do need active heating. An overview of the subsystems and their protection requirements is given in table 6.7.

Table 6.7: Thermal system overview

Active heating	**Air cooling**	**Radiation protection**
Batteries	Batteries	Batteries
Actuators	Engines	Autopilot
Payload	Autopilot	Sensors
Sensors		

For optimal performance, the batteries require constant monitoring. To control the temperature at which the batteries operate, active heating and passive insulation will be applied, as well as cooling. The passive insulation will work as radiation protection and will be the first defence against heat increase or heat dissipation. The use of multi-layer insulation film, with a range of -100°C to 150°C [11], is paramount to protect from temperature differences between shadow and sun. The active heating

[11] URL: http://www.dunmore.com/products/multi-layer-films.html [Retrieved on 16-6-2017]

takes the form of trace heating wiring [12], which will run around the elements mentioned in the first column of table 6.7. After which these elements and their wiring will be wrapped with the insulation, to minimize the heating required. All the other elements that require active heating will undergo a similar process.

The active cooling is a combination of valves and tubing, as can be seen in figure 7.8. The intakes and outlets will be designed, using the idea of NACA-intakes on the side of the pods as shown in figure 6.9, since they have clear advantages when comparing them to scoops, mainly because we do not need a high mass flow and therefore a high ram-pressure.[27] These cooling systems will be implemented in every pod. The most critical scenario for the cooling system will be during take-off and during ground tests due to the limited speed, the NACA-intakes are dependent on the propeller wash. More detailed design analysis needs to be done on the cooling system. However; this is considered to be outside of the scope of this conceptual design and will be postponed until more detailed design phases. Since the platform is flying at altitude over 20 km, it is more prone to damage from radiation. A multi-layer insulation foil will be used to insulate the systems from heat during the day, the cold air during the night and the radiation the whole day long.

6.5. Verification & Validation

For the power and propulsion system design, two self-made tools were used: A tool to calculate the climb rate and a tool to size the complete power system for cruise. The verification and validation of the power system sizing tool has already been thoroughly performed in the midterm report [10], but will again be shown here for completeness.

Verification

Since the climb rate program only contains one loop with some simple equations, the verification process did not need to be too extensive. Three tests were done: First of all, it was tested if the power required for flight increases with increasing altitude. Secondly, it was checked that the different inputs had the correct effect. For example, an increase in weight should lead to a decrease in climb rate for the same power available. Lastly, the final outcome of the program was checked by hand calculations and stating that the required power output was actually the lowest possible power output with which the climb rate requirement can be fulfilled.

The verification of the overall model was done by means of a system test. The system test was done by inspection. All values were plotted over the complete flight time and checked whether they made sense. The following things were tested:

- Battery charge

[12] http://uk.rs-online.com/web/c/cables-wires/electrical-power-industrial-cable/trace-heating-cable/ [Retrieved on 20-6-2017]

- During the flight, the battery charge always remains between 0 and the maximum battery energy.
- The battery never charges while there is no solar radiation
- The battery does not charge if there are no solar panels
- The battery always charges if the maximum battery charge is not reached and the available power is bigger than the power required for flight.

• Velocity
- Flight velocity increases with increasing altitude
- Flight velocity increases with increasing mass

• Altitude
- Altitude always remains between the minimal operating altitude and the given altitude ceiling.
- Altitude always decreases to the minimal operating altitude before the battery power is used by the engines.

• Power available from the sun equals zero during the night.

In addition to this, the different efficiencies were checked for their effects. An increase in efficiency should (in general) result in an increase in endurance and a smaller gap between input and output power.

Validation

The climb tool was validated by finding an aircraft with a known time-to-climb. Using the tool, the required motor power was estimated and compared with the real motor power. The aircraft which was selected was the Electric Extra 330LE [13], that reached a time-to-climb to 3000 m of 262 seconds [14]. The other aircraft parameters can be found in table 6.8. The resulting required motor power calculated using the tool was 260.5 kW. When compared to the validation value of 260 kW, which was the real power of the electric engine in the aircraft, the difference is very small and the tool is considered validated. Of course there are uncertainties in the values in table 6.8, however; these cannot be removed due to the lack of validation data.

Table 6.8: Data found or estimated for the Extra 330 LE

Parameter	Value	Note
Surface area [m^2]	10.7	From Siemens[12]
Aspect ratio [-]	6.0	Calculated from Siemens[12]
Oswald efficiency [-]	0.7	Estimated based on [28]
Zero-lift drag coefficient [-]	0.325	Estimated based on [28]
$C_L^{\frac{3}{2}}/C_D$ [-]	9.3	Estimated based on [28]
Propeller efficiency [-]	0.6	Estimated based on actuator disk theory
Motor efficiency [-]	0.95	From Siemens[12]

[13] URL: https://www.siemens.com/press/pool/de/events/2016/corporate/2016-12-innovation/inno2016-aerobatic-airplane [Retrieved on 26-6-2017]

[14] URL: https://www.siemens.com/press/pool/de/pressemitteilungen/2016/corporate/PR2016120105COEN.pdf [Retrieved on 26-6-2017]

The validation of the density and solar intensity tools for the complete power system sizing is done by comparing them to actual measurements from different researches. The results of the validation of the solar intensity tool can be found in table 6.9. The reference data was retrieved from the university of Waterloo [15].

Table 6.9: Solar model validation

Parameter	**Model**	**Waterloo**
Elevation angle [°] (21-12, 40N)	26.6	26.5
Maximum irradiance [W/m^2] (21-7, 45N)	794.1	795.0
Daylight hours [-] (21-7, 45N)	14.85	15

The overall simulation was validated in a stage of the design where it was undecided if the final design would be hybrid or purely solar powered. Since data on solar-powered aircraft is scarce, the validation was done using a fuel-powered long endurance aircraft and checking if the endurance calculated matched the actual aircraft's performance. This changes the way the power is made available, but still validates the power required and the way that the power system works. Since the main input for the amount of power available has been validated by the solar model validation, the entire model is validated using this method. The chosen aircraft is the Grob 109B, as sufficient data was available to do an initial validation. Data of the Grob 109B can be found in table 6.10.

Table 6.10: Data of the Grob 109B. Information compiled from Jane's all the world's aircraft [16], the Grob 109B flight manual [29] and the 1986 article in Flight Magazine [30]

Parameter	**Value**
Wing Area [m^2]	18.95
MTOW [kg]	850.0
Empty Weight [kg]	632.8
Usable fuel [kg]	70.8
Minimum sink rate (sea level) [m/s]	1.1
Fuel consumption (V = 33.5 m/s, RPM = 1800, h = 0 m) [L/h]	6.8

From the engine operating manual [31], the performance graph is extrapolated to the RPM of 1800 to find an approximate brake specific fuel consumption (BSFC) of 320 g/kWh. Assuming some average values for propeller efficiency (0.8) and a power of the generator of 500 W, the program can be run and an endurance of 19 hours was found at sea level. From the fuel consumption, a real endurance is found of 15 hours using the tank capacity of 100 L. The difference between these two numbers is significant but understandable. First of all, the fuel consumption in the table is only valid at MTOW, whilst the program assumes a variable fuel consumption with weight. Secondly, the fuel consumption is valid for a velocity of 33.5 m/s, which is higher than the optimum velocity for maximum endurance. Finally,

[15]URL: http://www.civil.uwaterloo.ca/beg/arch264/arch264-sun.pdf - retrieved on 18-5-2017
[16]URL: https://www.ihs.com/products/janes-worlds-aircraft-development.html

there is an uncertainty in the engine and especially in the propeller efficiency.

To conclude, there is some uncertainty from the validation. This stems from the fact that there is simply not a whole lot of validation data available for solar powered long endurance aircraft. However, the simplicity of the calculations and the validation of the individual parts of the simulation give good confidence that the current analysis is sufficiently accurate for the initial design stage.

7. Structural design

This section will present the design choices made and the methods used during trade-offs applicable to the structural integrity of the aircraft. First the main structure trade-offs are done in section 7.1. Second the load factor determination is presented in section 7.2. After that the individual components of the structure including the rod, skin, ribs, mid section, pod structure, landing gear and payload connection are designed in sections 7.3 to 7.9. Then the production of other components is quickly touched on in section 7.10. Last the verification and validation for the tools used is presented in section 7.11.

7.1. Main structure trade-offs

Several options for the inner structure which will carry the load are considered: A rod, a wingbox and a rod with a plate underneath it for convenient storage space. A combination of a rod and a middle wingbox section is also considered. In table 7.1 the merits and disadvantages of each option can be seen.

Table 7.1: Pros and cons of different structure types

Structure concept	Pro	Con
Rod	-Lightweight -Simple design -Easy inspection -Easy manufacturing	-Low impact resistance -Low storage volume for components
Rod + plate	-Lightweight -Easy component storage -Easy accessibility -Simple design	-Low impact resistance -Difficult component isolation
Wingbox	-High impact resistance -High storage volume -Easy component isolation -Easy joining to other elements -High inertia	-High weight -Cutouts necessary -More difficult manufacturing
Wingbox + rod	-Easy component storage -Easy component isolation -High impact resistance -High inertia	-High weight -Complex -More difficult manufacturing

The rod has been chosen. The most important reason for this is that it is the lightest option. The skin for such a low weight aircraft will already be low impact resistant, so a high impact resistance for the inner structure is not important as impact will still lead to skin failure. The low storage volume is a problem, but can be worked around by adding pods and payload attachments in the structure, as explained in section 7.7 and section 7.9. The low complexity of this option also facilitates a straightforward manufacturing process and easy inspection.

A rectangular rod cross section or a circular cross section can be used. A rectangle would be stronger in bending, but less efficient in torsion. The circular rod will be advantageous in attaching the ribs if twist is present, because the cut-out in the rib does not have to be directional and the ribs can be put into the right orientation before being joint to the rod. For a non circular cross section, the cutout has to be precisely manufactured.

7.2. Load factor determination

The critical load case was determined to occur due to upward gusts at altitudes below 1500 feet, while flying at a velocity close to stall. The load factor due to gusts is greater than any maneuver load as the maneuverability of the aircraft is limited by small allowed bank angles. Furthermore, the low wing-loading and flight velocity result in gusts having stronger effect on the aircraft.

The load factor due to gusts is dependent on the gust velocity. The maximum gust velocity was determined using data collected during a lifetime of a Boeing 747.[32] A number of probability density functions (PDF) were found that looked visually similar to the distribution of the statistical data. Next, a Levenberg-Marquardt optimization algorithm was applied to find the best fit values of the PDF parameters. Finally, the Cauchy distribution was determined to be the best fitting as it possessed the smallest root-mean-square error. The resultant PDF and Cumulative Distribution Function can be found in figure 7.1.

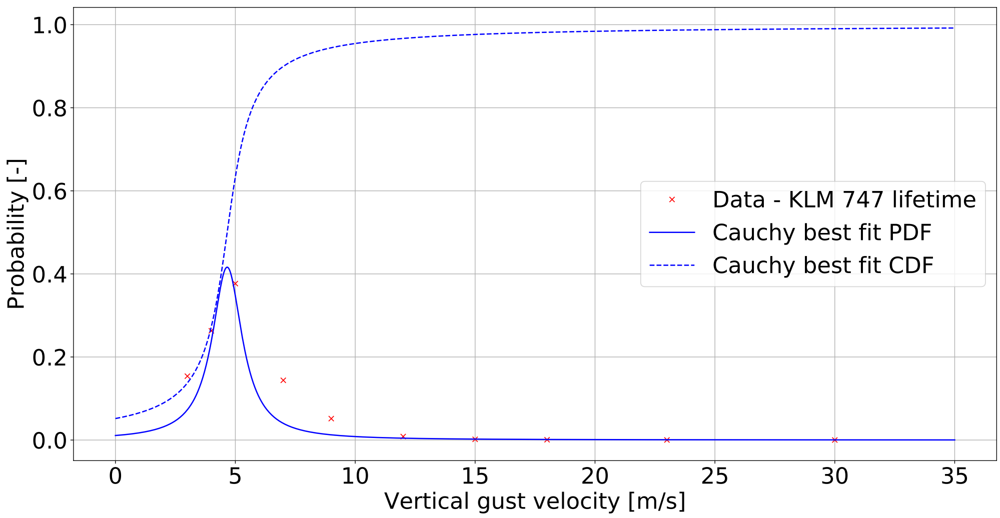

Figure 7.1: Best fit Probability Density Function (PDF) and corresponding Cumulative Distribution Function (CDF) and data for Boeing 747 lifetime

Using this plot a decision has been made that the structure shall be designed to withstand a gust speed for which there is only 1% chance that a gust of greater speed shall occur while the aircraft is below 1500 ft. This results in a 51.6% probability over the aircraft lifetime (72 take-offs and landings) that a gust speed faster than the one it is designed for shall be encountered. This probability is acceptable as the aircraft can delay take-off/landing until favourable conditions are present (the 747 flew through most weather). Furthermore, the gust load factor is multiplied by 1.5 as an additional safety precaution. These two considerations should allow for safe operation of the aircraft over its lifetime. Thus the critical load case factor is 2.7 and with the safety factor the ultimate load factor is 4 for a gust velocity of 21 m/s.

7.3. Rod

The load carrying structure is a circular rod as chosen in section 7.1. The cross section was chosen to be circular to avoid shear stress concentrations, as these turned out to be relatively high in non-circular cross sections due to sweep. The rod is placed at a quarter chord to minimize the torque due to misalignment of the aerodynamic center and the rod. It runs from the wingtip to the connection of the wing and the middle section. The rod has been divided into span wise segments, and for each of these segments the aerodynamic loads were obtained through XFLR5. [33]

The aerodynamic loads together with the weights and propulsive forces determine the maximum direct and shear stresses along the wingspan. The ultimate load factor is four, as described in section 7.2. To account for fatigue an additional safety factor of 1.1 is applied. In [34] it is stated that it is common for transport aircraft manufacturers to apply a load enhancement factor of 1.15. As the designed aircraft will undergo less cycles under less extreme conditions, the factor has been lowered.

The material used has to be as light as possible because weight drives the design of all other subsystems. Carbon fiber has a high-strength-to-weight ratio and low density in comparison with metal.[35] Because of this carbon fiber composites were chosen over a metal structure. Next the choice between a thermoset resin, thermoplastic resin or a sandwich structure had to be made. Sandwich structures have a relatively high moment of inertia, but are susceptible to trapping dirt in the core and absorbing moisture[1] and the extra area within the sandwich structure is unneeded, which is why this option was discarded. Thermoplastic resin composites tend to have very good mechanical properties, but the production techniques are not yet capable of producing a rod of up to 20 meters long out of one piece. Because for a thermoset composite it is possible to produce rods of such dimensions, it is decided to go for thermoset carbon fiber composite. The composite used is unidirectional carbon fiber with epoxy resin cured at 120° in an oven[2] and it has a 60 % fiber volume ratio. The carbon fiber is high strength,

[1] URL: https://www.faa.gov/regulations_policies/handbooks_manuals/aircraft/amt_airframe_handbook/media/ama_Ch07.pdf [Retrieved on 12-6-2017]

[2] URL: https://www.acpsales.com/upload/Mechanical-Properties-of-Carbon-Fiber-Composite-Materials.pdf [Retrieved on

as the specific strength is important for keeping the structure lightweight. It is chosen because of its high tensile and compressive strength, as these will be the highest stresses present in the structure. The mechanical properties of the composite can be found in table 7.2.

Table 7.2: Mechanical properties unidirectional carbon fiber with epoxy resin

Mechanical property	**Value**
Young's Modulus 0°	135,000 [MPa]
Young's Modulus 90°	10,000 [MPa]
In-plane Shear Modulus	5000 [MPa]
Major Poisson's Ratio	0.3 [-]
Ult. Tensile Strength 0°	1500 [MPa]
Ult. Compressive Strength 0°	1200 [MPa]
Ult. Tensile Strength 90°	50 [MPa]
Ult. Compressive Strength 90°	250 [MPa]
Ult. In-plane Shear Strength	70 [MPa]

The two production methods that are able to make a 20 m long cylinder are filament winding and braiding. Both of the methods do not allow to discontinue a single ply over the length of the rod, meaning a constant laminate thickness will have to be used over the entire length of the rod. Between these two methods braiding can be used for a larger fiber direction range. Due to that braiding will be used for producing the rods.

Because of the circular cross section the diameter of the rod and thickness together with ply orientation are the variables. Due to the constant thickness of the laminate, the laminate was designed to withstand the highest occurring loads. To analyze all the possible laminate designs a specialized excel sheet, which uses classical lamination theory, was used. [36] To find the optimal combination of laminate design and rod diameter an iterative process was used. During the first analysis the maximum available height within the airfoil minus a small margin for ribs was used as the diameter, this was equal to $chord_{local} \cdot \frac{t}{c} - 0.01$. The compressive load and shearflow are shown in figure 7.2. They are presented as Newton per millimeter in sideways direction. It is clear that maximum loads occur at the root. The laminate has been designed to be able to withstand the loads at the root according to the Tsai-Hill criterion.[37] The laminate design can be seen in figure 7.3.

21-6-2017]

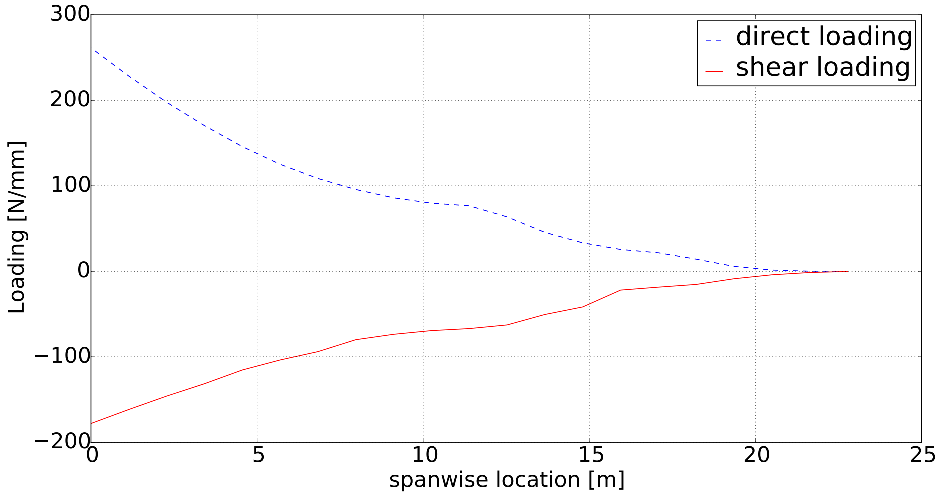

Figure 7.2: Maximum cross-sectional direct and shear loading along the wingspan, before minimizing rod diameter

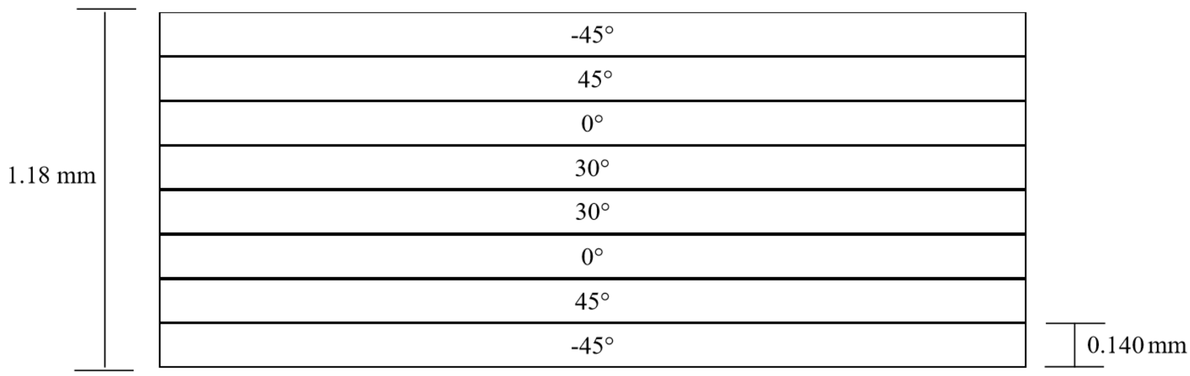

Figure 7.3: Laminate design with ply orientations

The laminate has been designed to be balanced and symmetric. No plies have been put in the 90° direction to save weight. Within the laminate six out of eight plies are placed to withstand shear stresses. Due to this high amount they can substitute the 90° ply. Once manufactured the exact orientation of the plies will differ somewhat from the design presented in figure 7.3. This is due to the weaving of the fibers during the braiding process.

The ideal situation would be where the loads are constant over the entire length of the rod. Due to constant thickness of the laminate only the diameter of the rod can be changed to approach the ideal situation of constant stress. By iteration the taper of the rod was increased with respect to the taper of the wing, while assuring that loads in the rod did not become higher then loads at the root. Another constraint was that the diameter could never increase from root to tip, otherwise the mould could not be removed after production. The updated load distribution can be found in figure 7.4. Without extra taper the weight entire rod was 82 kg, with extra taper the weight decreased to 60 kg. The diameter of the rod runs from 400 mm at the root to 100 mm at the tips. The rod design can be seen in figure 7.5.

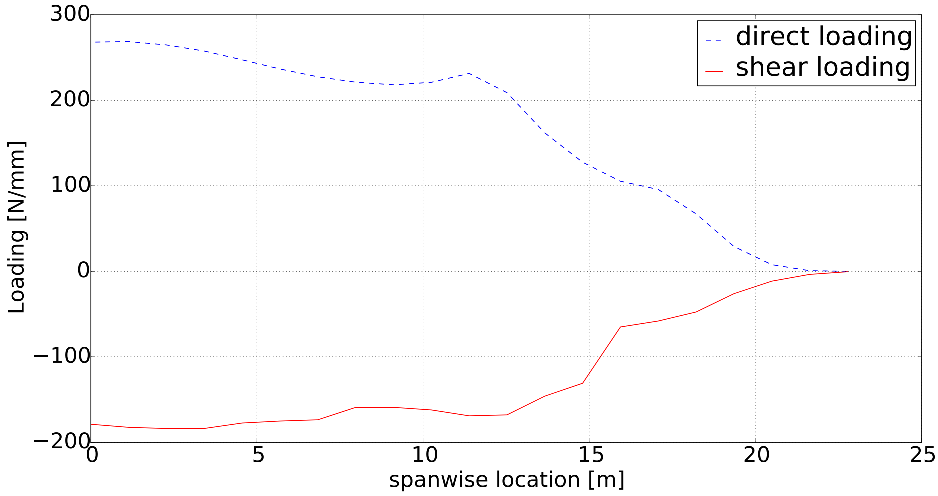

Figure 7.4: Maximum cross-sectional direct and shear loading along the wingspan, after minimizing rod diameter

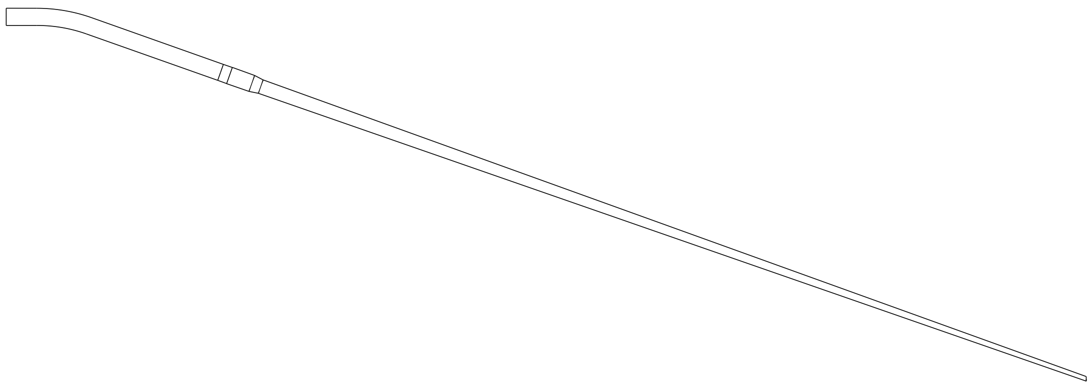

Figure 7.5: Design of one side of the rod

7.4. Skin

Because of the low wing loading of the aircraft the skin does not have handle loads as high as an conventional aircraft. Therefore it is possible to look into more light weight materials for the skin. Because of the light weight and ease of form-ability the choice was made to go with a thin foil. The foil has to be functional at extreme temperatures of up to ±70°C, furthermore the foil shall have a high Young's modulus (E) in order to ensure that it keeps the aerodynamic shape. In table 7.3 three kinds of films which were identified to be possible options, and some of their important parameters can be seen. From this the decision is made to use the Mylar Polyester film mainly due to its relatively high Young's modulus.

Table 7.3: Plastic film trade-off

	$\mathbf{T_{min}}$ $[C]$	**E** $[MPa]$	**UTS** $[MPa]$
Mylar Polyester film	-70	3380	200
Kapton Polyimide film	-269	2550	165
Tedlar PVF	-72	2140	55

7.5. Rib

The skin cannot carry compressive and shear loads, therefore the method used to design the rib spacing is based on cable theory. Cable theory assumes that each element can only carry tensile loads and therefore has to deform in order to cope with the distributed transverse loads acting on the wing in the form of pressure differences. [38]

The rib spacing is based on two parameters, the maximum vertical deviation of the foil and allowed tensile stress of the foil. The allowed vertical deviation is stated as 1% of $(t/c)_{max}$. These values were chosen such that the change in airfoil shape is minimal.

The rib spacing is dependent on the foil thickness because a thicker foil will experience smaller stresses for the same force and thus rib spacing can be larger. An optimum can be found, however one needs to also take into account impact resistance of the foil. To assure this, the minimum thickness of the foil is set to 0.1 mm which is higher than the optimum. With this thickness the rib spacing is 260 mm for the earlier stated deviation of 1% of chord length.

The ribs shall be a structure which features struts supporting an airfoil outline. In the quarter chord location a cutout shall be present which allows the rib slid on the rod to the required location. The ribs are placed perpendicular to the rod. The attachment to the rod will consist of two blind rivets along with an adhesive. The qualitative drawing of the rib design can be seen in figure 7.6.

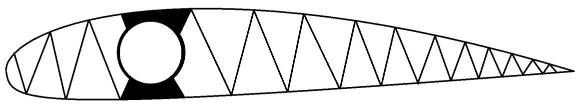

Figure 7.6: Qualitative drawing of the rib design concept. Circular part to be slid onto the rod for simpler assembly.

In order to minimize structural mass and avoid galvanic corrosion it has been decided that the part shall be made of a plastic. Research into manufacturing methods has shown that no traditional production method like Resin Transfer Moulding or Pressing can achieve the desired part complexity. [39] Thus it was decided that the optimal process is 3D Printing. The preferred 3D printer is the Leapfrog Xcel [3] due to its accuracy, maximum product size and the localization of its producer in the Netherlands. With this method, the estimated volume of material required to manufacture one rib is

[3]URL: https://www.lpfrg.com/en/xcel/ [Retrieved on 22-06-2017]

112.000 mm^3. Due to small thicknesses in the rib design a small extruder nozzle will have to be used. Based on the data provided in the technical specification sheet [4] the manufacturing time of all ribs for all the aircraft is 3 years with one 3D printer. This estimate assumes that the printing can occur at 80% of max speed. In order to shorten the production time to 1 year 3 3D printers should be purchased.

An important factor in the rib design is the material. The chosen printer can use Polyactic acid (PLA) however there may be a possibility to adapt it to use Acrylonitrile Butadiene Styrene (ABS) due to similar glass transition temperature. The criteria to be considered in the material selection are the tensile and compressive strengths, density, price, maximum service temperature, glass transition temperature and UV resistance, biodegradability and CO2 footprint. Table 7.4 compares these properties for both of the materials.

Table 7.4: Comparison between properties of Polyactic Acid (PLA) and Acrylonitrile Butadiene Styrene (ABS).[39]

Criteria	**PLA**	**ABS**
Tensile strength [MPa]	47	33.1
Compressive strength [MPa]	66	49.6
Density [kg/m^3]	1240	1050
Price [USD/kg]	2.8	2.5
Maximum operational temp. [°C]	50	70
Glass transition temp. [°C]	56	104
UV resistance	Good	Poor
Biodegrade	Yes	No
CO2 production footprint [kg/kg]	2.8	3.6
Other	Transparent	Printer adjustement required

From table 7.4 it can be seen that PLA has better mechanical properties even when taking into account the material density. Furthermore, it is more ecological due to its biodegradability and lower CO2 production. However, use of PLA would reduce the operational capabilities of the aircraft as the maximum temperature at which it could operate would be 50°C. This is a significant disadvantage as the aircraft would not always be capable of taking-off and landing in the middle-east. Taking into account all the factors ABS is a material better suited for use in the ribs. However, anti-UV coating will have to be applied to the ribs to prevent the UV rays reflected from clouds or bodies of water from degrading the mechanical properties of ABS. With this material the average rib should weigh 0.12 kg.

Some ribs shall carry servos for operation of control surfaces. These ribs will be additionally reinforced to carry the aerodynamic forces caused by surface deflections.

7.6. Wing sectioning

The aircraft is split up into 3 separate segments, 2 wing segments and one centerpiece. The centerpiece consists of two main structural components, being the attachments of the centerpiece to the wings

[4]URL: https://www.lpfrg.com/en/xcel/ [Retrieved on 22-06-2017]

as well as the corner segment in the root. Because the individual segments must remain modular for maintenance and transport the connections cannot be attached by means of welding or gluing. Therefore, the choice was made to do this attachment by means of bolts and a sleeve(mid-section will serve as a sleeve) into which the outer wing piece will fit. While the cross-section of the wing sections is mostly circular, close to the attachment this will change to slightly elliptical. The qualitative drawing of this concept can be seen in figure 7.7.

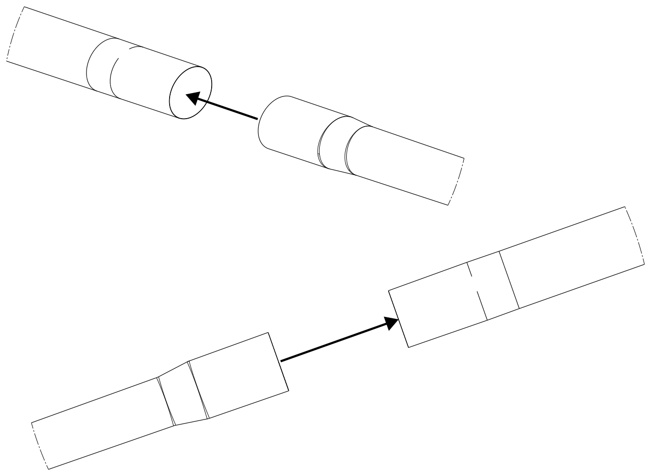

Figure 7.7: Attachment of the outer-wing piece into the middle section.

The bolts and the eccentric shape make sure the shear loads are transferred to the center piece without rotating the wing. The midsection will be made of the same material as the outer sections in order to keep the mechanical properties the same. Furthermore, ribs will be spaced such that when the outer wing section is slid into the sleeve, the outermost rib of the midsection will come together with the innermost rib of the outer wing section so that the aircraft skin remains continuous.

7.7. Pod design

To establish a reliable connection and easy to maintain system, a pod was designed for the propulsive system, as well as for the landing system. Two different types of pods are used: with landing gear and without landing gear, figures 7.8a and 7.8b respectively. The aft part of the pod is detachable from the straight part, so it is easy to access. This will serve as one of the two primary maintenance access points.

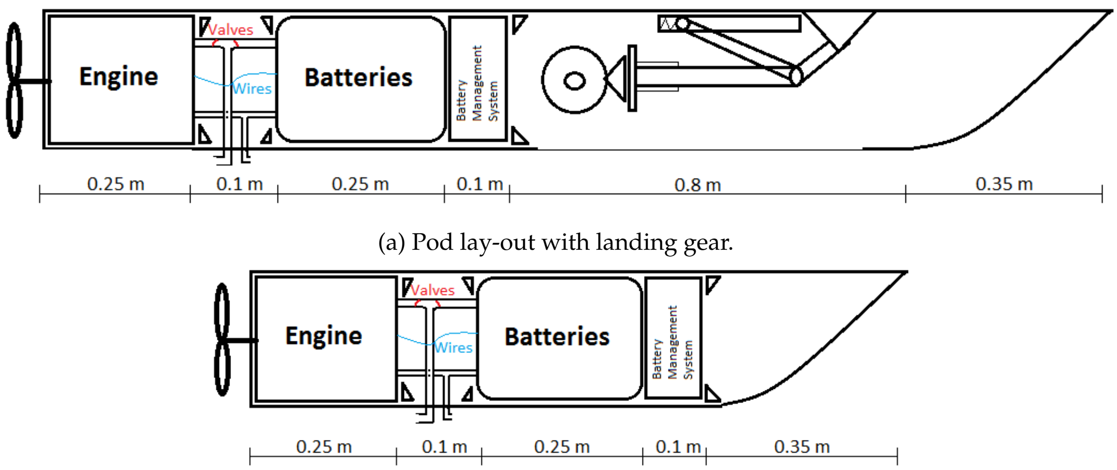

(a) Pod lay-out with landing gear.

(b) Pod lay-out without landing gear.

Figure 7.8: Technical lay-out of the pods.

Important parameters are given in table 7.5. These values are required to fit the systems in the pods. These are not the values used in the final design of the pods, since those are sized to fit on the wing with a reliable hard point connection. A more detailed overview of the pod is given in the CATIA models shown in chapter 9.

Table 7.5: Estimated pod parameters

	Pod with landing gear	**Pod without landing gear**
Diameter [m]	0.2	0.2
Length [m]	1.85	1.05
Material [-]	Carbon Composite	Carbon Composite

The valve system works as follows: due to the forward motion, the inlet, which will be a NACA intake, will have an over pressure, which will cool the engine and batteries by the cool air that is being sucked in. The valves on top will regulate the air flow, and therefore the rate and limits of cooling. Due to the under pressure at the outlet, the incoming air will be sucked back out.

One of the distinct characteristics of the engine pod is that it should be have a hole, for inserting internal elements and deploying landing gear for those pods where landing gear is located. For this resin transfer molding and vacuum infusion are applicable methods of production. A smooth surface is only needed on the outside, so vacuum infusion can be used instead of resin transfer molding. This has the advantage of being cheaper, although it is also slower.

The attachment of the pod to the wing rod is done through a mount system which can be seen in figures 7.9 and 7.10.

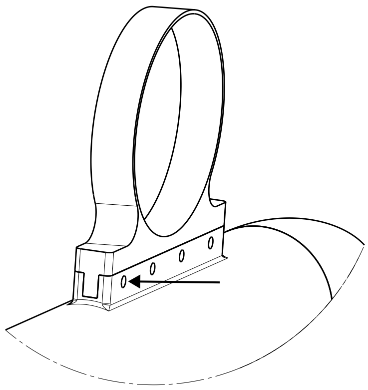

Figure 7.9: Pod connector closed, arrow indicates location of bolt.

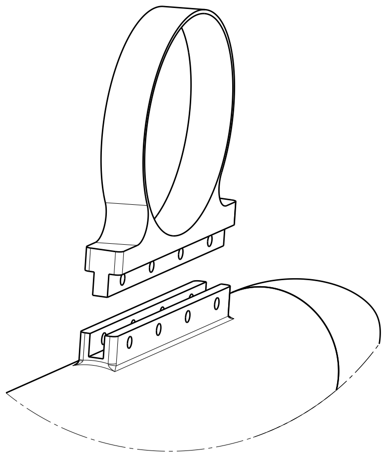

Figure 7.10: Pod connector open.

7.8. Landing gear

Three landing gears are used. One is placed in the middle and two in the engine pods furthest from the middle, as wheels farther out spanwise decrease the downwards deflection of the tip and allow for a larger bank angle at landing. The landing gear is not used for take-off, therefore a gear which has to be manually put back in place after landing is used. This has the main advantage of decreasing the amount of actuators, and thus the reliability is increased. As the aircraft attitude is susceptible to cross-winds, the wheels will be allowed to swivel to make a crabbed landing possible. The maximum swivel angle is 15°. The landing gear will be stored in the engine pods, behind the engines. The deployment of the landing gear is done by releasing a rod attached to the main landing strut which is propelled by a loaded spring, which also acts as a drag brace. Then the wheel will tear through foil on the bottom side of the pod. The foil is made thin enough to make sure the wheel will break through. After each landing the landing gear has to be put back into the spring and new foil has to be placed over the hole in the pod. This mechanism is shown in figure 7.11 and figure 7.12.

Furthermore, the landing gear does not feature any braking or steering mechanism due to the low landing velocity. Such systems would increase aircraft weight while providing unneeded functionality. A shock damper of 10 cm is used to relieve some of the loads in the structure introduced by touchdown. The tires have a tire pressure of 0.345 MPa in order to cope with rough landing surface. Using this the wheels have a width of 90 mm, calculated with the Torenbeek method.[40] The outer diameter of the wheels have been sized using the maximum diameter possible in the pod which corresponds to a diameter of 175 mm. The mass of the rim is 1.1 kg [5] and the mass of the tire is estimated at 1.5 kg [6]

As composites are rarely used in landing gear and are thus less reliable, metals are used for the landing gear. Aluminum, titanium and high strength steel [41] are considered. The designed landing strut properties can be seen in table 7.6. Only the tensile strength is shown, as data on compressive strength was not available for all materials. A compressive strength equal to the tensile strength is assumed for materials without sufficient information. Data for high strength steel on the density was not available, so a density of AISI Type 304 Stainless Steel[7] is assumed. Due to titanium giving the lowest weight, it is chosen. The main disadvantage is the cost, but as this will be dominated by the solar panels, it is not deemed an important factor for the landing gear.

Table 7.6: Landing gear strut material trade-off

Material	**Mass** [kg]	**Thickness** [mm]	**Density** [kg/m^3]	**Tensile strength** [MPa]
Titanium Ti-6Al-4V[8]	1.1	1.0	4430	880
Aluminum 6061-T6 [9]	1.3	2.0	2700	276
High strength steel	1.3	0.6	8000	1400

An impact of 2.5g is assumed, with a safety factor of 1.5, leading to a factor of 3.75 on the static loading. The struts have been sized to carry this load while not encountering yield or buckling failure. A maximum bank angle of 3° with a landing angle of attack of 2° results in a landing strut height of 0.55 m. The struts have a radius of 75 mm, to ensure they will fit into the engine pod, and a thickness of 1 mm. The drag brace has been estimated to weigh 50 % of the strut weight.

In table 7.7 the mass of each component of the landing gear can be found. The total mass is 1 kg over budget, which is less than 1 % of the total weight. This is insignificant on the whole weight, so the design is not adjusted to the increased weight of the landing gear.

Table 7.7: Landing gear weight

Component	**Mass** [kg]
Wheel	1.1
Tire	1.5
Strut	1.1
Drag brace	0.6
Total (1 landing gear)	4.3
Total (3 landing gears)	13

[5]URL: http://www.beringer-aero.com/file/brg_catalogues/9/cata_fichier/3_europe-in-english.pdf - [Retrieved on 3-7-2017]
[6]URL: http://www.aps-aviation.com/db_airdatabook.pdf - [Retrieved on 3-7-2017]
[7]URL: http://www.aps-aviation.com/db_airdatabook.pdf - [Retrieved on 4-7-2017]
[8]URL: http://asm.matweb.com/search/SpecificMaterial.asp?bassnum=mtp641 - [Retrieved on 4-7-2017]
[9]URL: http://asm.matweb.com/search/SpecificMaterial.asp?bassnum=ma6061t6 - [Retrieved on 4-7-2017]

To make the general shape of the landing gear, forming is used. This has the advantage of producing high quality parts and it also allows for hollow sections. The more complex shapes present in the landing gear will be made with milling, which has the disadvantage of producing lots of waste material. Therefore it is not used for all the structural landing gear parts.

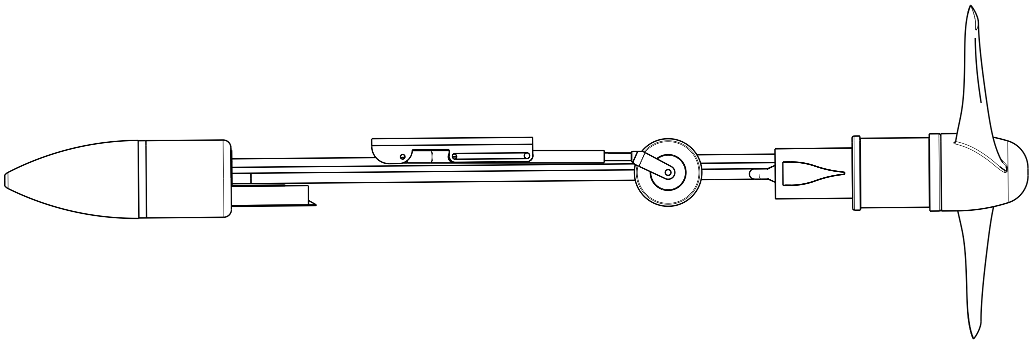

Figure 7.11: Landing gear retracted. (Strut and drag brace not decipted correctly)

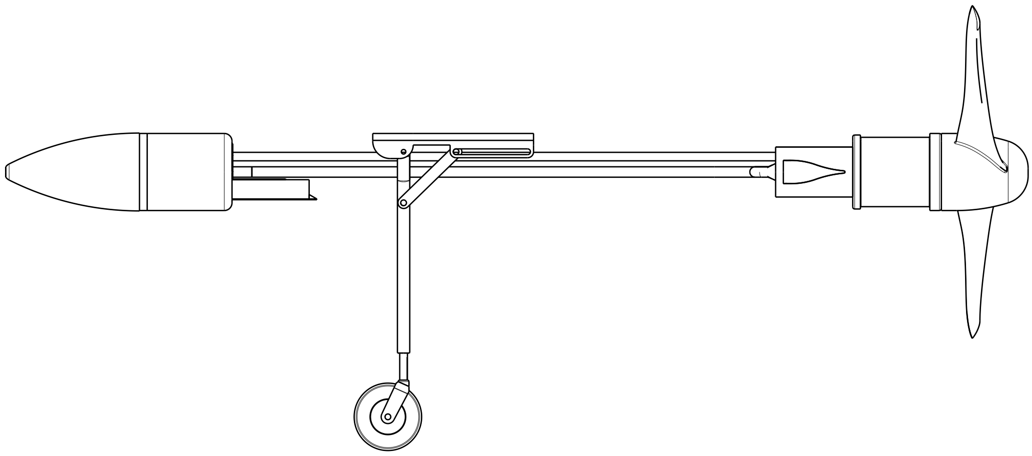

Figure 7.12: Landing gear deployed.(Strut and drag brace not decipted correctly)

7.9. Payload integration

One of the requirements for the payload is that it has a non obstructed view on the ground in order to fulfill its mission successfully. Therefore the pod has to be mounted partially outside of the wing. However in order to reduce the negative aerodynamic effect the payload pod is integrated in the wing as much as possible. This led to a rail system, attached to the wing rod on which you can slide the payload pod. The consequence is a hole in the leading edge of the root chord when the payload pod is removed. In figure 7.13 this mechanism is shown.

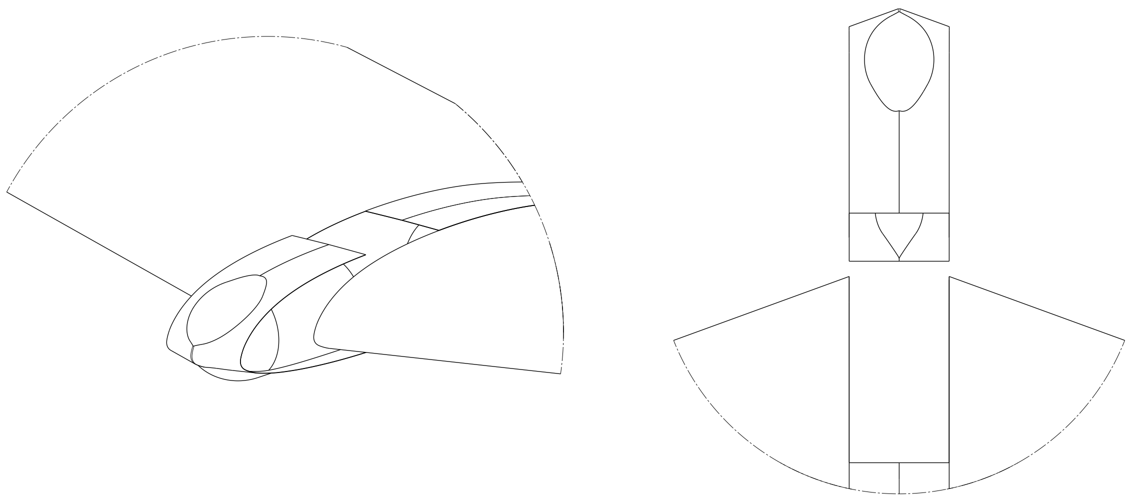

Figure 7.13: The integration of the payload in the root section of the wing.

7.10. Production of propeller

Even though an exact design of the propeller has not been made yet, a production method can still be chosen. Those relevant to a propeller are shown in figure 7.14. Vacuum infusion and resin transfer molding have the disadvantage of needing some kind of joint, as hollow sections cannot be made. This creates a weight penalty, thus these options are avoided. Of the two remaining options, braiding allows for more freedom in laminate design, as multiple fiber directions can be incorporated into one part. Therefore braiding is used for production.

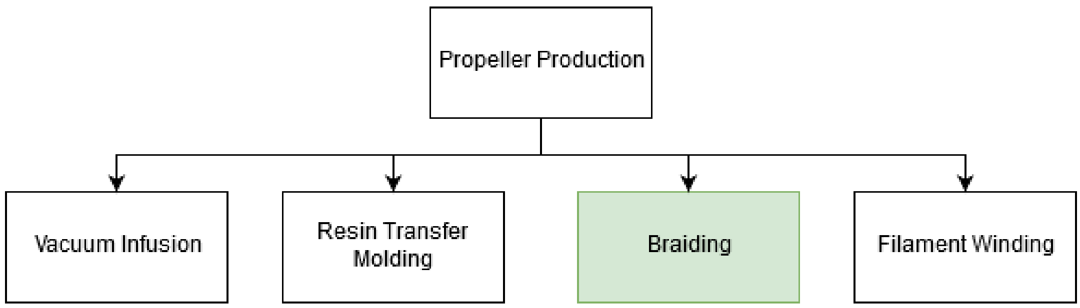

Figure 7.14: Propeller production design option tree.

7.11. Verification & Validation

Rib spacing

In order to verify the rib spacing program first an infinitely thin and thick foil is used from which a rib spacing of zero and infinite should be the outputs. Furthermore a hand calculation is done for the rib spacing, rib weight and foil weight with standard input parameters, in table 7.8 these results can be seen.

Table 7.8: Verification of the ribspacing program

Parameter	**Hand calculation**	**Program**
Rib spacing [m]	0.304	0.304
Rib mass [kg]	16.437	16.437
Foil mass [kg]	26.880	26.880

For validation of the program the amount of ribs of the Zephyr have been determined[10] and been used together with the span to calculate the rib spacing, giving 0.39 m. This value is slightly larger than the calculated rib spacing, however as this aircraft is also heavier than the zephyr this is sensible.

Stress determination

The stress determination script determines the shear and normal stresses in the wing rod given the properties of the wing(structure mass, location of engines and etc.) and aerodynamic load case obtained from XFLR5.

The verification of the tool consisted of comparing the program computations with manually performed calculations. Furthermore, the program was checked for proper flow control by assessing the entry into correct statements in test cases. Multiple errors have been identified and corrected such as incorrect computation of structure weight which did not include the length of the wing rod.

Validation of the tool has been performed by inputting multiple test cases into the program the first of which was a no load situation. This correctly has returned no stresses throughout the structure.

Furthermore, a point load situation has been investigated during which only a single load is applied to the structure. This test has been performed by inputting a straight wing with no taper and mass. A single point load has been applied such that no torque is generated about the quarter-chord location. The test was passed as the normal stress began to grow linearly towards the root while the shear stress stayed constant. Another test has been performed with two point loads of same magnitude but opposite direction has been performed. The test was also passed and the results can be seen in figure 7.15.

[10]URL: https://cdn.arstechnica.net/wp-content/uploads/sites/3/2016/02/Zephyr_8_under_construction_Airbus_press_pic-980x653.jpg - retrieved on 23-6-2017

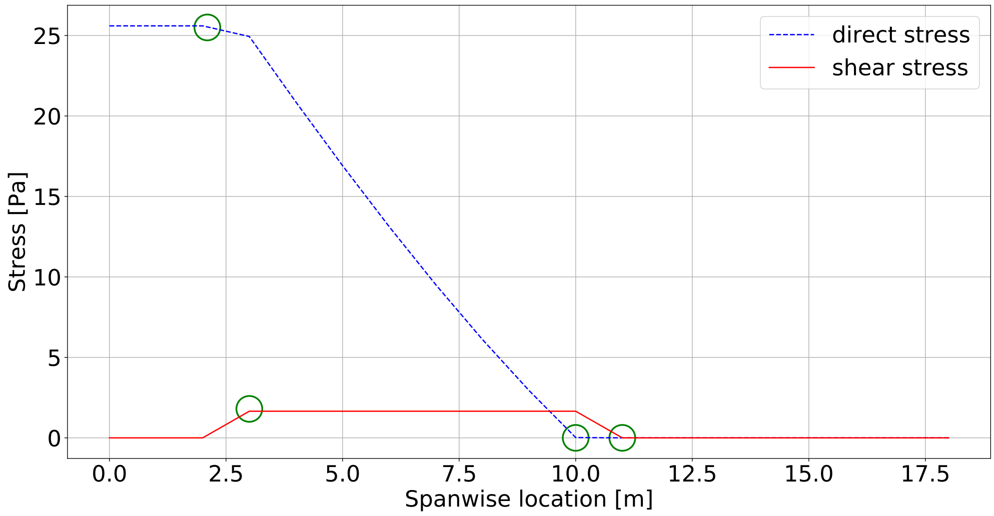

Figure 7.15: Two point load test. Same magnitude, opposite direction. Point load effects indicated at about 3m and 11m.

Another test that has been performed to check if the relief from the structure weight is modeled correctly. A point load was applied in the opposite direction of wing weight while keeping the structure mass nonzero. The test was passed and the result can be seen in figure 7.16.

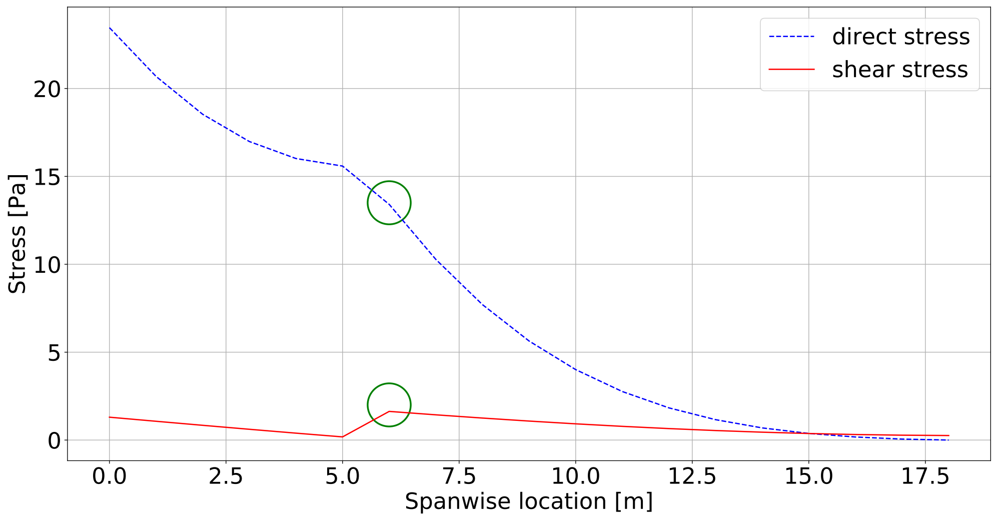

Figure 7.16: Distributed load and point load in the opposite direction test. Point load at about 6m and effect indicated by green circles.

8. Operations

In this chapter, the operation of the aircraft and ground system is explained. First, the mission profile is shown in section 8.1. After that, the most important operational considerations are discussed in section 8.2. Thirdly, the transportability is evaluated in section 8.3. The control automation and sensors and the hardware and software integration are discussed in sections 8.4 and 8.5. Finally, the design and operational considerations of the ground station is given in section 8.6.

8.1. Mission profile

As described in chapter 1, the system that is designed has to provide surveillance of a large area. Like most surveillance aircraft, this is done by loitering at a high altitude for a long period of time. Hovering over a certain area for a long period allows for the gathering of intelligence in terms of activity and enables the confirmation of certain pattern, if this is present. By having a group of aircraft flying in a specific pattern, a very large area such as a border or trade routes can be covered.

A typical mission profile for the surveillance aircraft design in this report is shown in figure 8.1. This mission profile includes a loiter phase of 30 days, which is one of the driving requirements. Since the aircraft is only powered by solar energy, the mission can be extended in case no failures arise and the solar conditions allow for it. It should be noted that the descent phase shown in the figure is done with inoperative engines, which means that the aircraft glides down to ground level. It is possible to decrease the descent phase to about half a day by maneuvering the aircraft appropriately. Also noticeable is the ascent to 23 km at the end of each day, and the descent back to 18 km during the night. This potential energy is combined with the stored battery power to fly through the night. The initial climb also goes up to the surface ceiling, as it climbs during the day and thus the loiter phase starts during the night. Other mission profiles could include a cruise phase, in case the aircraft has to travel to or between different locations, or a second climb starting during descent in case of an emergency situation.

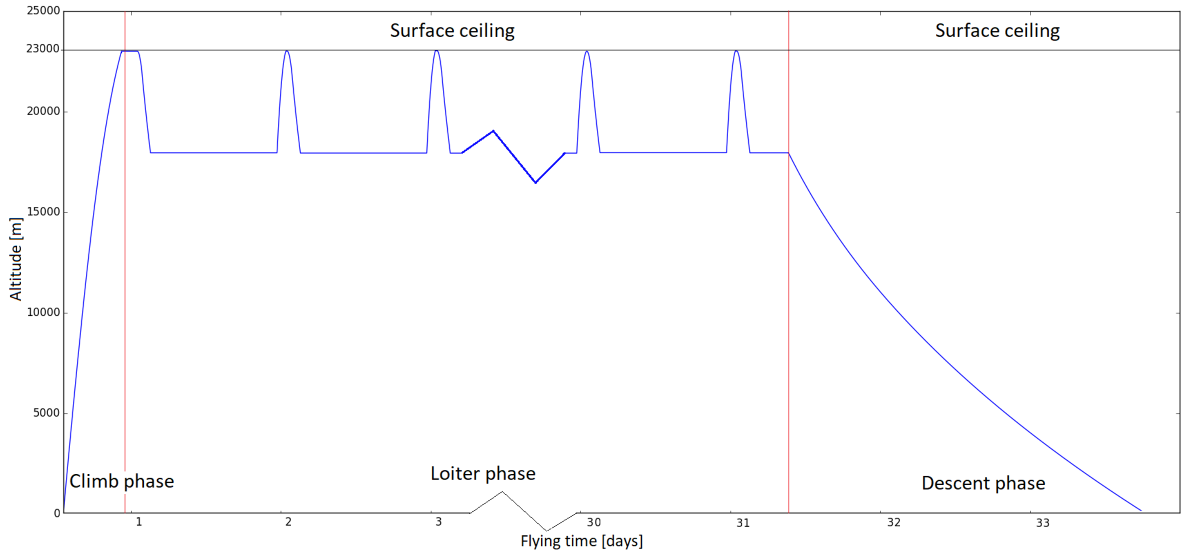

Figure 8.1: Typical mission profile

8.2. Operational considerations

The aircraft will serve as an alternative to satellites and fuel powered drones by providing a continuous presence while at a high vantage point within the atmosphere. In addition, quick deployment time will be possible due to its ease of transportability.

Due to weather limitations and airport availability, the C-17 might need to land some distance away from the desired operational zone of aircraft. Thus, there exists a possibility that it might be faster to fly the aircraft from the home base in the Netherlands to the operational location rather than bring the aircraft with the C-17. Assuming that the assembly of the aircraft takes 8 hours, the C-17 and the aircraft cruise at 800 km/h[1] and 100 km/h respectively, the C-17 should be used instead of direct flight of the aircraft if the flight distance exceeds 1700 km.

If a C-17 deployment is used, the take-off location for the aircraft must be chosen based on multiple factors. First, does the location have enough solar energy reaching it during the day for the aircraft to remain capable of continuing mission after taking-off which is dependent on latitude and day of year. This is visualized in figure 8.2.

[1]URL http://www.af.mil/About-Us/Fact-Sheets/Display/Article/104523/c-17-globemaster-iii/ [Retrieved on 20-6-2017]

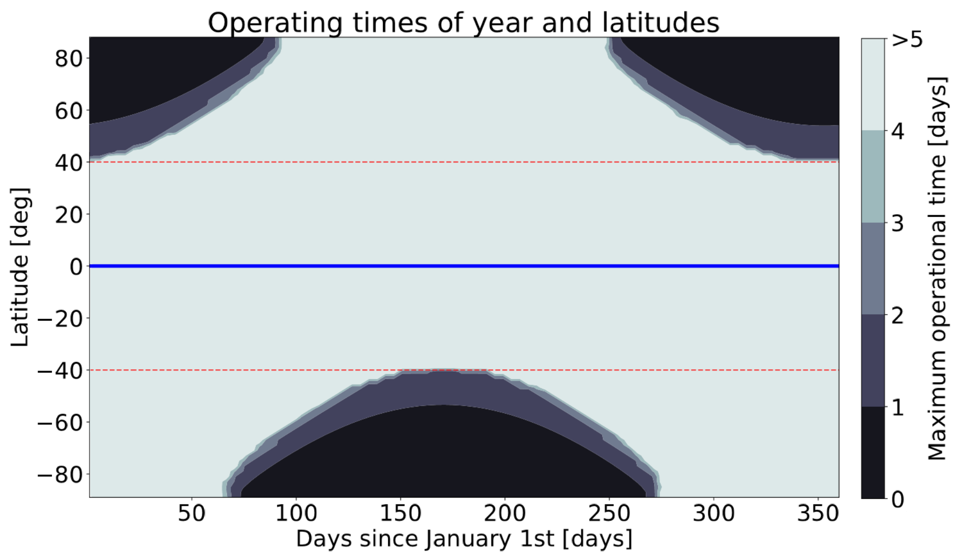

Figure 8.2: Aircraft operational time based on day of year and latitude. An operational time greater than 5 days is theoretically infinite. The blue line indicates 0 latitude (equator) and the red dashed lines the design latitude (40 deg) for the aircraft.

Another important factor for aircraft operation are the weather conditions. The aircraft cannot fly through certain types of cloud cover due to risk of turbulence and precipitation within them. Furthermore, there must be no risk of lighting as the aircraft does not posses the capability to deal with a lighting strike. The wind speed limit for take-off and landing is estimated at 3 on the Beaufort scale or about 5 m/s. Higher wind speeds will be capable of impacting the aircraft's attitude, thus making it dangerous to handle. Figure 8.3 shows that during the most windy time of the year in Mali there is less than 10% probability that wind will be greater than 5 m/s. However, higher wind speeds may be encountered in different locations, so it is recommended that the weather conditions are monitored closely for each stage of the flight.

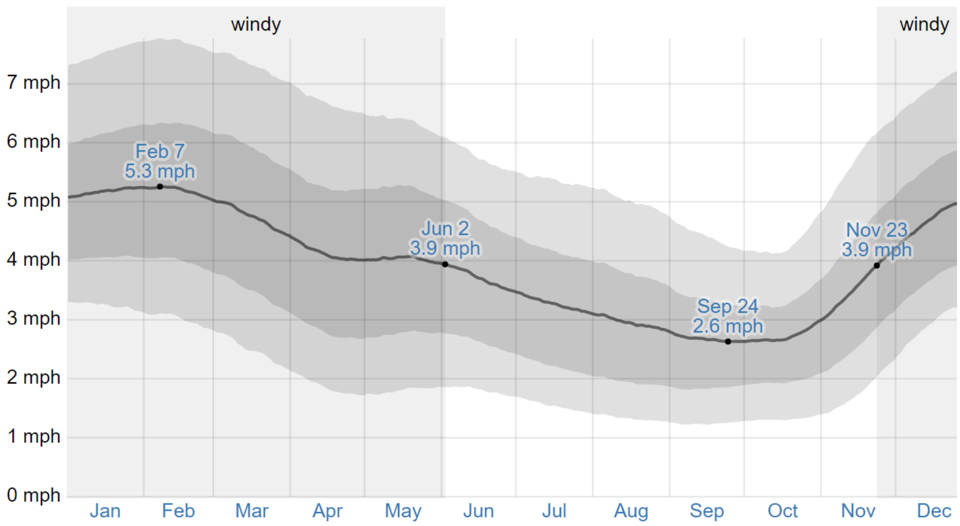

Figure 8.3: Windspeed in Bamako - Mali (RNLAF operating location). Dark gray area limits 10th percentile probability and light gray limits 90th percentile windspeed.

Another factor that is critical for the take-off/landing location is the location of the Jet Stream, which is a high altitude wind usually occurring between 9-16 km above sea level and spanning up to several hundred kilometers.[2] The mean wind velocities within it are between 120-200 km/h with known cases of the wind speed reaching 442 km/h.[3] During winter this phenomena is stronger in the Northern Hemisphere while weaker in the Southern. Figure 8.4 presents the Jet Stream wind speeds during its maximum strength in the Northern Hemisphere. Furthermore, turbulent conditions (Clear Air Turbulence) which could pose a danger to the aircraft can be present.[4] For this reason flying through the Jet Stream should be avoided unless there is a certainty that no turbulence will occur. The Jet Stream can be predicted with good accuracy up to a week, however the accuracy drops with forecasts further into the future.[5]

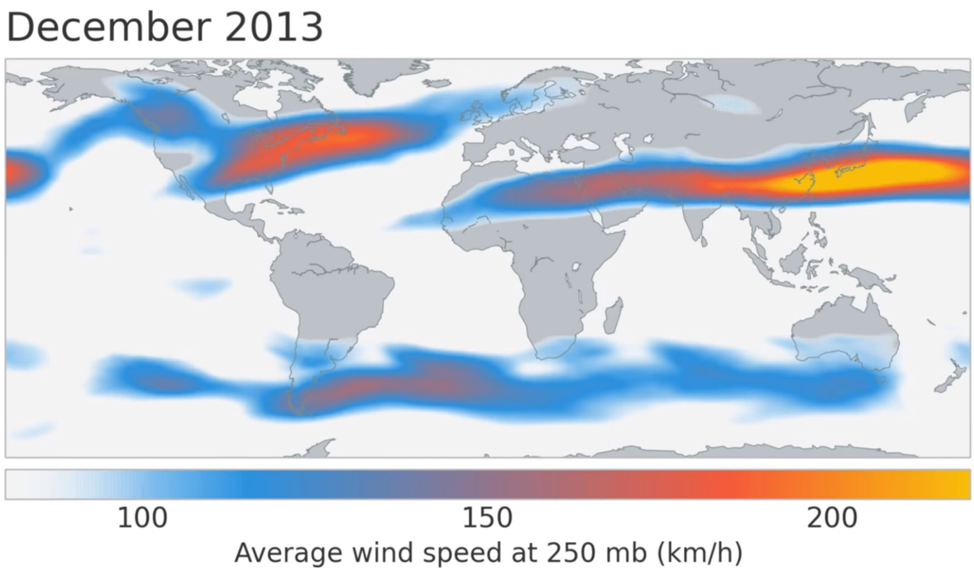

Figure 8.4: Jet stream wind speed for altitude of 10 km [6]

Once a suitable take-off location has been chosen and the aircraft is airborne, the main mission part begins. The flight strategy will be dependent on the payload being carried. However, in general the aircraft should be flown with a minimal amount of turns due to the increase in drag while turning.

Take-off

For take-off, the aircraft shall be situated on top of a trailer pulled by a car. The car will gradually accelerate to above the stall velocity of the aircraft. At that point the aircraft shall have enough lift force to rise from the platform and begin flight. No attachment/release mechanism will be used to connect

[2]URL: http://www.pbs.org/wgbh/nova/balloon/science/jetstream.html [Retrived on 21-06-2017]
[3]URL: http://www.srh.noaa.gov/jetstream/global/jet.html [Retrived on 21-06-2017]
[4]URL: URL:http://www.skybrary.aero/index.php/Jet_Stream [Retrived on 21-06-2017]
[5]URL: http://squall.sfsu.edu/crws/ensemble_fcsts.html [Retrived on 21-06-2017]
[6]URL: https://github.com/barentsen/jetstream.py [Retrieved on 27-6-2017]

the aircraft with the trailer as the take-off can be performed only in low wind conditions. Thus, the aircraft shall be placed unattached on top of the platform. This trailer can be seen in figure 8.5. These pictures are conceptual drawings and no calculations have been done on the structure. The support points can be shifted for- or backwards to account for sweep. The connection point to the car will be a stiff rod/beam. This way the trailer is easier to control than when using cables. The trailer will be approximately 1.5 m high and 25 m in length, with a width of 1 m. For transportation the connection points could be disassembled and put inside of the triangular beam. It is assumed that a truck is available at the takeoff location to pull the trailer and get up to a speed high enough for the aircraft to take-off.

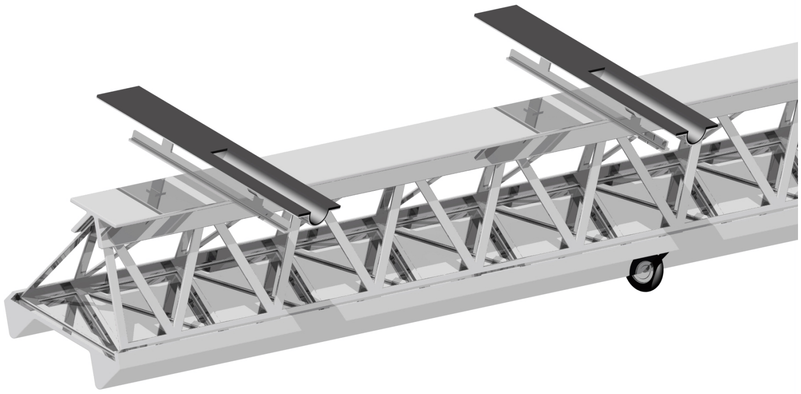

(a) Render of the take-off trailer: focus on support points

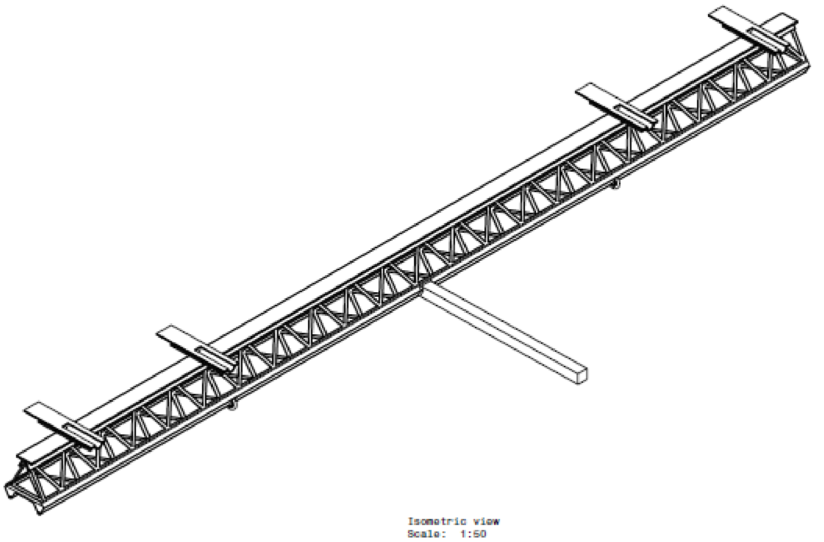

(b) Technical iso-view of the take-off trailer.

Figure 8.5: Renderings of conceptual take-off trailer design.

Landing

The landing shall be performed in low wind speed and non-gusty conditions. When the aircraft is a few meters above the ground the propellers are put in a horizontal position to prevent hitting the ground with the propellers. After coming to a stop the aircraft will be removed from the runway by either towing it or pushing it by the ground crew. Using an analytic method, with a ground friction coefficient of 0.1, gives a landing distance of less than 250 meter.[42] Thus the landing field length of less than 2300 meters of requirement MPS-PLAT-2.1 has been met.

8.3. Transportability and setup

Before the aircraft is deployed, it is stored in a condition that allows for immediate transport. That is, the main structural pieces of the aircraft, two wingtip sections and a mid section shall be kept in boxes. The wing sections contain the ribs, skin, engine pod attachments and solar film, which is not detachable from the wing. The engine pods are kept separately without batteries within them and with engine blades detached. This is done to make the pods accessible for checks and to make it easy to check the batteries, which are a vital component of the aircraft.

Once a decision is made to deploy, the aircraft with the required equipment are loaded onto a C-17 aircraft. This process is expected to take at maximum 4 hours if the aircraft requires fuel transfer (loading and fuel transfer have to be done separately). If not, the loading time is to take about 2 hours and 30 minutes.[43] These time estimates were made assuming that the aircraft to be loaded is considered as oversized cargo, as the wing pieces cannot be palletized due to their large size. A faster loading time may be achieved considering the low weight of the aircraft pieces. Three aircraft can be fit into a single C-17 together with the take-off trailer, as can be seen in figure 8.6, and as such requirement MPS-PLAT-4.1 is satisfied.

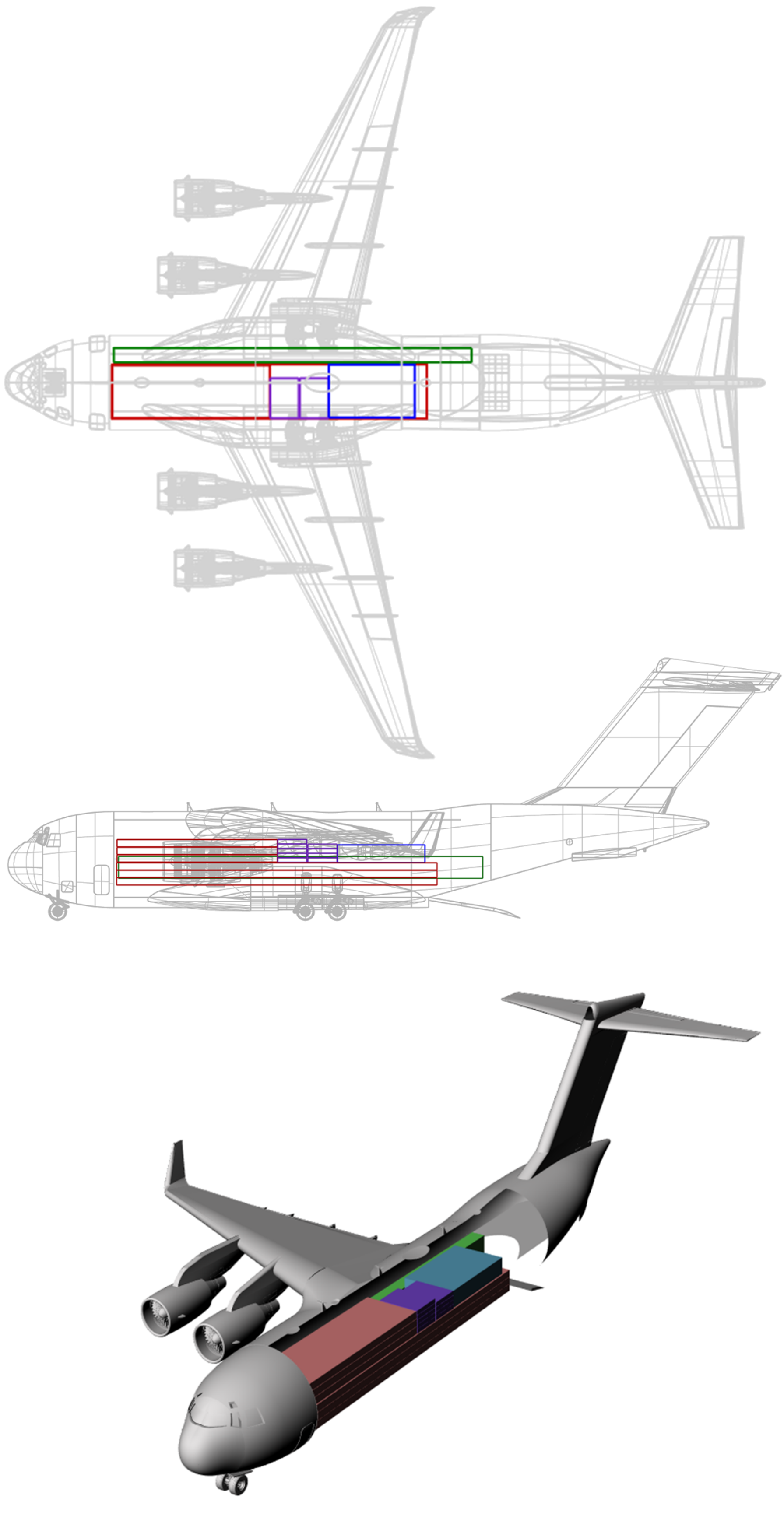

Figure 8.6: Fitting 3 aircraft inside a C-17.

In table 8.1 the dimensions and content of the boxes in figure 8.6 can be found.

Table 8.1: Content of the cargo boxes

	Content	**Dimensions** [mm]
Red box (Big)	2x Winghalves	22000 x 3800 x 500
Red box (Small)	Wing mid-section	11000 x 3700 x 500
Blue	Tools and other equipment	6000 x 3700 x 1200
Purple	2x Engine pod + propeller	2000 x 2800 x 300
Green	Trailer	25000 x 1000 x 1500

After landing, the C-17 is to be unloaded and the aircraft has to be assembled. The time for unloading is estimated at 3 hours. [43]

8.4. Control automation and sensors

In order to fully automate the aircraft, an autopilot module and a variety of sensors is required. GPS will be used in order to determine the position of the aircraft. By combining this information with accelerometers and gyroscopes, the heading and velocity can be obtained. This combination of sensors should be sufficient for the aircraft, except gust states, which are indistinguishable from accelerometer bias. [44] Therefore, a static and dynamic pressure sensor, and angle of attack and side slip angle vanes are added.

The Veronte autopilot by Embention [7] will be used to control the aircraft. This is a lightweight package capable of autonomously controlling the platform and already has GPS, gyroscopes, accelerometers, magnetometers and pressure sensors included. The pressure sensors, however, are not sensitive enough to measure the low static pressure at 50,000 ft. Therefore, external pressure sensors will be added, as well as angle of attack and side slip angle sensors. For each sensor a simple op-amp based amplifier can be used to attenuate the output voltage into the analog input range for the autopilot controller (0-3V). A simple lightweight camera is added to the system as well, such that, if needed, the operator has a visual aid when manually controlling the system.

Finally, for the elevons and drag rudders, actuators need to be present in the system in order to operate these devices. Furthermore, an electronic speed controller is needed to control the output power, and thus the thrust, of each engine.

Communication, navigation and antennas

In order to control the aircraft, a data link with the ground station is needed. For operation of the aircraft in the vicinity of the ground station a line of sight (LOS) half-wave antenna, design for 900 MHz is used. As this antenna is omnidirectional, there is no need for a pointing mechanism. This LOS communication system allows contact with the ground station within a 90 km radius, allowing for a

[7] URL:https://products.embention.com/veronte/uav-autopilot [Retrieved on 7-6-2017]

live feed of telemetry and payload data, as well as manual control.

Furthermore, a satellite communication system will be included for beyond line of sight (BLOS) communications. This BLOS system will be based on the iridium network, which has world wide coverage. It will be a low bandwidth system which is used to send navigation and payload commands. Furthermore, this system is used to send back telemetry data, such as aircraft location, to the ground station. However, the bandwidth is not sufficient to give a live feed or to transmit output from the on-board camera. Therefore; either a relay system needs to be used, allowing the LOS antenna to be used, or a separate data link for the payload is needed. Such a separate BLOS data link will, in that case, be part of the payload package.

In figure 8.7 the communication flow diagram can be seen, visualizing the flow of data through the system.

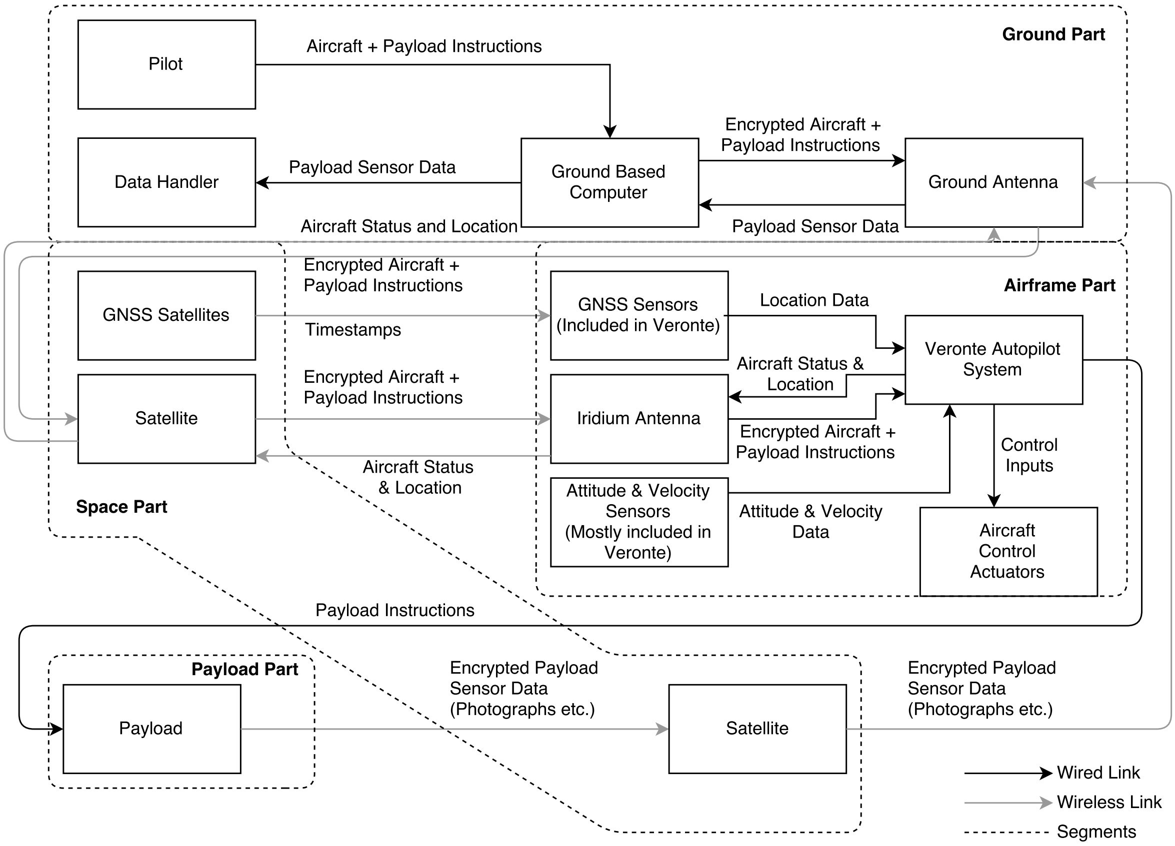

Figure 8.7: Communication flow diagram of the system

8.5. Hardware/software integration

In the aircraft, different types of hardware and software have to work simultaneously and sometimes together to perform the different tasks. How these systems are integrated, can be seen in figure 8.8. On the Veronte autopilot system, one can attach different types of actuators and even thermometers, as there are 5 analog inputs and 4 digital inputs as well as 12 digital PWM outputs and a usb connection which can be used. One can program the Veronte autopilot system for different applications.

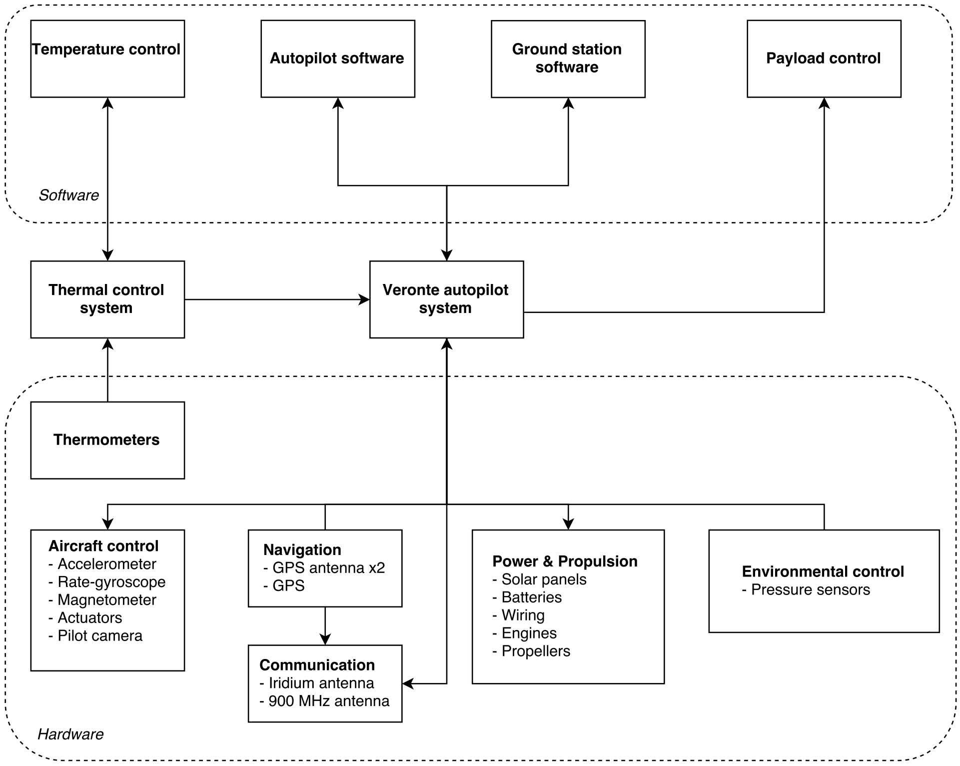

Figure 8.8: Hardware/software integration

A more detailed block diagram showing the data handling of the autopilot can be found in figure 8.9. As described in section 8.4 the LOS- and Iridium antenna's will be used for aircraft and payload commands and control. They will also be used to receive aircraft status updates such as location and possible failures. The payload measurements will be communicated through a separate communication system in the payload.

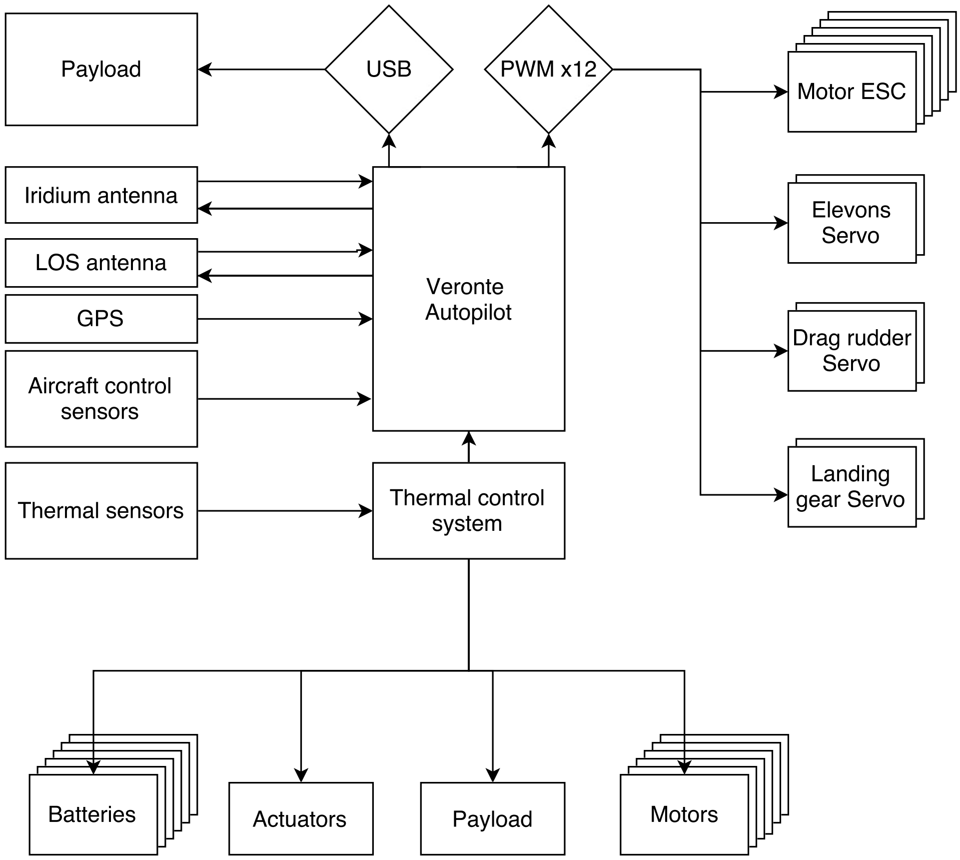

Figure 8.9: Data handling diagram of the autopilot

8.6. Ground station

The ground station for the aircraft consists of several elements. Firstly, a tracker antenna is used for the LOS communication with the aircraft. As this is a high gain antenna, a higher bandwidth can be achieved than with a omni-directional antenna. Furthermore, a Veronte Autopilot CS is used as interface between the aircraft and a control PC. This device is capable of controlling the tracker antenna, as well as weather stations, alarms and similar systems. Also, the on-board sensors allow more advanced flight commands on the aircraft,such as flying home and following the ground station.

A regular PC is used to control the Veronte Autopilot CS. The Veronte Pipe Software allows full control of the aircraft from a computer. When controlling up to ten aircraft it is recommended to have multiple monitors available, such that a map view of all aircraft, as well as telemetry data can be viewed at the same time. When operating using BLOS communication, this computer system does not need to be placed in the area where the system is operated. Instead, the system can be operated form an airbase in the home country. This ground station could be build into a container-like homebase, with antenna and air-conditioning unit. The advantage of doing this, is the possibility of moving this ground station to the crisis zone, when required. A concept of the ground station is rendered in figure 8.10. This type of ground station requires less personnel to be deployed and reduces the cost of a mission, as well as decreasing the amount of required protection and space at the crisis zone. For quick deployment of the system, a Veronte HCS Suitcase can be used for operation with LOS communication. This allows the system to be used without setting up a ground station. Such a suitcase system will be used for testing the aircraft on the ground and for hand-control during take-off and landing, if necessary.

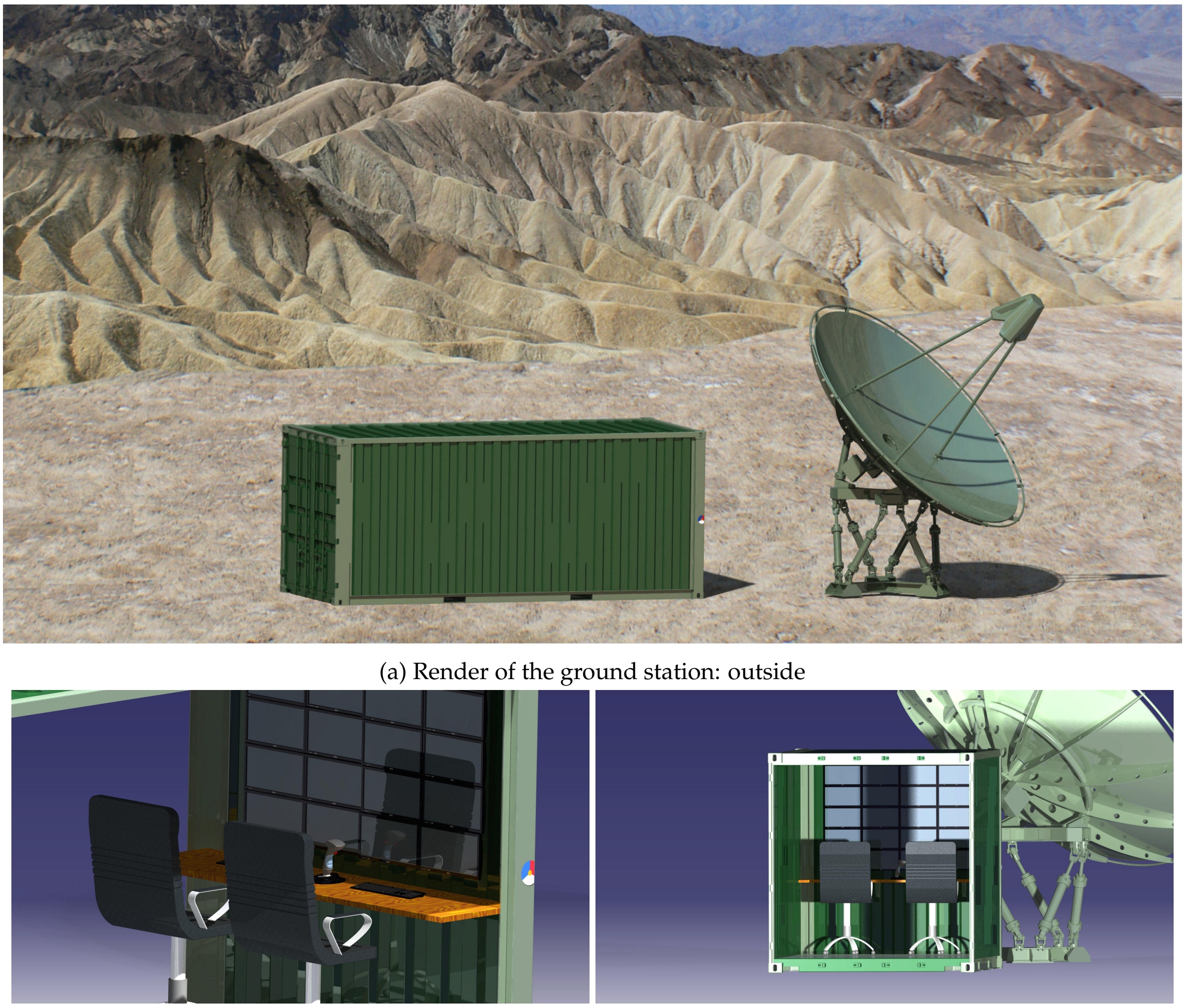

(a) Render of the ground station: outside

(b) Render of the ground station: desk

(c) Render of the ground station: inside

Figure 8.10: Rendering of the ground station.

9. Design Evaluation

To ensure that the aircraft is able to perform its mission within the design constraints, the design is evaluated in this chapter. First the main parameters are summarized in section 9.1. Afterwards the most important drawings of the design are shown to increase clarity in section 9.2. After this the compliance with the requirements is checked in section 9.3. In section 9.4 the reliability, availability, maintainability and safety (RAMS) of the design is analyzed. Finally the assumptions made during the design are checked on their sensitivity in section 9.5.

9.1. Main parameters

The technical design of the aircraft is strongly driven by the combination of high-altitude and long endurance flight. The flying wing aircraft is designed to cruise for 30 days between 18 and 23 km and can reach distances of up to 72,000 km during its 30 day flight, at an average cruise velocity of about 100 km/h.

The aircraft reaches cruise altitude in 9 hours, 20 minutes. During the day the solar panels charge the batteries and the aircraft ascends to 23 km. Using its batteries and the gained potential energy the aircraft flies through the night while descending back to 18 km.

It reaches the endurance because of a combination of low weight and an fully electrical power train. The structure weighs 140 kg, the power train 131 kg, a payload of 25 kg and other systems add up to 37 kg. The structure consists of a carbon fibre, circular rod carrying all torsional and bending loads. The rod weighs 58 kg and carries the 41 kg skin and ribs. The rod is split into 3 parts for transportability in the C-17 and is fitted together using 10kg joints. The structure is designed using a load factor of 4. It also carries the total of 13 kg landing gear in the circular pods.

These 6 cylindrical pods positioned at 30%, 49%, and 68% span also hold the engines and batteries. An overview can be found in section 7.7. The 6 brushless DC engines produce 80 N of thrust and an run at 93% efficiency using 2 m diameter fixed pitch propellers. The total propulsion train has a 78% efficiency. The engines are powered by their corresponding battery pack which are discharged to 20%, and charged by 78 m^2. Alta solar film with an efficiency of 31.6% is used in the design. This energy is used to power the engines and is stored in batteries with a specific energy of 450 Wh/kg.

All these subsystems come together in the wing. The aircraft has a surface area of 83 m^2 and a span of 45.6 m. A sweep angle of 20 degrees, a taper ratio of 0.6 and a twist angle of 1.8°(root to tip) are incorporated to ensure stability and trim. While cruising L/D equals 52 at a $C_{L_{cruise}}$ of 0.8. To add some yaw stability the aircraft is equipped with relatively small wing tips which are 0.7 m high. For longitudinal and lateral control the aircraft has elevons measuring 0.2c and 0.52$\frac{b}{2}$. The drag rudders also measure 0.2c and 0.45 m. They are positioned as close as possible towards the wingtip for maximum control capabilities. More about the aircraft controllability can be found in section 5.2.3.

Finally, the aircraft entails a range of smaller subsystems. It is equipped with passive and active thermal control to optimize battery performance. Navigation and communication is done by the Verone autopilot system by Embention. The payload is removable and interchangeable from the nose of the aircraft using a rail system and provides it's own communication link. Take-off will be performed using a trailer towed by a car or truck.

Some of the most important weights and parameters are listed in table 9.1.

Table 9.1: Summarized final design

Parameter	Value	Parameter	Value	Parameter	Value
S [m^2]	83	$\mathrm{M_{to}}$ [kg]	307	$P_{cruise_{shaft}}$ (18 km) [kW]	2.1
AR [-]	25	$\mathrm{M_{oew}}$ [kg]	283	$P_{cruise_{shaft}}$ (23 km) [kW]	3.2
b [m]	45.6	$\mathrm{M_{structure}}$ [kg]	139	$P_{climb_{shaft}}$ [kW]	4.5
Taper ratio [-]	0.6	-$\mathrm{M_{Rod}}$ [kg]	58	$\eta_{Solarpanels}$ [%]	31.6
Tip chord [m]	1.3	-$\mathrm{M_{Ribs}}$ [kg]	20	$\eta_{Batteries}$ [%]	98
Root chord [m]	2.2	-$\mathrm{M_{Skin}}$ [kg]	23	$\eta_{Propulsiontrain}$ [%]	78
$\mathrm{Sweep_{LE}}$ [deg]	20	-$\mathrm{M_{landinggear}}$ [kg]	13	$\eta_{Propeller_{cruise}}$ [%]	85
t/c [%]	18	$\mathrm{M_{Powertrain}}$ [kg]	131	$\eta_{Propeller_{climb}}$ [%]	75
W/S [N/m^2]	35.8	-$\mathrm{M_{Solar}}$ [kg]	19	η_{Engine} [%]	93
W/P [N/W]	0.89	-$\mathrm{M_{Power\ storage}}$ [kg]	92	Number of engines [-]	6
L/D [-]	52	-$\mathrm{M_{Propulsion}}$ [kg]	14	Propeller diameter [m]	1.5
$C_L^{\frac{3}{2}}/C_D$ [-]	45	$\mathrm{M_{other}}$ [kg]	12		
$\mathrm{V_{cruise}}$ (18 km) [m/s]	26	$\mathrm{M_{payload}}$ [kg]	25		

9.2. Drawings

Overview drawings of the aircraft can be found in figure 9.1 and figure 9.2. The drag rudders and elevons can clearly be seen near the wingtips in detail A. The main landing gear, together with one of the engines can be seen in detail B. Furthermore, the payload bay and middle landing gear can be seen in detail C. Detail D shows the size of the wingtips. Figure 9.3 shows one of the engine pods containing the landing gear, and all internal components. The tubing in this pod is to transport the air for cooling through the pod. Finally, the breakaway cover under the landing gear can be seen.

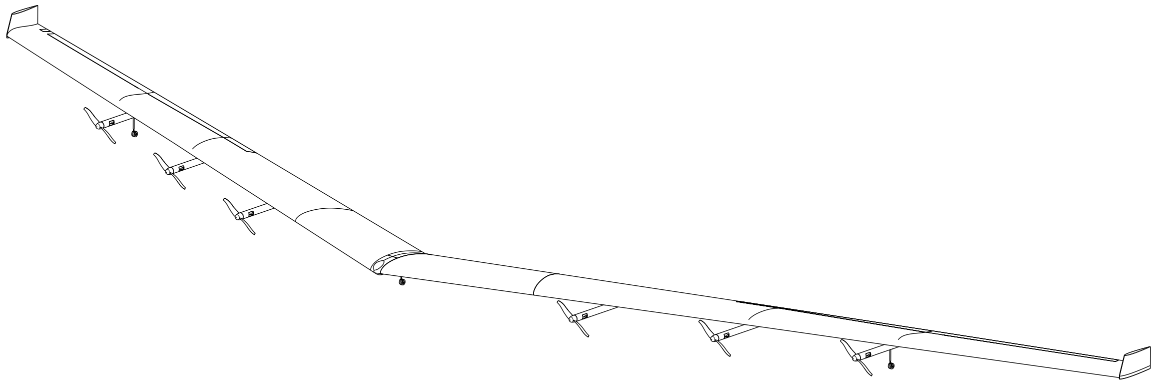

Figure 9.1: Isometric view of the aircraft.

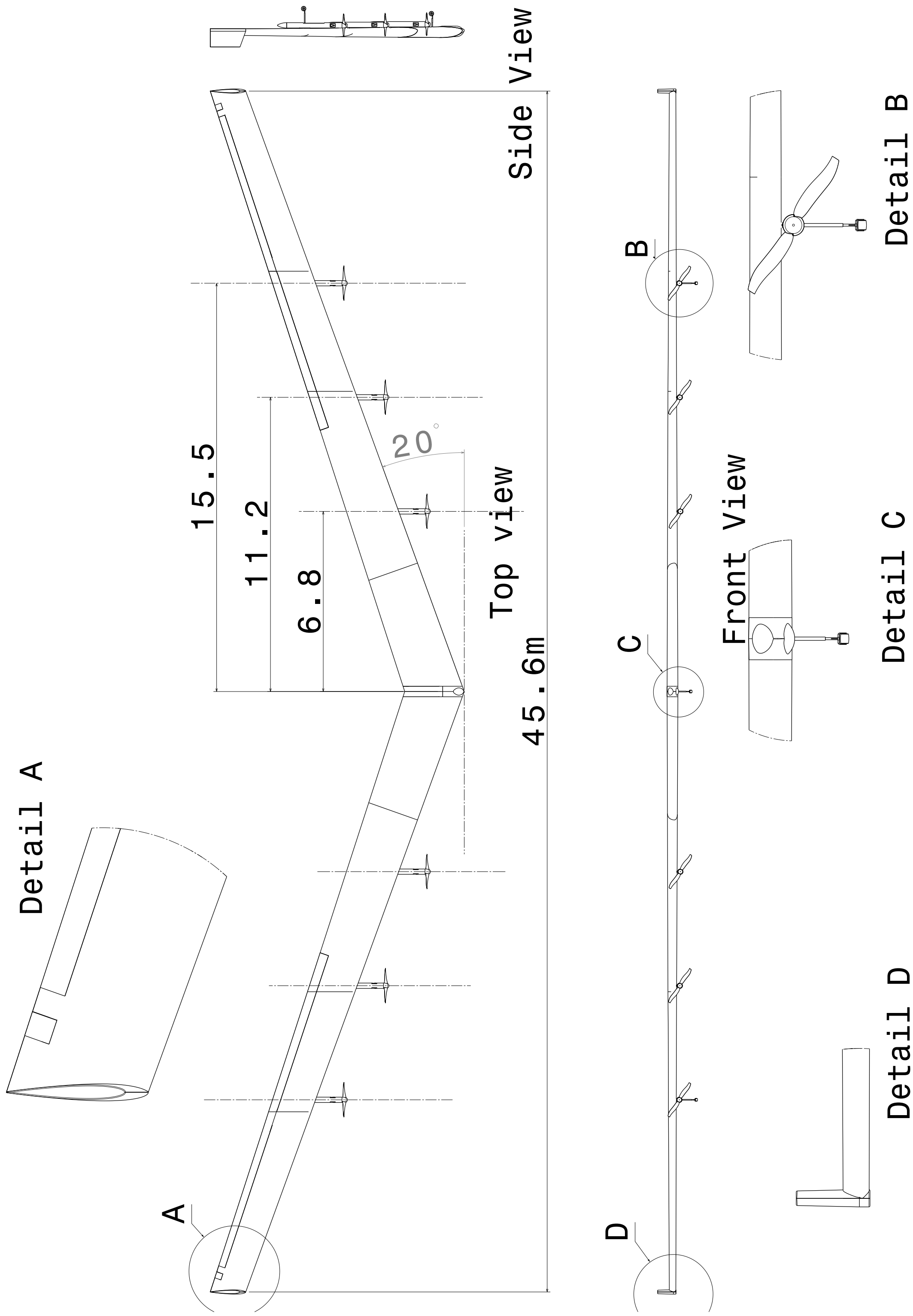

Figure 9.2: An overview of the outer shape of the aircraft.

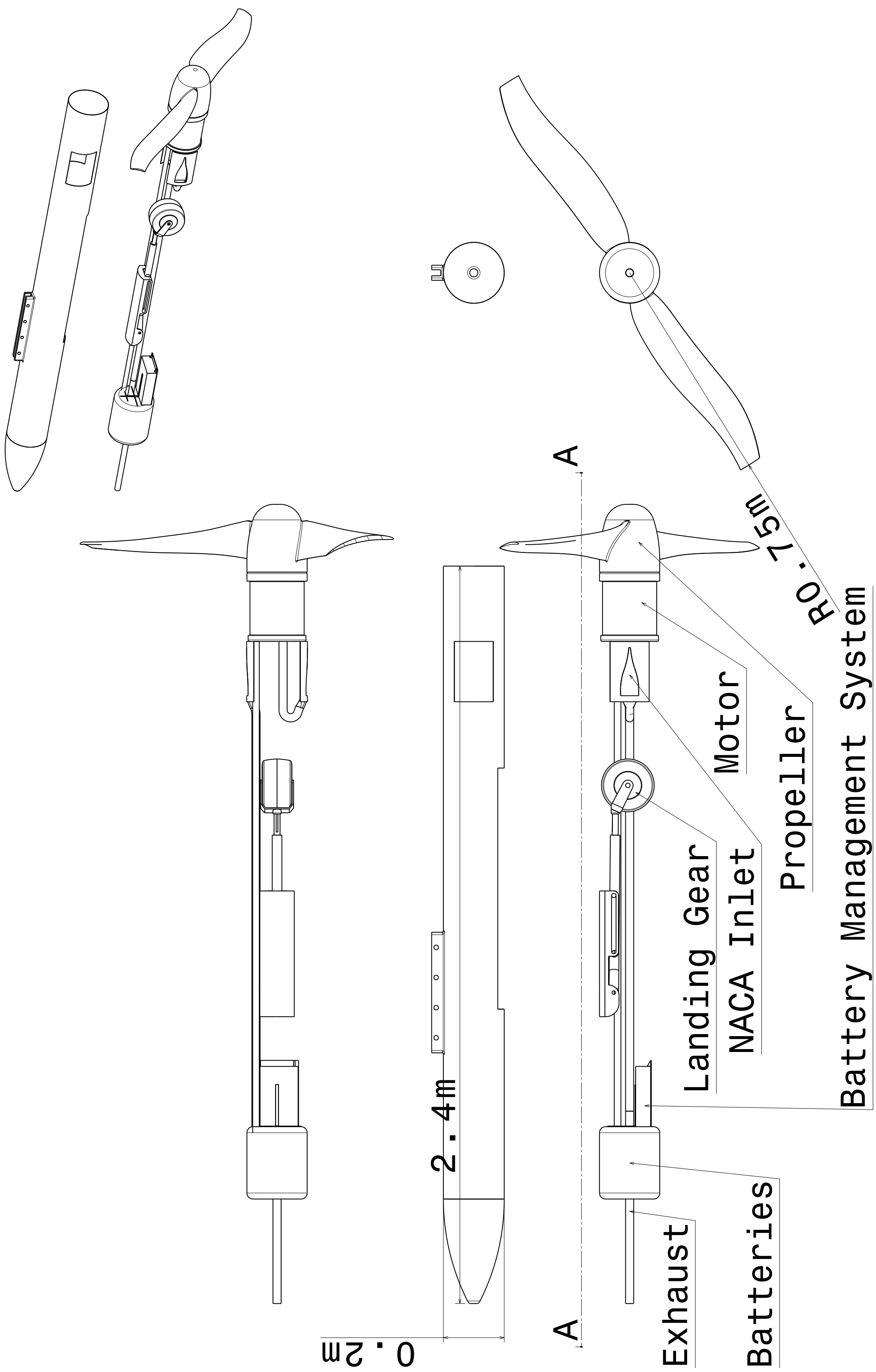

Figure 9.3: An overview of one of the outer engine pods, including internal components.

9.3. Compliance Matrix

Table 9.2 shows which requirements are fulfilled by the design (✓), which are not (**x**) and which requirements can not be evaluated yet (**-**). After that, the reason for potential scores in these last two categories are explained.

Table 9.2: Compliance matrix

Number	Requirement	
MPS-FLT-1	The station keeping altitude shall be more than 50,000 ft.	✓
MPS-FLT-2	The loiter time of the aircraft shall be more than one month, unrefuelled.	✓
MPS-FLT-3	The mission radius shall be more than 800km.	✓
MPS-FLT-4	The aircraft should be operable year-round between $\pm$ 40° latitude.	✓
MPS-FLT-5	The aircraft shall be able to climb to its ceiling in 9 hours, 20 minutes	✓
MPS-PLAT-1	The aircraft shall be able to fly autonomously.	✓
MPS-PLAT-2.1	The take-off and landing field length shall be less than 2300 m.	✓
MPS-PLAT-2.2	The aircraft shall be able to take-off from a gravel surface.	✓
MPS-PLAT-3	The operational lifetime shall be more than 20,000 flight hours.	✓
MPS-PLAT-4.1	Three aircraft with support material shall fit in the cargo hold of one C-17.	✓
MPS-PLAT-4.2	The weight budget of the total system to be transported with the C-17 shall be less than 77,000 kg.	✓
MPS-PLAT-5	The preliminary design shall be a fixed-wing aircraft.	✓
MPS-PLAT-6	The platform shall be operational in a temperature range of $\pm$70° Celsius.	✓
MPS-PLAT-7	The clearance angle during take-off and landing shall be more than 3°.	✓
MPS-PLD-1	The aircraft shall be able to continuously provide 400 W of power to the payload.	✓
MPS-PLD-2	The aircraft shall be able to support a payload of 25 kg.	✓
MPS-PLD-3	The on-board computer shall be able to store up 500 GB worth of data.	✓
MPS-PLD-4	The payload shall include its own telecommunication system for receiving and sending data.	✓
MPS-PLD-5	The aircraft shall be able to carry a payload which is no larger than 40 cm in diameter and 50 cm in length.	✓
MPS-PLD-6	The payload shall be positioned to obtain a clear view towards the ground.	✓

MPS-COST-1	The fly-away cost per aircraft shall be less than €10 million.	✓
MPS-COST-2	The ground station cost shall be less than €30 million.	✓
MPS-COST-3	The maintenance and take-off material cost shall be less than 10% of the aircraft cost.	✓
MPS-COST-4	The annual maintenance cost shall be less than 5% of the aircraft cost.	✓
MPS-PRD-1	75% of the total design & production cost shall be contracted to Dutch parties.	X[1]
MPS-PRD-2	The system shall enter service in 2023.	✓
MPS-PRD-3.1	The production of the complete system shall be carried out with zero effective CO_2 emissions.	✓
MPS-PRD-3.2	No production processes shall be employed where toxins or other environmentally harmful by-products are being produced.	X[2]
MPS-MISC-1	A fleet of 10 aircraft shall be able to be controlled by 2 operators.	✓
MPS-MISC-2	The third-party probability of fatal injury shall be lower than 10^{-9} per hour.	–[3]

1. The biggest reason for not complying to this requirement is the expenditure on solar panels. High-efficiency solar panels are not available from Dutch manufacturers causing all of this expenses to be ordered from Alta devices, an American company.
2. The production of both solar panels and batteries can not be carried out using non-toxic products. This is the case for both the high- and lower efficiency systems, as explained in section 6.1.
3. The third-party probability of fatal injury is not yet assured in this design phase as this relies on a more detailed design of the complete structure. The required failure rates for these components are evaluated in section 9.4.4.

9.4. RAMS analysis

The final evaluation done on the conceptual design is on Reliability, Availability, Maintenance and Safety (RAMS). A good implementation of these criteria early in the design stage is vital to creating a good design. The reliability of the system is discussed in section 9.4.1, followed by the analysis of the availability in section 9.4.2. Next, the maintainability is addressed in section 9.4.3 and finally the safety is discussed in section 9.4.4.

9.4.1. Reliability

According to [45], reliability is defined as '...the probability that a system will perform in a satisfactory manner for a given period of time ...'. In other words, reliability is the probability that the aircraft will be able to fulfill its mission. This depends on the functioning of all of the different subsystems. All critical systems have a redundancy. The servos for example are one time redundant, while the autopilot is three times redundant. For the structure, the system is made redundant through the use of a safety factor. However the aircraft will immediately return to base in case of a failure in a critical component, even if it would technically still be possible to complete the mission (see section chapter 8). This is done to ensure safe operations at all times. The critical systems that can cause mission failure are shown in figure 9.4. Note that the aircraft will also return to base in case of a payload failure, but since the payload will be designed by the air force or potential other customers themselves, this is not taken into account here.

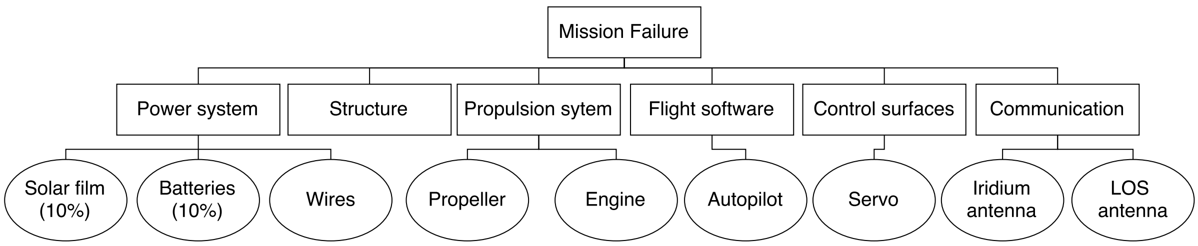

Figure 9.4: Critical systems that can cause mission failure

The "10%" values under the batteries and solar panels indicate that this system is only determined to 'fail' once 10% of the power (stored or generated, respectively) is lost due to this failure, unless it can not fly continuously with this loss of power. A failure can for example occur when all of the systems connected to one engine pod fail. For all other systems, which have a lot less redundancy, a single part failure will always cause the aircraft to return to base or look for a safe landing site in case a return to base is not possible.

To estimate the chance of a mission failure, each of these critical subsystems is analyzed and a failure rate is estimated. This rate is very dependent on the design, so it should be taken into account in the future project. The table with failure rates is shown in table 9.3. As described in chapter 8 , the autopilot is three times redundant, and as such a single failure will not directly cause a crash. However, a single failure in the autopilot is indicative that there is a fault within the system. For the structure, there are many causes which can cause failure. For this preliminary design phase, the failure rate is taken from general UAV statistics. All of the failure rates should be updated in future design phases once more information is available.

Table 9.3: Failure rate of critical subsystems

System	**Failure rate** $[1/hr]$	**System**	**Failure rate** $[1/hr]$
Solar flim (Cell)	$9.8 \cdot 10^{-5}$ [46]	Propeller	10^{-7} [47]
Solar film (10%)	$\approx 1 \cdot 10^{-10}$	Engine	$2.6 \cdot 10^{-8}$ [48]
Batteries (Cell)	$7.5 \cdot 10^{-5}$ [13]	Autopilot (single failure)	10^{-6} ([1])
Batteries (10%)	$\approx 3.6 \cdot 10^{-9}$	Servo (single failure)	$5 \cdot 10^{-5}$ [24]
Wires (short circuit)	$2.5 \cdot 10^{-8}$ [24]	Iridium antenna	$6.5 \cdot 10^{-7}$ ([2])
Structure	$5 \cdot 10^{-6}$ [24]	LOS antenna	$1.38 * 10^{-4}$ [24]

To find the mean time between failure (MTBF), all failure rates are added and the inverse of that outcome is taken. This leads to a MTBF of 5157 hours. The weak points in the system are the LOS antenna and the Servo's, even though these are one time redundant as well. Since the LOS antenna is only used during landing and possibly during take-off and testing, it is only active for less than 10% of the time. Therefor, the failure rate per aircraft flight hour is reduced by a factor 10. If one of the line of sight antenna's need to be replaced during the operational lifetime of the aircraft, this system is easily accessible. Other systems are not expected to fail within their first 20000 operational hours, although the possibility is of course always there. However, with proper maintenance and inspection, the operational lifetime should easily surpass the 20000 hour requirement (except for the batteries, as described in section 6.1).

9.4.2. Availability

The availability can be expressed as a percentage using the MTBF and Mean Down Time (MDT) and equation (9.1). The MDT includes all the possible moments when it is not flying, so repair, failure repair but also logistics. How the MDT is determined can be seen in table 9.4. With this, an availability of 99% could be found. This value might seem very high, but that is mostly due to the very long endurance, due to which the MDT is relatively low. [24]

$$A = \frac{MTBF}{MTBF + MDT} \tag{9.1}$$

[1]URL: https://www.embention.com/en/news/redundant-autopilot-for-drones [Retrieved on 23-6-2017]
[2]URL: https://www.novatel.com/support/known-solutions/mtbf-specifications-for-gps-700-series/ [Retrieved on 23-6-2017]

Table 9.4: Maintenance tasks and the estimated times

Task	**Time**
Repair & maintenance	1-3 days
Failure	1-3 days
Logistic tasks	
Disassembly	2 hours
Packing	2 hours
Load C-17	2 hours
Fly C-17	1-15 hours[3]
Unload C-17	2 hours
Unpack	2 hours
Assembly	2 hours
Checks	2 hours

9.4.3. Maintainability

Maintainability can be quantified by means of the Mean Time To Repair (MTTR). This is the average time it takes to repair one component or device. For this system, the after flight MTTR equals 5.6 hours. All the maintenance tasks and their estimated times can be found in table 9.5. For the propeller and battery pods, this time can be very short if there are extra pods at the ground base, so maintenance on those pods can be performed when the aircraft is simply flying with other pods. The rod, rib and propeller repair can take up a long time if material has to be produced, so in an ideal situation, there are always spare parts. The times have been split in pre-flight and after flight scenarios, the latter of which includes more detailed inspection and repairs. There are tasks that can be performed simultaneously.

Due to degradation, the batteries will need to be replaced approximately every 5000 flight hours. This can be done quickly if replacement pods are available at the landing location. In this case, the replacement pods can be placed in the aircraft after which the batteries in the dis-attached pods can be changed in the workshop. The aircraft skin will be easily and regularly inspected. The rod and other stress-carrying structures on the other hand are more difficult to inspect since the skin will have to be removed. As they have been designed to withstand fatigue (similar to other composite aircraft), detailed inspection of the carrying structure will only be required in very large (D-type) checks. In commercial airliners, this can be after 30,000 flight hours[4], which is already beyond the required life-time for this platform. Therefore; detailed inspection of the rod has been omitted from the regular maintenance checks.

[3]URL: http://janes.ihs.com/Janes/Display/1343224#[Retrieved on 24-6-2017]
[4]URL: https://www.lufthansa-technik.com/aircraft-maintenance [Retrieved on 23-6-2017]

Table 9.5: Maintenance tasks and the estimated times

Maintenance	Preflight	After flight
Skin inspection & replacement	2 hours	24 hours
Solar film inspection & replacement	2 hours	24 hours
Rod inspection & repair	2 hours	6 hours
Rib inspection & repair	2 hours	6 hours
Landing gear inspection & repair	-	2 hours
Control surface inspection & repair	1 hour	2 hours
Payload inspection and/or change	1-2 hours	1-2 hours
Propeller and battery pod inspection & repair	2 hours	24 hours
Autopilot inspection & testing	1 hour	1 hour
Thermal and electrical wiring system inspection	1 hour	6 hours
Attachment / connections inspection & repair	1 hour	4 hours
Perform ground test (i.e. control surfaces)	1 hour	2-3 hours
Ground system inspection & repair	1 hour	2 hours

In case of large failure, where for example the rods or the ribs are damaged beyond easy repair, the aircraft will have to be moved to the Netherlands for repair.

9.4.4. Safety

To keep a high standard of safety, the system should be as much free from possible hazards as possible. These hazards do not only occur from system failures; human errors, environmental conditions and simply an unsafe design may also cause unsafe situations. These situations can occur in any phase of operations, even during the downtime. However, as the take-off, landing, maintenance and transport only involves trained staff, no unsafe situations should occur during these phases if the safety regulations are followed. Third-parties, such as the local population, can only be involved during failures in the airborne phases. The events that can lead to fatal injury of third parties are indicated in the fault tree in figure 9.5. Events that can occur under the 'catastrophic' failure are for example an on-board explosion, which is extremely unlikely given that there are no fuels on board. Autopilot failure can include a complete shutdown of the system and redundant systems or a wrong interpretation of the waypoints. Note that pilot error and environmental conditions are not included in the fault tree as these factors don't stem from the reliability of the aircraft itself.

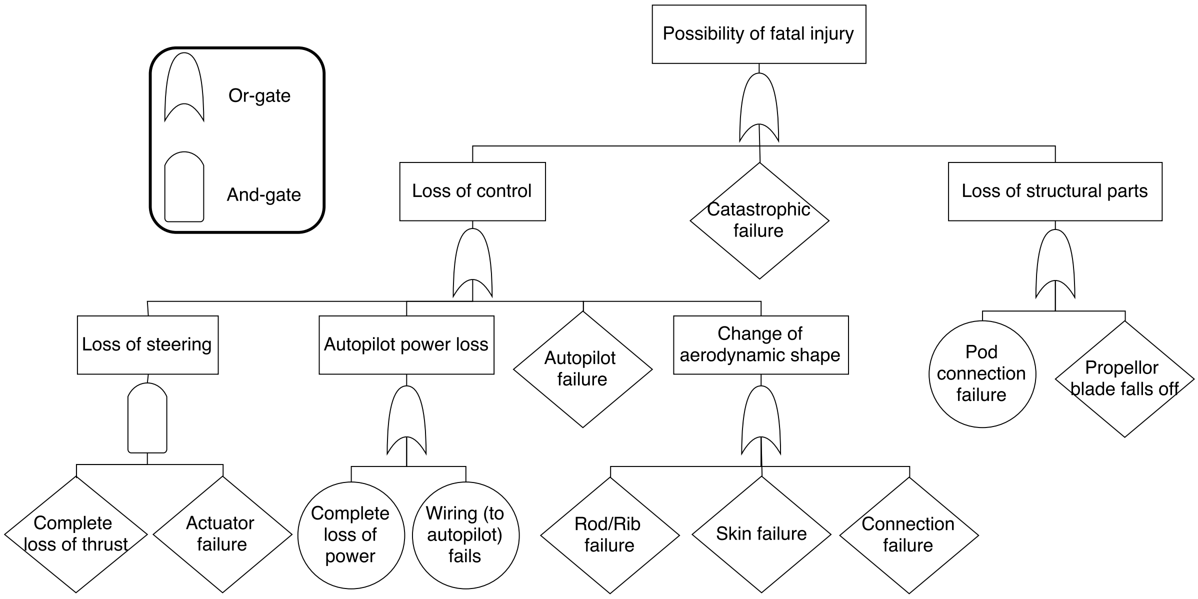

Figure 9.5: Fault tree with failures that can result in casualties.

Some of the failure modes that can lead to fatal injuries are already have a known failure rate. To quantify the maximum failure rate for the other failure possibilities, equation (9.2) from Weibel is used [49]. From Weibel it can be found that the Espected Level of Safety (ELS) should be 10^{-7}. Filling in the variables in this equation (which come from the requirement) and with an average population density of $56.6 people/km^2$ [5], it is found that the MTBF equals $1.59 \cdot 10^6$ hours for failures that can cause fatal injuries.

$$MTBF = \frac{\rho_{people}}{ELS} A_{exp} P_{fatal} \tag{9.2}$$

This MTBF leads to a failure rate of approximately $6.29 * 10^{-7}$. This is very low when compared to the average rate of losses of UAV's, which is close to 1 every 10000 flight hours. However, that includes small and cheap consumer-targeted UAV's which do not make use of aerospace-grade components. A better comparison is made with regional airliners, which have a Class A mishap rate (where the aircraft is destroyed and fatality is very likely [6] close to 10^{-7}. [24] This is much closer to the required failure rate for the current design. In table 9.6, the (required) failure rate for all of the different causes in figure 9.5 is given. Some of these are already known from the reliability analysis in section 9.4.1, while others function as a requirement for the detailed design.

[5]URL: http://data.worldbank.org/indicator/EN.POP.DNST [Retrieved on 21-6-2017]
[6]URL: http://www.public.navy.mil/NAVSAFECEN/Pages/statistics/mishap_def.aspx [Retrieved on 22-6-2017]

Table 9.6: Required failure rate of different subsystems

Known failure rate		Required failure rate	
System	**Failure rate** $[1/hr]$	**System**	**Failure rate** $[1/hr]$
Loss of steering	≈ 0	Catastrophic failure	10^{-8}
Complete loss of power	≈ 0	Loss of structural parts	10^{-8}
Wiring (to autopilot) fails	$3 \cdot 10^{-8}$	Severe change of	
Autopilot failure (4x)	10^{-7}	aerodynamic shape	$4.8 * 10^{-7}$

The loss of structural parts and catastrophic failure are cases that should absolutely be avoided. Therefore, these are given a value of 10^{-8}. A complete loss of steering and a complete loss of power is very unlikely, as these systems are very redundant and have multiple causes that all need to happen simultaneously. Therefore the failure rate of these events is set to 0. This leads to a maximum rate of failure where the aerodynamic shape is changed severely of $4.8 \cdot 10^{-7}$, which is higher than the typical structural reliability described in table 9.3. Therefore, the structure should be particularly well designed in order to meet the fatal injury requirement.

9.5. Sensitivity Analysis

A sensitivity analysis is performed to find the effects of the assumptions which were made during the design process. For this process, one assumed parameter of the design was changed and the resulting design was evaluated. In sections 9.5 and 9.5 it can be seen that especially the battery density is an important factor in the complete design. Therefore; thorough research should be done early in the next design phases to make sure that this assumption is valid.

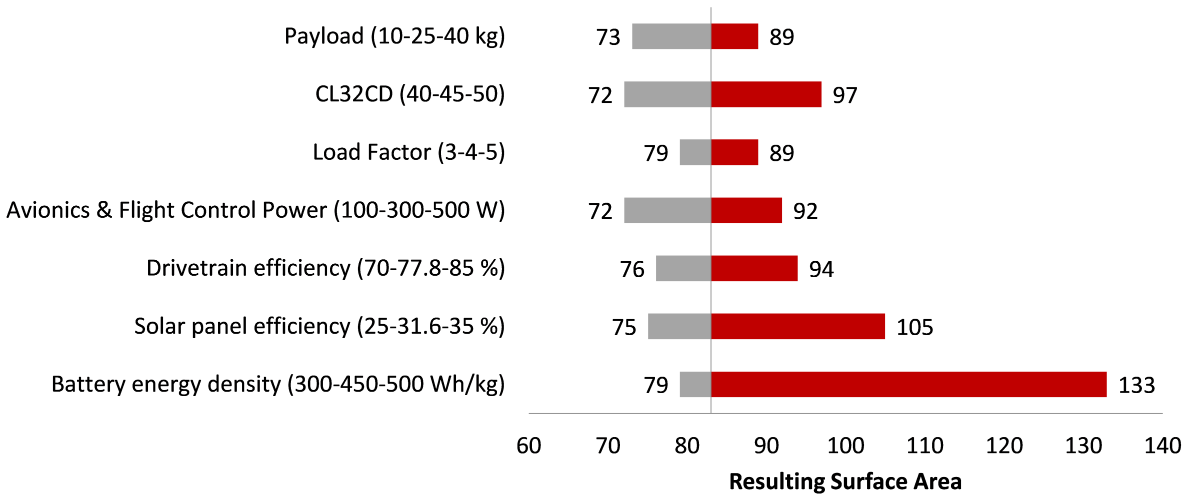

Figure 9.6: Effect of assumptions on resulting wing area.

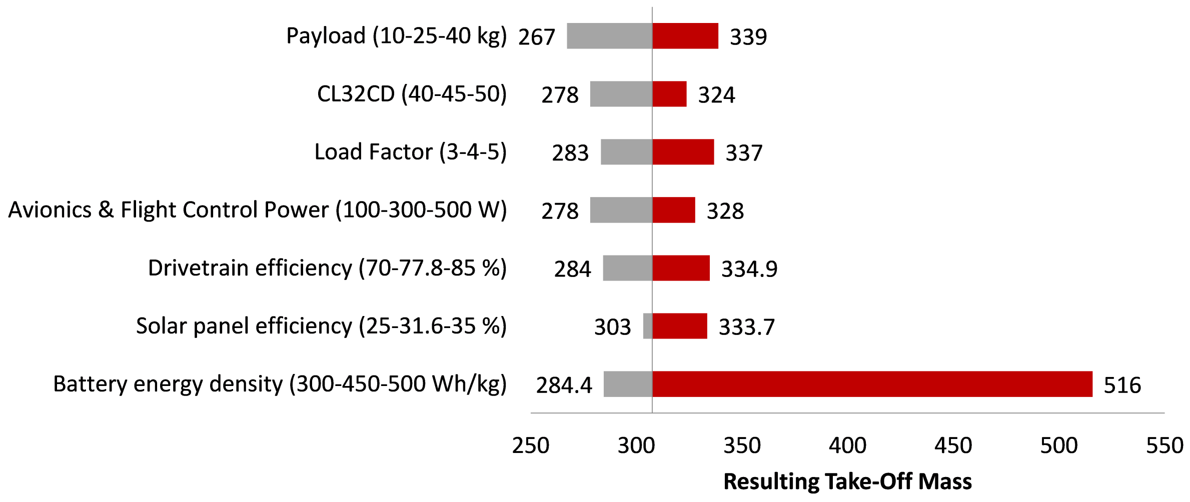

Figure 9.7: Effect of assumptions on resulting aircraft mass.

10. Resource allocation

This chapter includes the resource allocation for the design in terms of cost and production facilities. First, a detailed cost analysis is done in section 10.1. This includes the expected return on investment based on possible events that could be prevented by the aircraft system. Then, the manufacturing is described in section 10.2. Finally, the project development logic and future project planning are given in sections 10.3 and 10.4.

10.1. Cost/budget breakdown

In this section the cost will be analyzed to be able to calculate the edge the HAPS has over the competition. This is done by evaluating the production, development and maintenance costs and looking at the return on investment.

10.1.1. Cost Analysis

The final cost of building the HAPS is given in table 10.1. These costs comply with requirements: MPS-COST-1, MPS-COST-3 and MPS-COST-4. The cost with maintenance is given for 3 years and is calculated using 3 battery replacements and a monthly disassembly/assembly.

Table 10.1: Final cost estimation

Class	**Total lifetime cost**
With maintenance	€ 5.500.000,00
Without maintenance	€ 5.000.000,00
Support system	€ 110.000,00

To calculate the cost a lot of parameters were used, these can be found in table 10.3. As seen in table 10.2, the design process was split up in 4 different parts, spread out over 6 fiscal years (FY). These parts are further explained in section 10.4.

Table 10.2: Timeline of the design process

Phase	**Fiscal year**
Conceptual design	FY17
Conceptual & preliminary design	FY18
Preliminary & detailed design	FY19
Detailed design	FY20
Detailed design	FY21
Detailed design & manufacturing	FY22

Table 10.3: The parameters used in calculating the cost

Parameter	Value	Parameter	Value
Yearly rate	2.35%	Hours in a year/engineer	2087
Hourly rate of student engineer	€ 75	Solar array area [m]	78.9
Hourly rate of software engineer	€ 150	Solar array cost/m^2	€ 25,000
Hourly rate of senior engineer	€ 250	Thermal area [m^2]	400
Hourly rate of project engineer	€ 175	Thermal cost/m^2	100
Hourly rate of mechanic	€ 100	Battery weight [kg]	90
Hourly rate of Air Force mechanic	€ 30	Battery cost/kg	€ 2000
Hourly rate of Air Force engineer	€ 60	Structure weight [kg]	139
Inboard navigation cost	€ 30,000	Amount of aircraft	50
Price carbon fiber	€ 300	Unforeseen cost	15%
Price Mylar film cost/m^2	€ 3.10	Rod weight [kg]	58
Amount of pods per aircraft	6	Skin area [m^2]	200
Landing gear weight [kg]	13	Pod weight [kg]	10
Profit margin	0%	Price of resign cost/kg	€ 150
% Fibre in composite	60%	3D printer cost	€ 35,000
Rib material [cost/kg]	€ 2.5	Total rib weight [kg]	20

10.1.2. Cost Breakdown

The cost is split up in different sections as discussed in section 10.1.1. The preliminary cost is estimated using the senior engineers from table 10.4, while the detailed design is estimated using every engineer, excluding the manufacturing.

Table 10.4: Amount of jobs per group for the design and construction of the HAPS

	Stability & control	Power & propulsion	Structures	Aero-dynamics	Systems engineering	Manu-facturing
Senior engineers	3	3	3	2	2	2
Project engineer	4	6	5	4	-	3
Software engineers	5	2	1	1	-	1
Executive	-	-	-	-	1	-
Mechanics	-	-	-	-	-	6
Total	12	11	9	7	3	12

In figure 10.1 the cost breakdown for the whole project is shown. It is obvious that the further the progress, the higher the cost is. This is mainly due to the extra work force, but also because of expensive testing. The reason there is a bump in figure 10.1 at FY19 is that the preliminary design and detailed design overlapse, together with expensive testing.

In figure 10.2a the manufacturing process is broken down. This is basically the cost of the aircraft without the research and development. It is obvious that the Power and Propulsion part is the most expensive. This is due to the high cost of the solar panels (25000 euros/m^2), which is 92% of the P&P subsystem cost and 70% of the total manufacturing cost. The work cost is 11% of the total cost because a hangar has to be bought/build to do the final assembly. This cost was estimated using a cost of 6 million euros to buy land to build on and another 5 million to build the factory and put tools in it. The structural part, which is just 9.5% of the total cost, is further broken down in figure 10.2b. 54% is taken by the wing, which consists out of the rod (93.5%), the ribs (5.0%) and the foil (1.5%). The biggest cost of the rod is the construction process, explained in section 7.3. The biggest cost of the rib production is the acquisition of 3 3D-printers, as explained in section 7.5.

The cost of the ground station will fall well below 30 million, and therefore will satisfy requirement MPS-COST-2, even though the cost is not estimated accurately. The suitcase option, shortly explained in section 8.6, only costs 8000 euros[1]. This suitcase is only for quick deployment. The larger ground station will exist out of a container (acts as a cage of Faraday), with 10 screens and two control panels (keyboards), a satellite up-link and an air-conditioning unit. All of these units combined will not reach a 30 million euro cost.

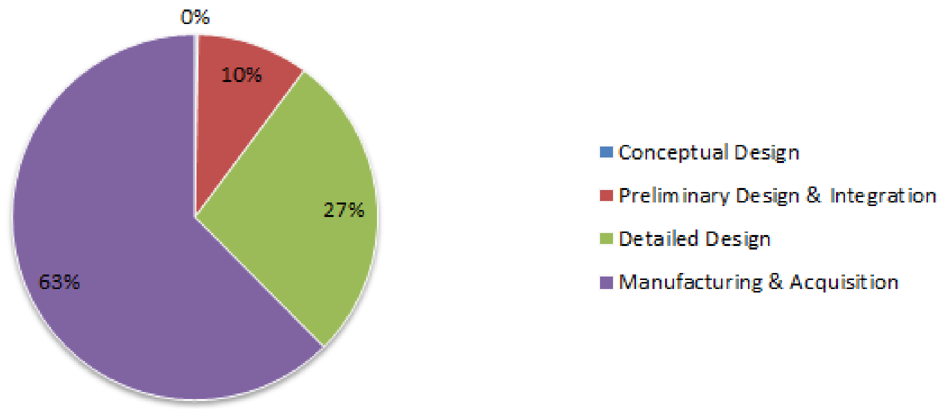

(a) Breakdown of the development cost

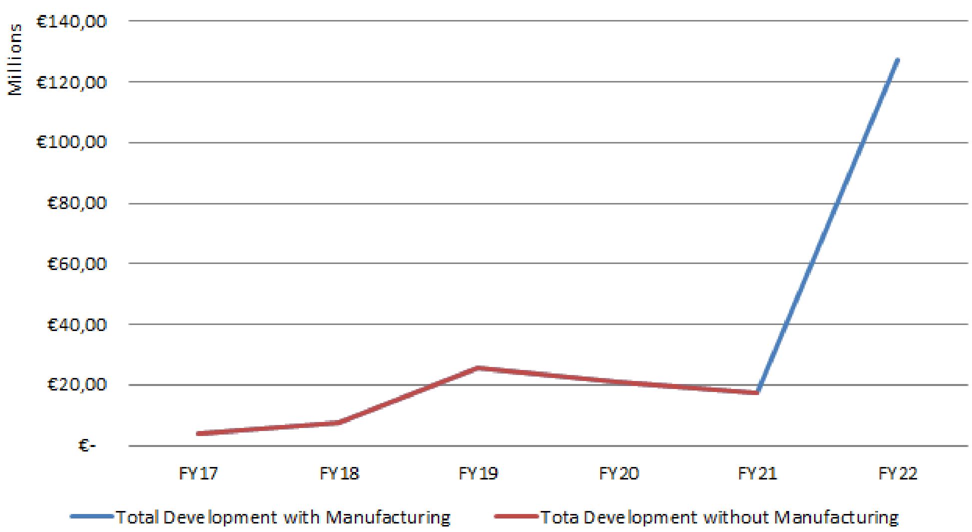

(b) Progress of the development cost

Figure 10.1: Development cost of the HAPS.

[1]URL: https://products.embention.com/veronte/control-station/hcs-suitcase [Retrieved on 23-06-2017]

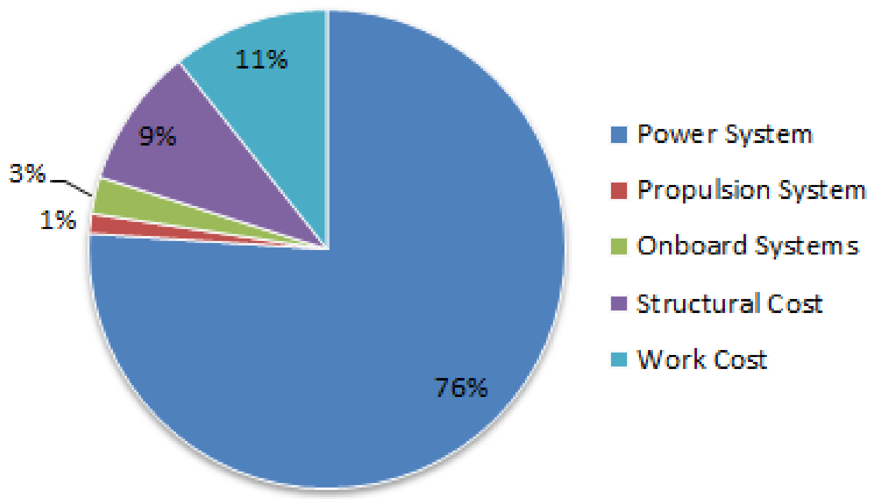

(a) Breakdown of the manufacturing cost

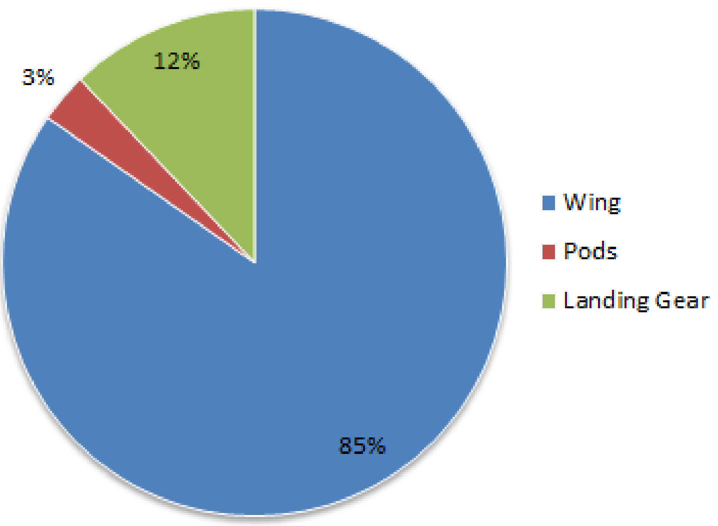

(b) Breakdown of the structures cost

Figure 10.2: Breakdown of the manufacturing costs

To check for requirement MPS-PRD-1 figure 10.3 is introduced. From figure 10.3a it is clear that this requirement is not met. This is due to the massive cost of the the solar foils. Without taking the solar films into account, it is clear that most of the extra costs go to the Netherlands. These are mostly high-paying research jobs.

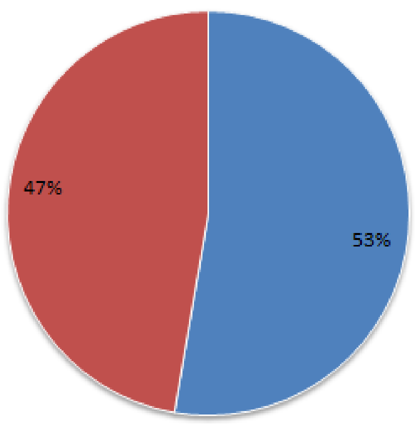

(a) Cost breakdown of the spending per country.

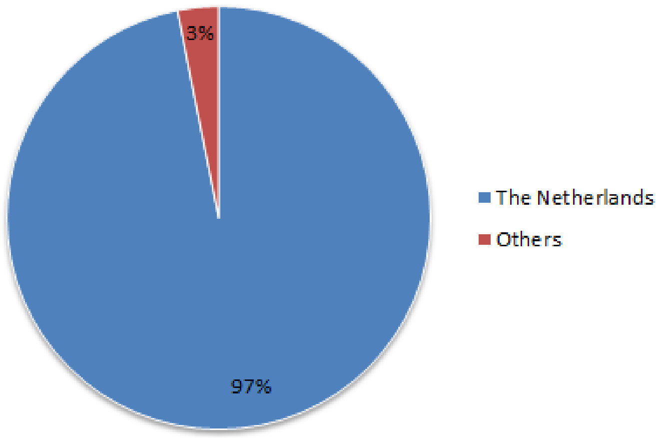

(b) Cost breakdown of the spending per country, excluding the solar films.

Figure 10.3: Cost breakdown of the spending per country.

10.1.3. Operational Profit

The major part of the operational cost is the cost of the aircraft per flight hour. To calculate this, the cost of the aircraft, the maintenance required, the transportation of the aircraft (C-17 flight cost)[2] and two data analysts working around 24/7 [3] was taken into account. All these costs combined result in a cost/flight hour of approximately 260 euros per hour, as can be seen in table 10.5.

Table 10.5: Cost breakdown per flight hour

Parameter	Cost	Explanation
Cost of aircraft	€ 5.000.000,00	1 aircraft
Cost of maintenance/cycle	€ 40.000,00	Cycle = 30 days
Cost of transportation	€ 100.000,00	Transport every half year, over a 5000 km distance
Cost of pilots	€ 110.000,00	Cost per year for 1 data analyst / pilot
Cost/flight hour	€ 260,00	

When comparing multiple aircraft with similar missions; surveillance, detection, communications or espionage, it is obvious from figure 10.4 that the high-altitude platform being designed in this document is the cheapest possible alternative. This creates extra incentive for possible clients to buy this product instead. It needs to be stressed that the platform that is designed should be seen as a supplement, not a substitution.

[2]URL: http://nation.time.com/2013/04/02/costly-flight-hours/ [Retrieved on 22-06-2017]
[3]URL: http://www.payscale.com/research/US/Job=Data_Analyst/Salary [Retrieved on 21-06-2017]

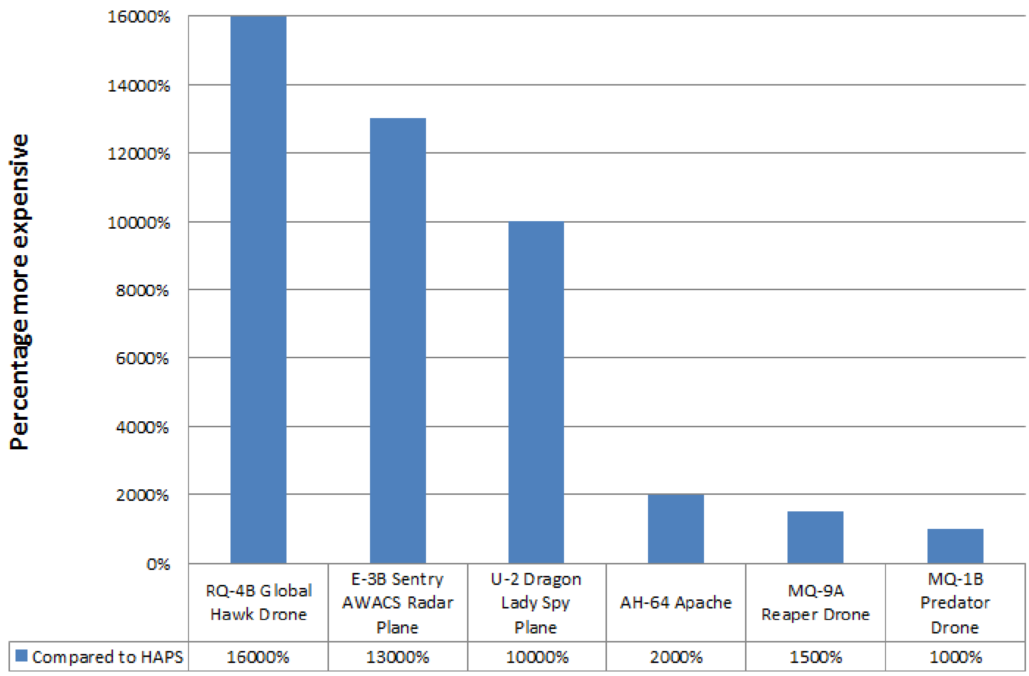

Figure 10.4: Comparison of cost/flight hour to other aircraft with similar missions. [4]

10.1.4. Return on Investment

Even though most of the alternative surveillance platforms cost more, the acquisition of a multi-million euro system is still an important decision. To be able to sustain the platform, it needs to perform to a certain standard and return on the investment made. To estimate possible ROI's table 10.6 is shown. In this table 3 different possible missions are laid out. The first handles a growing problem in these recent years: terrorism. It is estimated that every terrorist attack does an average of 19 million dollars in damages[5,6]. Every year there is an average of over 3000 terrorist attacks globally, in which, on average 9.62 people get killed [7].[50] If the platform could prevent one attack from happening, this damage would be avoided and therefore it could be stated that the return investment is: (Damage Avoided - Price of platform)/Price of platform.

The second mission is avoiding the drug trafficking via high-speed boats using AIS detection[8]. One boat can approximately carry 1 ton of illegal drugs, worth over 30 million euros[9,10]. The apprehension of these drugs is critical to protect the civilians and the economical system.

[4]URL:http://www.globalsecurity.org/military/systems/aircraft/rotary.htm [Retrieved on 22-06-2017]
[5]URL: http://fortune.com/2015/11/17/terrorism-global-economic-cost/ [Retrieved on 20-06-2017]
[6]URL: http://www.nato.int/docu/review/2008/04/AP_COST/EN/index.htm [Retrieved on 20-06-2017]
[7]URL: https://www.start.umd.edu/gtd/images/START_GlobalTerrorismDatabase_TerroristAttacksConcentrationIntensityMap_45Years.png [Retrieved 20-06-2017]
[8]URL: https://mscconference.wordpress.com/category/the-illegal-movement-of-people-illicit-cargoes-at-sea/ [Retrieved on 27-06-2017]
[9]URL: http://www.dailymail.co.uk/news/article-3880654/Coast-Guard-shows-two-ton-cocaine-haul-drug-smuggling-submersible_setting-12-month-record-5-6BILLION.html [Retrieved on 20-06-2017]
[10]URL: http://www.dailymail.co.uk/news/article-2913854/Drug-cartels-using-new-very-fast-boats-INVISIBLE-radar-Central_American-smuggling-missions.html [Retrieved on 20-06-2017]

The last mission is providing a mobile network to a certain part of a city (in this case a quarter of an average city). An average city in the United States counts approximately 270,000 people[11], of which 17% fall below 12 years [12]. To calculate a possible return on investment, the population of the city was first divided by 4 after which 83% was taken to account for the non-users (mostly young children). The average customer is worth approximately €1100 to a mobile provider, yearly [13].

Table 10.6: Return on Investment for 3 different missions.

Parameter	Value
Average damage/acting terrorist (terrorist attack)	€ 19.050.000,00
Terrorist attacks/year	3000
Damage/year	€ 57.150.000.000,00
ROI of 1 avoided terrorist attack	315%
Price of ton of illegal drugs	€ 33.000.000,00
ROI of catching 1 ton of illegal drugs	615%
Average city population	270,000
Average value/person/year	1100
ROI mobile providers/quarter-city	1300%

10.2. Manufacturing Assembly & Integration

The aircraft is a fairly novel and specialized design. Due to this specific production, assembly and integration methods are required. First an overview of which company produces the required parts, as well as the production method used, will be provided. Secondly and overview of the complete production process is presented along with a cut through of the sections and an exploded view. The chapter is concluded with a design of the factory for final assembly.

10.2.1. Manufacturing

Most of the components are manufactured, or bought off the shelf, by an external company. Due to the initial small amount of aircraft produced (50 according to section 3.1) it is financially more efficient to sub-contract most of the production, instead of investing in more equipment and production space. An overview of which company produces or sells which component is presented in table 10.7. It also states the production method and estimated production time for the parts for one aircraft.

[11]URL: https://factfinder.census.gov/faces/tableservices/jsf/pages/productview.xhtml?src=bkmk [Retrieved on 20-06-2017]
[12]URL: https://www.childtrends.org/indicators/number-of-children/ [Retrieved on 21-06-2017]
[13]URL: http://bgr.com/2014/01/17/most-expensive-cell-phone-service-us/ [Retrieved on 20-06-2017]

Table 10.7: Aircraft components with their manufacturer,production process and time to produce all components for one aircraft.

Component	Manufactured by:	Production method	Production time
Skin foil	DuPont Teijin Films	Off the shelf	-
Solar film	Alta Devices	Off the shelf	-
Rod	NLR	Braiding	1 day
Ribs	RNLAF	3D printing	7 days
Actuators	Volz	Off the shelf	-
Wiring	Fokker	In house	-
Landing gear	Fokker	Forming & Milling	-
Pod	KVE Composites Group	Vacuum infusion	7 days
Batteries	Sion Power	Off the shelf	-
Engines	AE Group	In House	-
Ground system suitcase	Embention	Off the shelf	-
Propeller	NLR	Braiding	1-2 days
Autopilot	Embention	Off the shelf	-

10.2.2. Assembly and Integration

Several specialized techniques are required for the production of the aircraft. As a result a factory will be built in which the final assembly and integration of the aircraft will be performed, as well as the production of a small amount of components. Initially only 50 aircraft will be built. To keep the initial investment costs of the factory and training personnel down, most of the subsystems will be bought off the shelf or the production is sub-contracted. An exploded view of the aircraft showing the manufacturer of each part is shown in figure 10.5 and figure 10.6. Assembly of all the parts will be performed as parallel as possible. Because the aircraft is designed to be modular for transport, assembly will take place in separate parts: wing, mid-section, engine pod. In figure 10.7 an overview is given of the assembly and integration process.

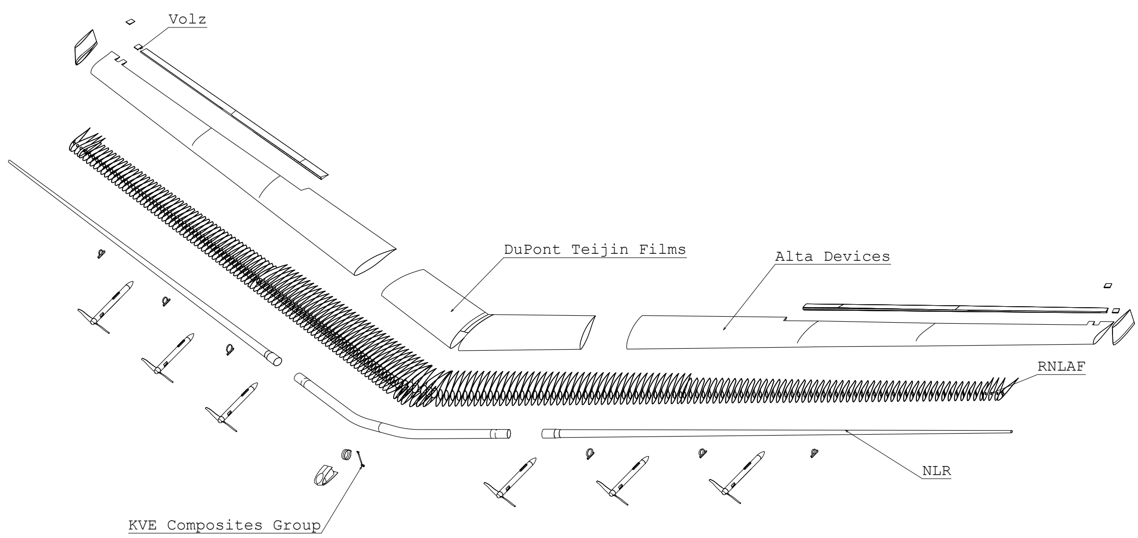

Figure 10.5: Exploded view of the aircraft with manufacturer per part

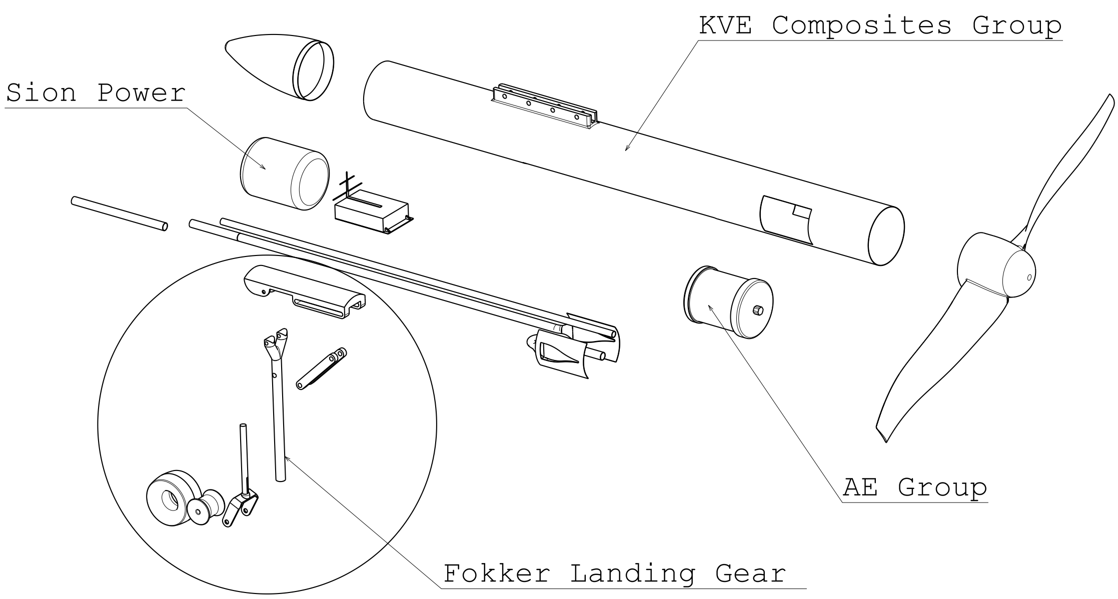

Figure 10.6: Exploded view of the pod with manufacturer per part

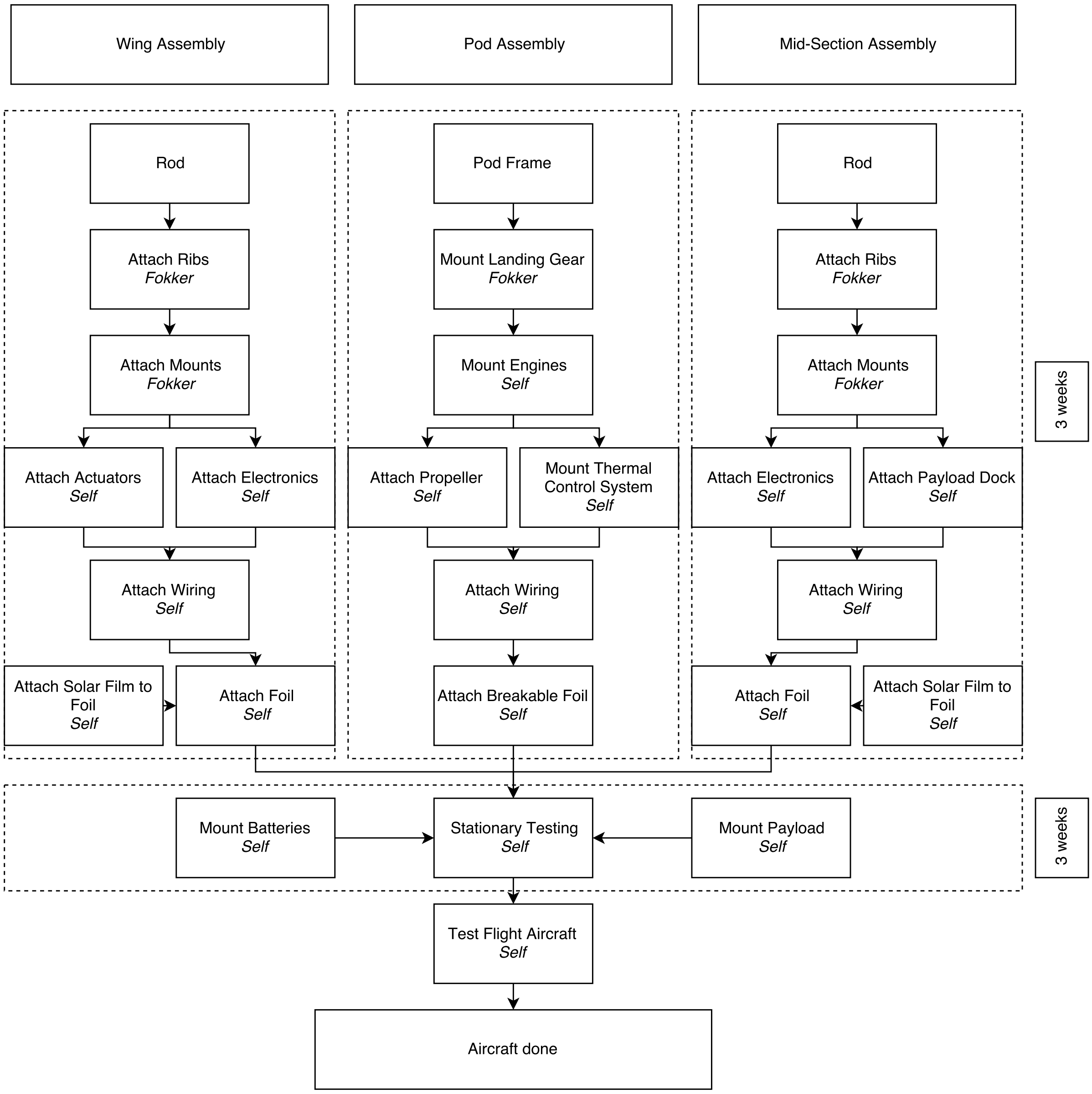

Figure 10.7: Assembly and Integration flow

Attaching the ribs, mounts and landing gear will be sub-contracted to Fokker Aerostructures. Making use of their services saves a lot on investment costs in equipment. Placing the ribs under the right angle will require high precision as there is a twist of 2 degrees throughout halve the wingspan. To do this properly a jig will be provided to Fokker Aerostructures. The method for attaching the ribs to the rod is presented in section 7.5.

Further assembly will be performed at the factory designed for the aircraft. The factory will be located at or near the terrain of the military airbase Woensdrecht, the main support base for the RNLAF. [14] Working close to airbase Woensdrecht allows for easy flight testing of the finished aircraft, usage

[14]URL: https://www.defensie.nl/organisatie/luchtmacht/inhoud/vliegbases-en-luchtmachtonderdelen/woensdrecht - [Retrieved on 23-06-2017]

of facilities and tools already available, and good infrastructure for transportation of big products is present. Transport will be a critical factor during assembly and integration due to restrictions on trailer sizes. Transport is possible by truck, but a permit has to be supplied in order to allow for trailers up to 25.5 meter to be used[15].

Due to the high price of the solar film (section 10.1.2) the skin will be split into panels. In case of damage to the skin only one panel has to be replaced. The panels of foil will be hot-glued to the ribs, after which the solar film is glued to the upper surface of the foil. The solar film will be the outer layer to ensure maximum electricity production. The placement of the parts inside the wing, mid section and pod can be seen in figure 10.8, figure 10.9 and figure 10.10.

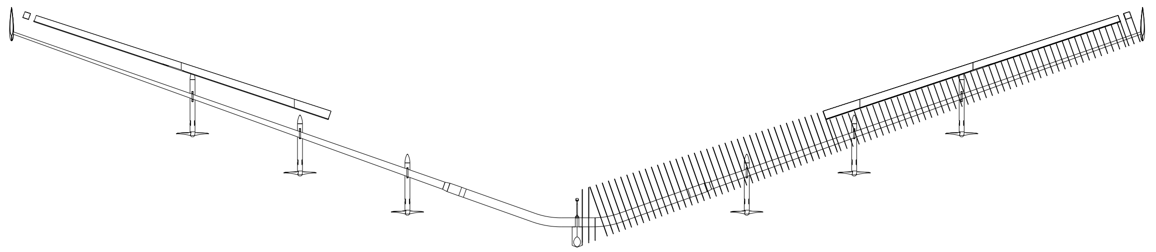

Figure 10.8: Top view cut through of the wing

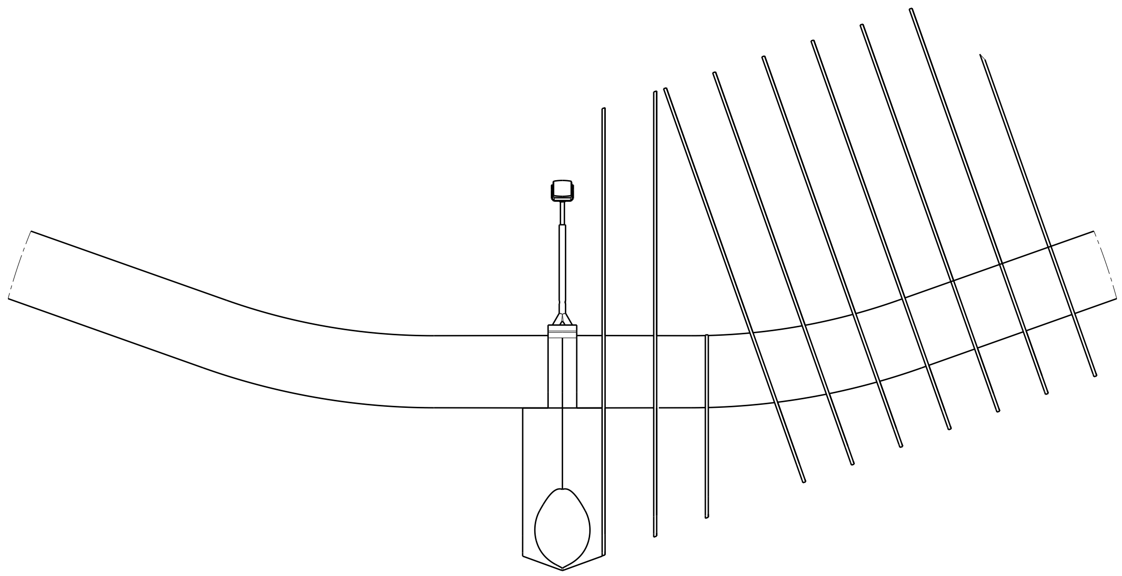

Figure 10.9: Top view cut through of the middle section

[15]URL: https://www.rdw.nl/sites/ontheffingen/Paginas/LZV.aspx - [Retrieved on 23-06-2017]

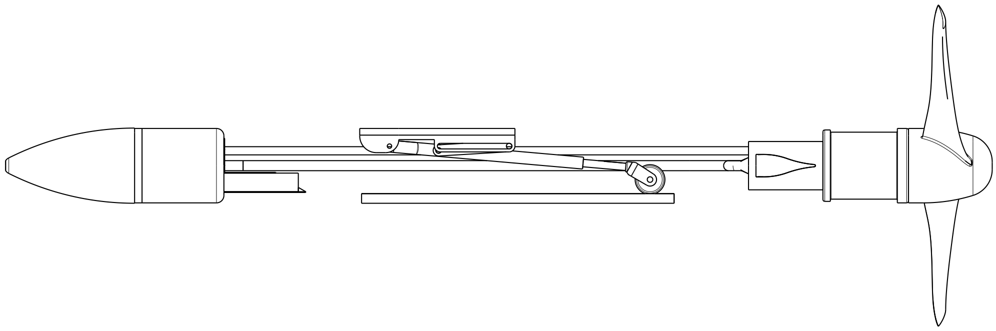

Figure 10.10: Side view cut through of the pod

10.2.3. Factory Design

The factory facilitates the final assembly and integration of the aircraft, as well as production of the ribs. It will consist of a big hall divided into different areas. Assembly of the three main parts, final assembly, manufacturing of the ribs and storage will have a dedicated area. Besides that the factory will have a canteen, dedicated meeting room and office space. The main production areas have been sized to accommodate the assembly of all parts for one entire aircraft. After the aircraft has been tested stationary it will be disassembled again to make sure it can fit through the doors. The layout of the factory can be seen in figure 10.11, the images of the aircraft parts are to scale.

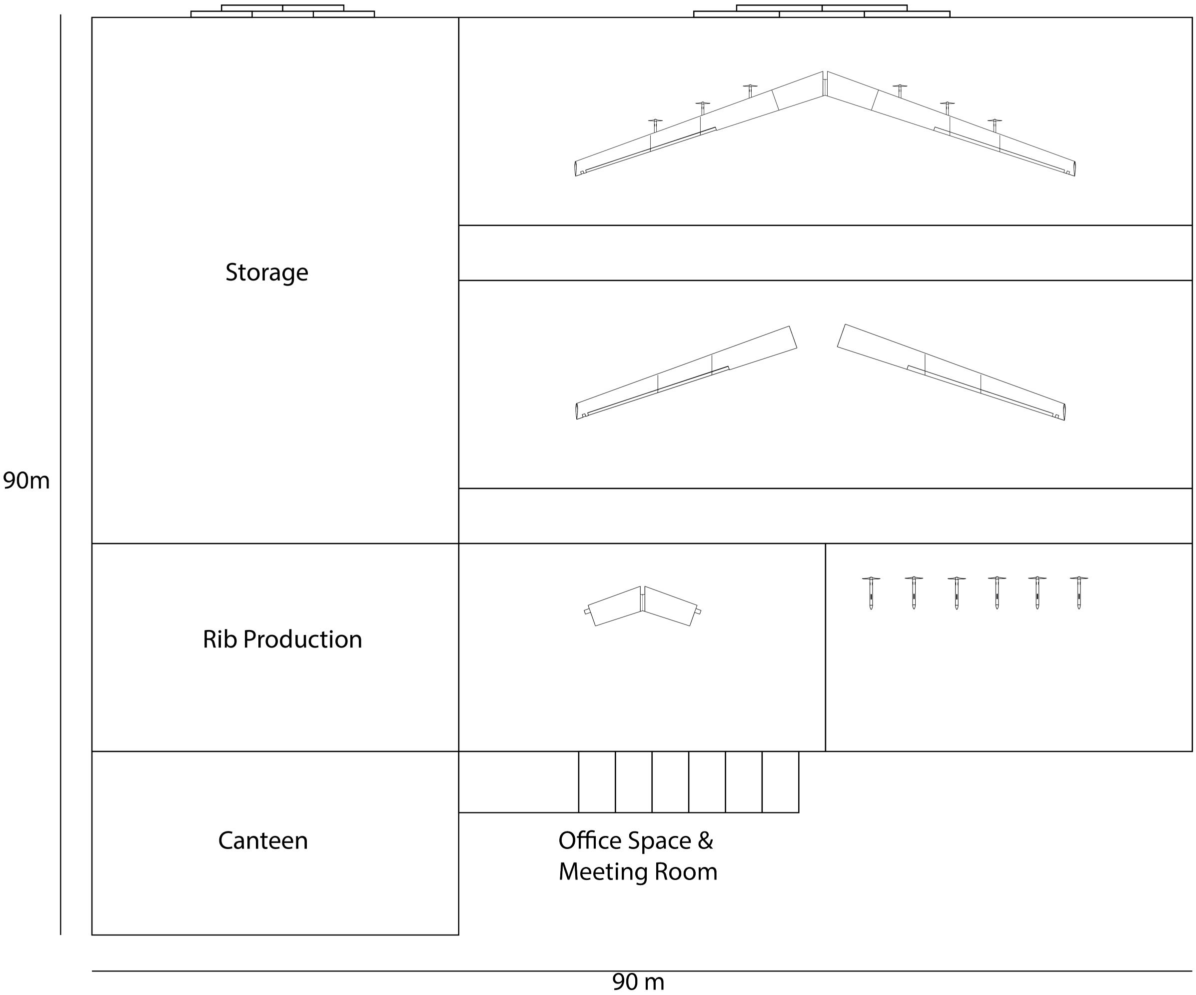

Figure 10.11: Factory layout

10.3. Project development logic

In this report, the conceptual design of an HALE pseude-satellite has been described. Howver; the project is far from complete. In figure 10.12 the complete remaining design process is described until the first aircraft will be delivered to the customer in 2023.

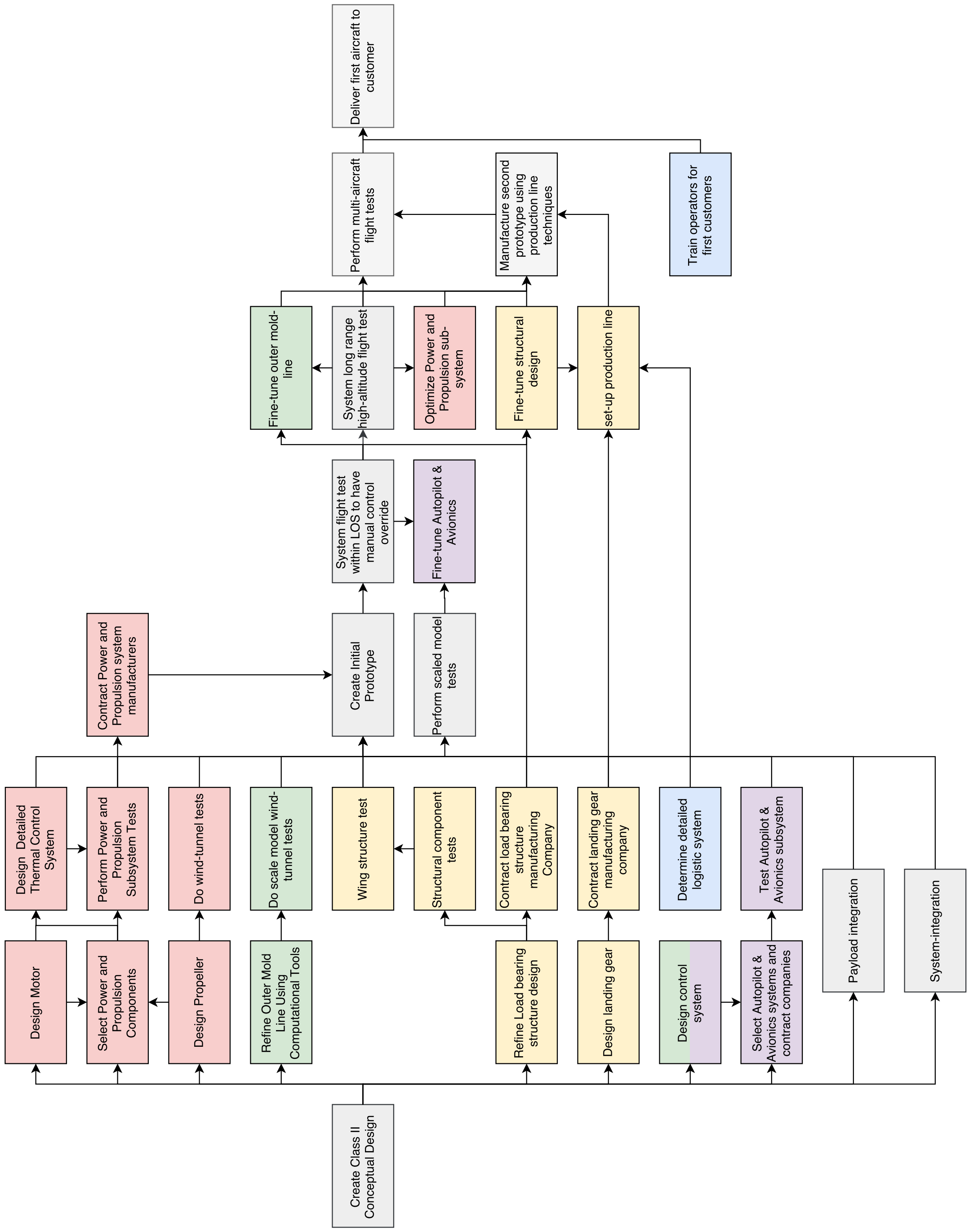

Figure 10.12: Chart depicting the steps to take for the project until delivery to the first customer.

10.4. Project Gantt chart

To guide to future research and development of the project, a Gantt chart (see figure 10.13) is made to give an estimated time-line. The chart is structured as follows: on the top level it is split up in Class II Conceptual Design, Preliminary Design and Detailed Design & Manufacturing. Below that are all the tasks that have to be done, all leading up to the production and marketing of the product. The most important stages and milestones are given in orange.

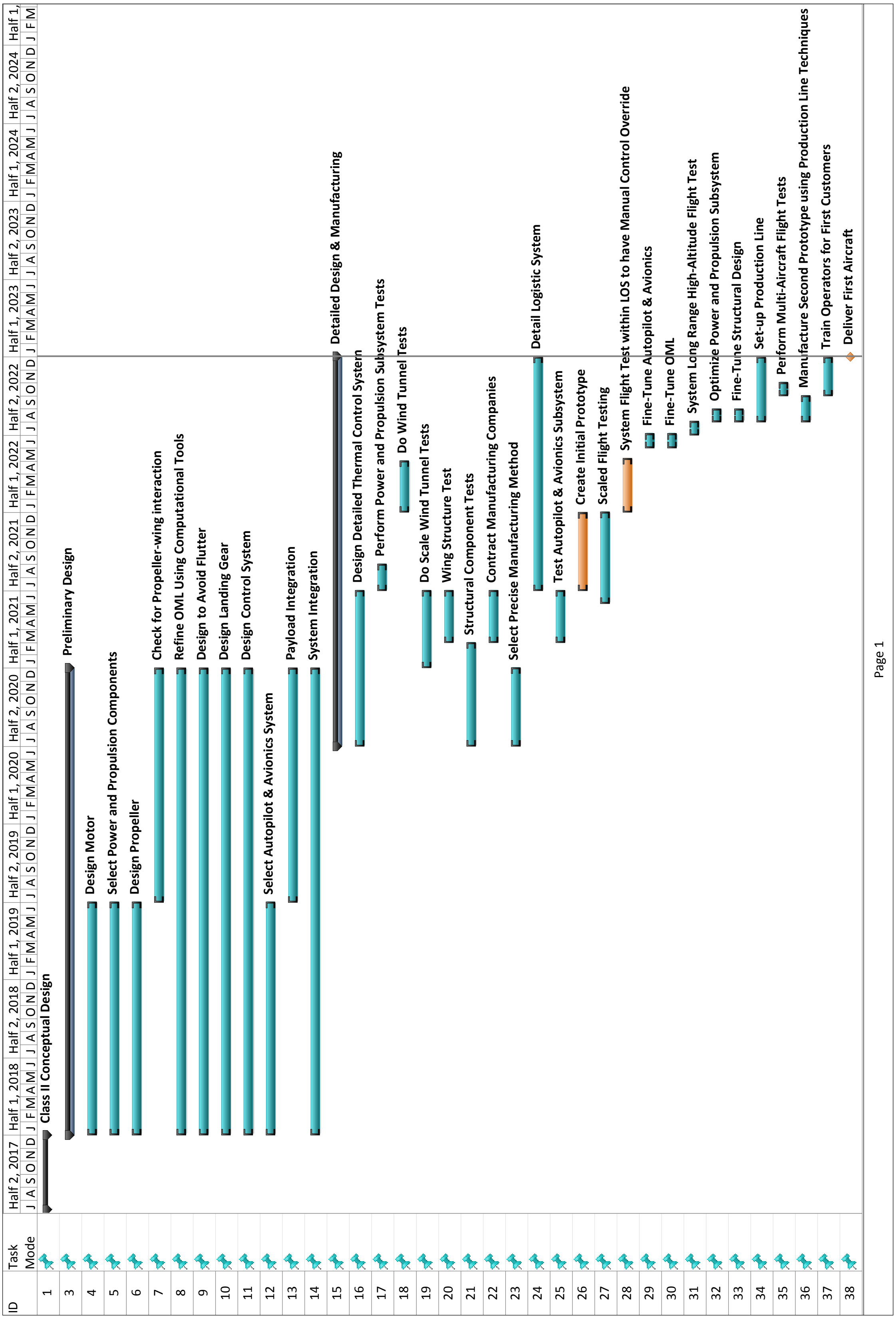

Figure 10.13: Project Gantt Chart

11. Sustainable development approach

Sustainable development has become an important part of the design process throughout the years. Therefore, in order to ensure a sustainable development, certain technologies have to be assessed for their sustainability. In this chapter multiple steps that contribute to a sustainable development are explained.

11.1. Sustainability of the project

Because the aircraft does not use any fuel it will already be considerably more sustainable than its current aircraft alternatives. Furthermore the surveillance platform does not have to be launched into space to loiter over an area for an undefined period of time.

However some measures can still be taken during the design and development of the aircraft to increase the sustainability. These steps are further explained in the next subsections: technologies, production and end-of-life solutions.

Technologies

A large part of the sustainability is dependent on the selection of technologies used in the aircraft. Due to high requirements and the expectations of a high-end product, there was limited room to choose between technologies. The batteries are created from lithium-sulfur as only they are capable of providing the required energy density. However as sulfur is available in abundance and easily recyclable from the batteries they do not have a higher impact than their lithium-ion counterpart.[51]

The solar-foil has a high impact on the sustainability of the product, mainly due to the high power requirements for production, which will be discussed in section 11.2. Also the toxicity levels of the materials involved play a big part in solar-foil selection and the determination of the sustainability.

Production

In order to increase the sustainability during production two basic methods will be incorporated, being; minimizing transport and utilizing minimizing wasted materials. Minimizing the transport falls in line with requirement MPS-PRD-1, 75% of the total design & production cost shall be contracted to Dutch parties, as this also implies that the transport will be relatively low. The CO2 emission will be discussed in section 11.2.

For the actual production waste will be re-used as much as possible in order to minimize the required amount of materials, to increase the sustainability and reduce the production costs.

End-of-life solutions

As this aircraft has a relatively short operational lifetime most subsystems and products can be re-used after its life. The actual end-of-life solution of the aircraft will be decided by the customer, however one of the possibilities for the RNLAF might be; sell/donate the solar-panels and batteries to the UN Peace Corps which can use it to power refugee camps and alike. This only requires that the batteries are replaced every year or that the depth of discharge is decreased to increase the battery life time such that the UN does not increase its costs.

11.2. CO2 emissions during production

One of the major parts of the sustainability is the CO2 emissions of the manufacturing process and operations of the aircraft. In order to group the emissions two groups have been formed for which the CO2 emission will be analyzed. Afterwards a plan will be proposed in order to achieve zero net CO2 emissions. The groups mentioned earlier are:

- Energy required for manufacturing
- Transport during manufacturing

In order to calculate the CO2 emission during manufacturing the assumption is made that all energy is generated by means of fossil fuel. This gives a representation of the energy required expressed in kg CO2. After which this value can be mitigated by different means. The values used in the calculation are 31 kg CO2 per kg manufactured carbon fibre composite, 2.5 kg CO2 per kg foil.[52]

For the solar-foil it takes 7.67 GJ to produce 1 m^2 of GaAs film [53]. However, as the factory is located in Sunnyvale - Silicon Valley, the majority of the energy supplied to the factory is already CO2 Neutral [1,2]. Furthermore, Altadevices is part of the Hanergy group, this group strives to have all their companies manufacture with zero net CO2 emissions.[54] Therefore the assumption is made that only 5% of this energy is produced by means of fossil fuels, leaving 64 kg CO2 per square meter of GaAs solar film that needs to be accounted for.

The final major element is the manufacturing of the batteries. As Sion power does not provide any data on their CO2 emission for manufacturing, 5 kg CO2 per kg batteries is used. This value is determined by using the CO2 emissions for manufacturing nickel-metal-hydride batteries which are worse than Lithium-sulfur batteries [3]. In table 11.1 the mass of the CO2 emissions from each segment can be seen as well as the total mass of CO2 emission which needs mitigation.

[1] URL:http://www.jointventure.org/initiatives/climate-prosperity/4-initiatives/climate-change/187-climate-task-force-success-stories [Retrieved on 20-06-2017]
[2] URL: https://www.kcet.org/redefine/silicon-valley-city-to-be-carbon-neutral-by-2017 [Retrieved on 20-06-2017]
[3] URL: http://ec.europa.eu/environment/integration/research/newsalert/pdf/303na1_en.pdf - recieved on 20-6-2017

Table 11.1: CO2 emission from manufacturing

Component	Amount	CO_2 [kg]
Carbon-fibre composite	110 kg	3500
Foil	23 kg	30
GaAs Solar film	80 m2	5050
Lithium-sulfur batteries	90.00 kg	450
Total (1 aircraft)	-	9000
Total (50 aircraft)	-	450000

For the CO2 emissions during transport only the transport from the US to the the Netherlands is considered for the amount of CO2 produced. Transport from within the Netherlands is negligible in comparison with the amount produced during intercontinental transport.

The parts that need to be transported from the US are the batteries, solar-film and thermal system. It is assumed that all these elements for 50 aircraft can fit inside one cargo aircraft. The emission of the cargo aircraft is assumed at 0.00103 kg CO2/km/kg for a Boeing 777. [55] The flight sizing the transportation C20 emission will be from San Francisco (SFO) to Schiphol (AMS), giving a total flight distance of 8800 km. The total mass to be transported by aircraft is 5300 kg, bringing the total amount of CO2 from transport to 50 tonnes of CO2.

However this amount can be decreased considerably when looking at transport using maritime solutions. The CO2 emission is calculated using 8.4 g CO2/tonne/km [4]. This gives a total amount of CO2 of 0.4 tonne, which is considerably smaller. Therefore the choice has been made to transport everything from the US by ship.

From this can be seen that the manufacturing is mostly sizing the CO2 emissions of the aircraft in comparison with the transport.

11.3. Emission Mitigation

The goal of the emission mitigation is to make the entire production process CO2 neutral. The first form of mitigation is done by doing the transatlantic transport by means of maritime transport instead of by aircraft. There is however still 450 tonnes of CO2 to be mitigated, the main contributors to the CO2 emissions are the production of the composite and the solar-film.

The majority of the emissions of the composite originate from the fibre production (51%) and the composite part production (35%).[52] Of this 86% again more than 50% of the carbon footprint is due to electricity and roughly 30% is due to release of gases from chemical processes. This last part can be mitigated by carefully monitoring the gases released and contain them before they reach the atmosphere. For the electricity it comes down to using green CO2 neutral electricity during the manufacturing,

[4]URL: https://www.ecta.com/resources/Documents/Best%20Practices%20Guidelines/guideline_for_measuring_and_managing_co2.pdf [Retrieved on 20-06-2017]

either by installing solar-panels on the factory roof or by using a green power supplier.

The majority of the emissions of the solar-film production are due to the power required for the manufacturing. Therefore the same mitigation method is used as for the composite production. Furthermore, an extra commission will be paid to all manufacturers that use green energy to ensure that the products will be developed CO2 neutral and to incentivize other producers to also switch to eco-friendly energy. All remaining unmitigated CO2 will be covered by buying emission credits[5].

[5]URL: https://ec.europa.eu/clima/policies/ets_en [Retrieved on 27-06-2017]

12. Conclusion & Recommendations

This report has described a class II conceptual design for an high altitude pseudo satellite to increase the surveillance, reconnaissance and communication capabilities of the Royal Netherlands Air Force (RNLAF). It was found that high efficiency, lightweight structures and especially batteries with a high energy density are of key importance to the feasibility of the design. The most optimal design turned out to be a solar-powered flying wing which is capable of flying at altitudes of up to 23 km for 30 days without refueling. The high altitude is needed for several reasons. First of all, it allows the aircraft to fly above the jet stream which for some parts of the year causes otherwise unflyable conditions. Furthermore it allows for the storage of potential energy. During daytime the aircraft will ascend from the lowest cruise altitude (18 km) to its ceiling to store potential energy, which it uses during nighttime by gliding down. Finally, it allows the payload to be able to scan a wide area.

Since the aircraft is dependent on solar power to charge its batteries, it is limited in the locations where it can fly. It can fly year-round up to a latitude of 40 degrees (north). During summer however; it is able to fly at higher latitudes even reaching the poles. The aircraft is kept lightweight by using a simple structure, with a circular composite rod serving as the main structural component while composite ribs and a skin out of plastic foil are used to define the aerodynamic shape. One aircraft consists of 2 outer wing sections, 1 middle section and 6 engine pods which can all be separated from each other. The final take-off mass is about 310 kg, where the biggest contribution comes from the batteries.

The aircraft can be developed and manufactured in the Netherlands where 53% of the total development and production costs can be allocated. This figure increases to 97% when not taking the solar film into account. The highly efficient solar film used on the aircraft is not available in The Netherlands, and using less efficient solar film would drive the design to an unacceptable extent. Due to the use of any solar film avoiding toxic materials during production can not be avoided. The design is created in such a way that three aircraft can be transported inside a single C-17. The aircraft can be ready within eight hours after the C-17 lands in a crisis zone. This means that this aircraft can be operational above the target location faster than solar powered designs of competitors. This is a clear advantage for military operations. On the other hand; this design still has the endurance and operational cost of a solar powered design, which is a great advantage for longer duration missions where a larger fleet of conventional UAV's would usually be needed.

Recommendations

The following aspects should be kept in mind during the next phases of the aircraft design:

- The Dutch roll of the aircraft has turned out to be only marginally stable. Analysis will need to be done to find out if a PID controller is able to improve the stability of the dutch roll.
- In general, for large, lightweight aircraft, gusts can be a large problem. The structure of the aircraft has been designed to withstand significant gusts. However; the dynamic and aeroelastic properties of the aircraft should be analyzed with respect to being able to land safely, even in gust conditions.
- As stated in chapter 5, more accurate analysis of the aerodynamic performance of the wing is needed by means of CFD analysis and/or real-life tests. Until that is done however; a more in depth analysis of the validity of the software used so far and compensation for potential biases should be done.
- High altitude propeller design is a complex process. At this phase of the design, there is still a large factor of uncertainty in the propellers. Enough resources should be spent towards developing an efficient propeller early on in the design.
- From the sensitivity analysis, it was found that battery energy density is of key importance to the design. Therefore; companies should be contacted early on to make sure that the proposed specific energies can be met by the time the first aircraft needs to be build. A slight increase of specific energy of the battery may already lead to a much more efficient design.
- The aircraft has been designed keeping transportability in mind. For this reason, the aircraft is able to be disassembled with relative ease. Concepts on how to do this have been established. The weight penalties on these concepts have been estimated but are still a relatively large factor of uncertainty. A team of structural experts should carefully reconsider the joint types and their effect on the design
- The usage of plastic foil has been done on aircraft wings, but usually not on aircraft of this scale and with a a lifetime as long as 20,000 flight hours. Research should be done on the fatigue life or degradation of these foils.
- The replace-ability or repair-ability of the plastic foil should also be taken into consideration during the further design phases since thin foil is relatively easily perforated.

- The wing rod has been designed to withstand the lifetime of the aircraft. However; more attention should be paid towards being able to maintain this structure if this turns out to be necessary.

Bibliography

[1] F.C.L.; Devezas T.C. d'Oliveira, F.A.; de Melo. High-Altitude Platforms - Present Situation and Technology Trends. *Journal of Aerospace Technology and Management*, 8:249 – 262, 09 2016.

[2] Claes A.P.K. Drenth M.K. Griffioen M.A. Groot D.J. Janowski J.T. Marchena Esteban C. Post P.J.A. Wedemeijer R. Willemsen J.D. Buller, M.B. Pseudo satellite for military purpose: Project plan. Technical report, Technische Universiteit Delft, 2017.

[3] Claes A.P.K. Drenth M.K. Griffioen M.A. Groot D.J. Janowski J.T. Marchena Esteban C. Post P.J.A. Wedemeijer R. Willemsen J.D. Buller, M.B. Pseudo satellite for military purpose: Baseline report. Technical report, Technische Universiteit Delft, 2017.

[4] Unified Teaching Staff. Aircraft design for stability and control: Planform and dihedral considerations. PDF, mar 2006. Massachusetts Institute of Technology.

[5] D.P. Raymer. *Aircraft Design: A Conceptual Approach*. AIAA, first edition, 1999.

[6] Military specification flying qualities of piloted airplanes. November 1980.

[7] M. Christopher Cotting. Aircraft control sizing, senior design class, February 2009.

[8] Bernd Chudoba. *Stability and Control of Conventional and Unconventional Aircraft Configurations: A Generic Approach*. Stoughton, Wisconsin, 2001.

[9] M.S. Selig G.K. Ananda, P.P. Sukumar. Measured aerodynamic characteristics of wings at low reynolds numbers. *Elsevier*, 2014.

[10] Claes A.P.K. Drenth M.K. Griffioen M.A. Groot D.J. Janowski J.T. Marchena Esteban C. Post P.J.A. Wedemeijer R. Willemsen J.D. Buller, M.B. Pseudo satellite for military purpose: Midterm report. Technical report, Technische Universiteit Delft, 2017.

[11] AltaDevices. Single cell technology performance. Data sheet, 2017.

[12] Y. Hishikawa W. Warta Martin A. Green, K. Emery and E. D. Dunlop. Solar cell efficiency tables (version 48). *Progress Photovoltaics Journal*, 24:905–913, 2016.

[13] Yuriy V Mikhaylik, Igor Kovalev, Riley Schock, Karthikeyan Kumaresan, Jason Xu, and John Affinito. High energy rechargeable li-s cells for ev application: status, remaining problems and solutions. *Ecs Transactions*, 25(35):23–34, 2010.

[14] infolytica corporation. Motorsolve 6: Electric machine design software. http://www.infolytica.com/en/products/motorsolve/, 2016.

[15] A. Rapinett. Zephyr: A high altitude long endurance unmanned air vehicle. Master's thesis, University of Surrey, Apr 2009.

[16] Duane C. Hanselman. *Brushless Permanent Magnet Motor Design*. The Writers' Collective, 2003.

[17] Giulio De Donato, Fabio Giulii Capponi, Giovanni Antonio Rivellini, and Federico Caricchi. Integral-slot versus fractional-slot concentrated-winding axial-flux permanent-magnet machines: Comparative design, fea, and experimental tests. *IEEE Transactions on Industry Applications*, 48(5):1487–1495, 2012.

[18] AJ Mitcham, G Antonopoulos, and JJA Cullen. Favourable slot and pole number combinations for fault-tolerant pm machines. *IEE Proceedings-Electric Power Applications*, 151(5):520–525, 2004.

[19] Nobuyuki Matsui. Sensorless pm brushless dc motor drives. *IEEE Transactions on Industrial Electronics*, 43(2):300–308, 1996.

[20] J.Whurr A.Rolt. *Distributed Propulsion Systems to MAximize the Benefits of Boundary Layer Ingestion*. University of Cincinatti, 2015.

[21] G.J.J. Ruijgrok. *Elements of Airplane Performance*. Vssd Pub., 2009.

[22] J.S. Vanderover and K.D. Visser. Analysis of a contra-rotating propeller driven transport aircraft. Clarkson Univeristy.

[23] Yaxi Chen, Peiqing Liu, Zhihao Tang, and Hao Guo. Wind tunnel tests of stratospheric airship counter rotating propellers. *Theoretical and Applied Mechanics Letters*, 5(1):58 – 61, 2015.

[24] J. Gundlach. *Designing Unmanned Aircraft Systems: A Comprehensive Approach*. AIAA, first edition, 2012.

[25] M.A.R. Silvestre J.C. Pascoa J. Morgado, M. Abdollahzadeh. High altitude propeller design and analysis. *Aerospace Science and Technology*, 2015.

[26] N.J. van Wonderen. Analysis of propeller slipstream effects on the directional stability using a potential flow model. Master's thesis, Delft University of Technology, jan 2017.

[27] Valentine Invanitski. Naca duct vs. scoop. http://www.ivanitski.com/naca-duct-vs-scoop/, 2013.

[28] Vos R. Zandbergen B.T.C. Melkert, J.A. Aircraft preliminary sizing (class 1 estimation method). Lecture slides, feb 2017.

[29] GROB-WERKE GMBH &Co. KG, 8939 Mattsies, Federal Republic of Germany. *Flight manual for the Grob 109B VH-GUM*, sep 1983.

[30] Eric Weiner. Grob g109b: Two-for-one sailplane. *Flying*, 113(8):66–78, aug 1986.

[31] Burkhart Grob Luft- und Raumfahrt GmbH&Co. KG, D-86874 Tussenhausen, Federal Republic of Germany. *Operations Manual Grob 2500 Aircraft Engine for Motorgliders*, issue 2 edition, jul 1994.

[32] R. NOBACK J.B. DE JONGE, A.J.P. VAN DER WEKKEN. Acquisition of gust statistics from aids recorded data. In *63rd AGAïlD Structures and Materials Panel Meeting*, 1986.

[33] Youngren H Drela, M. Xflr5. Software package, 2000.

[34] Department of Defense. *Composite Materials Handbook*. January 1997.

[35] Danna Qian, Limin Bao, Masayuki Takatera, Kiyoshi Kemmochi, and Atsuhiko Yamanaka. Fiber-reinforced polymer composite materials with high specific strength and excellent solid particle erosion resistance. *Wear*, 268(3):637–642, 2010.

[36] B. Jongbloed. Lamdpbt, January 2013. An excel sheet provided to us by the author, used to determine composite laminate properties.

[37] C. Kassapoglou. *Design and Analysis of Composite Structures with Applications to Aerospace Structures*. Wiley, 2010.

[38] Welleman J.W. Hartsuiker, C. *Engineering Mechanics Volume 1: Equilibrium*. Springer, 2006.

[39] UK Granta Design Limited, Cambridge. Ces edupack. software, 2009.

[40] Melkert J.A. Vos, R. Aerospace design and systems engineering elements i. Lecture slides, mar 2017.

[41] Helmut Spindler, Martin Klein, Rudolf Rauch, Andreas Pichler, and Peter Stiaszny. High strength and ultra high strength hot rolled steel grades-products for advanced applications.

[42] Mooij E. Voskuijl, W. Flight and orbital mechanics. Lecture slides, 2016.

[43] Ruth T. Berg James P. Stucker. *Understanding Airfield Capacity For Airlift Operations*. RAND, 1998.

[44] B.A. Hummelink. Fixed-wing uav integrated navigation with low-cost imu/gps, Jan 2011.

[45] Prof. dr. ir. M.J.L. van Tooren Ir. R.J. Hamann. *Systems Engineering and Management Techniques*. Tu Delft, 2006.

[46] R. Lacerda G. Bunea A. Terao D. Rose D. DeGraaff, S. Caldwell. Qualification, manufacturing, and reliability testing methodologies for deploying high-reliability solar modules. Technical report, Sunpower, 2010.

[47] U.S. Department of Transportation. Certification of propellers. Technical Report AC 35-1, Federal Avition Administration, 2008.

[48] R.Smith D.S. Wilson. Electric motor reliability model. Technical report, Rome Air Development Center, 1978.

[49] Roland E. Weibel. Safety considerations for operation of different classes of unmanned aerial vehicles in the national airspace system. Paper, jun 2005. MASSACHUSETTS INSTITUTE OF TECHNOLOGY.

[50] National Consortium for the Study of Terrorism and Responses to Terrorism. Global terrorism database. Excel, 2016. Retrieved from https://www.start.umd.edu/gtd/.

[51] D. Larcher and J-M. Tarascon. Towards greener and more sustainable batteries for electrical energy storage. page 19–29, 2014.

[52] Smyth B. M. Murphy A. Butterfield J. Chua, M. H. Understanding aerospace composite components' supply chain carbon emissions. 2015.

[53] M. A. J. Huijbregts A. Meijer L. Reijnders N. J. Mohr, J. J. Schermer. Life cycle assessment of thinfilm gaas and gainp/gaas solar modules. 2006.

[54] Hanergy. Hanergy holding group csr report 2014. 2014.

[55] K.J. Mason C. Miyoshi. Journal of air transport management. 2009.

A. Task division

Task	Responsible Person(s)	Extra help
Preface	Arno	
Summary	Max	
Introduction	Ryan	Max
Market analysis	Arno, Jakub	
Functional discovery	-	-
-Requirements	Mathijs	Max, Ryan
-Functional analysis	Mathijs	Max
-Technical risk assessment	Mathijs	Max, Ryan
General design	-	-
-Design approach	Bas, Daniel	
-General results	Daniel	
-Mass & Power budgets	Ryan	
Wing geometry, stability & control	-	-
-Wing geometry	Max	Mathijs
-Static & dynamic stability	Max	Mischa
-Controllability	Mischa	Max
-Verification & validation	Mathijs	
Power & propulsion	-	-
-Power system design & sizing	Ryan	
-Engine design	Arno	
-Propeller design	Daniel	Ryan
-Pod design	Arno	Ryan
-Thermal design	Arno	
-Verification & validation	Daniel, Ryan	
Structural design	-	-
-Main structure trade-offs	Christian	Bas
-Load factor determination	Jakub	
-Rod	Bas	Christian
-Skin	Jan	Bas
-Rib	Jakub	Jan
-Mid-section	Jan	Bas
-Landing gear	Christian	Bas, Jan
-Production of propeller	Christian	Bas, Jan
-Verification & validation	Jakub, Jan	

Task	Responsible Person	Extra help
Operations	-	-
-Mission profile	Ryan	Max, Arno
-Operational considerations	Jakub	
-Transportability and setup	Jan	Arno, Daniel
-Control automation and sensors	Mischa	
-Ground station	Arno, Mischa	
-Hardware/software integration	Daniel	
Design evaluation	-	-
-Main parameters	Max	
-Drawings	Mischa	
-Compliance matrix	Ryan	
-RAMS analysis	Ryan	Mathijs
-Sensitivity analysis	Daniel	
Resource allocation	-	-
-Cost/budget breakdown	Arno	
-Manufacturing, assembly & integration	Bas	Christian
-Project development logic	Daniel	
-Project Gantt chart	Arno	
Sustainable development approach	Jan	
Conclusion & recommendations	Daniel	Ryan, Bas
Catia Model Aircraft	Mischa	Arno